



National Steel Bridge Alliance

A Fatigue Primer for Structural Engineers

by

John W. Fisher

Geoffrey L. Kulak

Ian F. C. Smith

A Note of Caution

All data, specifications, suggested practices, and drawings presented herein, are based on the best available information and delineated in accordance with recognized professional engineering principles and practices, and are published for general information only. Procedures and products, suggested or discussed, should not be used without first securing competent advice respecting their suitability for any given application.

Publication of the material herein is not to be construed as a warranty on the part of the National Steel Bridge Alliance – or that of any person named herein – that these data and suggested practices are suitable for any general or particular use, or of freedom from infringement on any patent or patents. Further, any use of these data or suggested practices can only be made with the understanding that the National Steel Bridge Alliance makes no warranty of any kind respecting such use and the user assumes all liability arising therefrom.

A FATIGUE PRIMER
for
STRUCTURAL ENGINEERS

by

John W. Fisher
Lehigh University
Bethlehem, Pennsylvania, USA

Geoffrey L. Kulak
University of Alberta
Edmonton, Alberta, Canada

Ian F.C. Smith
Swiss Federal Institute of Technology
Lausanne, Switzerland

ACKNOWLEDGMENTS AND DISCLAIMER

Several US state highway departments and highway design firms or consultants supplied information on various bridge structures reported in this document. These include transportation departments in the States of Connecticut, Maryland, Massachusetts, Minnesota, Ohio, Pennsylvania, South Dakota, Virginia, and West Virginia and the firms DeLeuw Cather and Company, Fay, Spofford and Thorndike Inc., Greiner Engineering Sciences, Kozel Engineering Company, Modjeski and Masters Inc., and Wiss Janney Elstner Associates Inc. Their contributions are noted with thanks.

The document was proofread with great care by Jeffrey DiBattista, Graduate Student at the University of Alberta and helpful comments were provided on the technical content by Prof. Gilbert Grondin, also of the University of Alberta. Jeffrey DiBattista did many of the calculations associated with the example presented in Chapter 5. The contributions of Manfred Hirt, Professor of Steel Construction and Director of ICOM, Swiss Federal Institute of Technology, Lausanne, are gratefully recognized. Professor Hirt is the co-author of a principal source document (Reference 1). Figure 4 is taken from Hirt, M.A. "Anwendung der Bruchmechanik für die Ermittlung des Ermüdungsverhaltens geschweisster Konstruktionen," *Bauingenieur*, 57 (1982), and is used with his permission. The authors also thank Dr. Peter Kunz, formerly at ICOM, for his help with the preparation of Example 7.

The authors have taken care to ensure that the material presented is accurate. However, it must be understood that persons using the material assume all liability arising from such use. Notification of errors and omissions and suggestions for improvements are welcome. No part of this publication may be reproduced or distributed in any form or by any means without the prior written permission of the authors.

TABLE OF CONTENTS

1	Introduction	1
2	Basic Fracture Mechanics Concepts	
2.1	How to Account for a Crack	2
2.2	Fracture Limit State	6
2.3	Fatigue Limit State	8
2.4	Fracture Mechanics Used as a Qualitative Design Tool	11
3	Fatigue Strength Analysis	
3.1	Introduction and Historical Background	16
3.2	Sources of Flaws in Fabricated Steel Structures	18
3.3	Basis for Design Rules	22
3.4	Design Rules Given by the AASHTO Specification.....	25
3.5	Fracture Mechanics Analysis of Fatigue.....	29
4	Fatigue Assessment Procedures for Variable Stress Ranges	
4.1	Cumulative Fatigue Damage.....	34
4.2	Analysis of Stress Histories.....	40
4.3	Fatigue Limits.....	47
5	Fatigue Design According to the American Association of State Highway and Transportation Officials Specification (AASHTO)	
5.1	Introduction	51
5.2	Redundancy and Toughness.....	51
5.3	Fatigue Design in the AASHTO Specification	54
5.3.1	Fatigue Load and Frequency	54
5.3.2	Fatigue Resistance.....	56
5.4	Summary of AASHTO Requirements.....	58
5.5	Design Example	59

6	Distortion-Inducted Fatigue Cracking	
6.1	Introduction	73
6.2	Examples of Distortion-Induced Cracking.....	73
6.3	Further Examples of Distortion-Induced Cracking.....	76
6.3.1	Web Gaps in Multiple Girder and Girder Floor Beam Bridges	76
6.3.2	Web Gaps in Box Girder Bridges.....	79
6.3.3	Long Span Structures	81
6.3.4	Coped Beam Connections	82
6.3.5	Connections for Lateral Bracing	83
6.3.6	Other Examples	83
6.4	AASHTO Specification Requirements Relating to Distortion-Induced Fatigue	84
6.5	Design Examples.....	85
6.6	Summary.....	87
7	Inspection and Repair of Fatigue Cracks	
7.1	Introduction	88
7.2	Protocol for Fatigue Crack Investigation	88
7.3	Identifying the Causes of Cracking.....	89
7.4	Cracking at Low Fatigue Strength Details	90
7.5	Methods for Inspection of Fatigue Cracking.....	95
7.6	Repair of Fatigue-Cracked Members	97
7.7	Avoiding Future Cracking Problems.....	100
8	Special Topics	
8.1	Bolted or Riveted Members	102
8.1.1	Bolted Members	102
8.1.2	Threaded Rods.....	106
8.1.3	Riveted Connections.....	108

8.2	Environmental Effects; Use of Weathering Steel.....	110
8.3	Combined Stresses	114
8.4	Effect of Size on Fatigue Life	115
8.5	Role of Residual Stress.....	115
8.6	Quantitative Design Using Fracture Mechanics.....	121
	REFERENCES	124
	INDEX	128

Chapter 1. Introduction

Fatigue in metals is the process of initiation and growth of cracks under the action of repetitive load. If crack growth is allowed to go on long enough, failure of the member can result when the uncracked cross-section is sufficiently reduced such that the part can no longer carry the internal forces. This process can take place at stress levels (calculated on the initial cross-section) that are substantially less than those associated with failure under static loading conditions. The usual condition that produces fatigue cracking is the application of a large number of load cycles. Consequently, the types of civil engineering applications that are susceptible to fatigue cracking include structures such as bridges, crane support structures, stacks and masts, and offshore structures.

The first approach in the design and execution of structures is to avoid details that might be prone to cracking, and then to inspect the structure for cracks, both during fabrication and later in its life. However, it is inevitable that cracks or crack-like discontinuities will be present in fabricated steel elements, and it is the responsibility of the engineer to consider the consequences in terms of brittle fracture and in terms of fatigue. The fatigue behavior of a fabricated steel engineering structure is significantly affected by the presence of pre-existing cracks or crack-like discontinuities. Among other things, it means that there is little or no time during the life of the structure that is taken up with "initiating" cracks.

Probably the most common civil engineering structures that must be examined for fatigue are bridges. In North America and elsewhere, early steel bridge structures were fabricated using mechanical fasteners, first rivets and later high-strength bolts. In these cases, initial imperfections are relatively small. In addition, loading and load frequency were also low by today's standards. Consequently, fatigue cracking in these early structures was infrequent. In the 1950's welding began to be used as the most common method for fabrication. This had two principal effects related to fatigue. First, welding introduces a more severe initial crack situation than does bolting or riveting. Second, the continuity inherent in welded construction means that it is possible for a crack in one element to propagate unimpeded into an adjoining element.

Design rules at this period of time had been developed from a limited experimental base and the mechanism of fatigue crack growth was not well understood. Furthermore, most of the experimental results came from small-scale specimens. This is now known to be a

limitation in evaluating fatigue strength: reliance on small-scale specimens can result in overestimates of fatigue strength.

During the 1970's and 1980's there were many examples of fatigue crack growth from welded details now known to be susceptible to this phenomenon. Research revealed that the type of cracking observed in practice was in agreement with laboratory test results and supportable by theoretical predictions. Experience in the 1970's also exposed an unexpected source of fatigue cracking, that from distortions. This is also a phenomenon related largely to welded structures.

The purpose of this publication is to provide the student and the practicing engineer with the background required to understand and use the design rules for fatigue strength that are currently a standard part of design codes for fabricated steel structures. The approach adopted establishes the basis for the problem in terms of fracture mechanics, that is, an analytical tool that accounts for the presence of a crack in a structure [1]. The focus is then directed specifically upon the issue of fatigue.

It is intended that fundamentals are presented in a general way, but applications will refer to the specification for the design of steel bridges prepared by the American Association of State Highway and Transportation Officials (AASHTO) [2]. This specification is widely used in the United States, and the governing Canadian specification is nearly identical to it.

Chapter 2. Basic Fracture Mechanics Concepts

Use of the fracture mechanics method of analysis is relatively recent. Originally advanced to explain the rupture of glass specimens [3], its introduction into the field of structural engineering practice started when it was used in the 1940's to help explain the catastrophic failure of welded ship hulls. Currently, it is employed to assess the behavior of elements used in machinery, pipelines, automotive parts, spacecraft, turbine blades, and many other components.

In this Chapter, basic concepts of the fracture mechanics approach are described in order to assist the reader in understanding the fatigue design rules. In addition, for those who might need to design at higher levels of sophistication, it will provide the basis for further reading and self-instruction.

Only a summary of fracture mechanics concepts is given in this section. For simplicity, the discussion is limited to cases where the loads are applied at locations remote from the crack locations and normal to the crack surfaces, the so-called Mode 1 situation. (The different ways in which a crack can open, or *modes*, will be explained in Example 1). Excellent review articles provide more detailed information (for example, see Ref. [4–6]) and several reference books are available [7–9].

2.1 How to Account for a Crack

Five cases of a loaded plate containing a crack are shown in Fig. 1. It requires no knowledge of fracture mechanics to appreciate that cases 1 to 5 are placed in order of increasing severity. Taking Case 1 as the basis for comparison, the following important

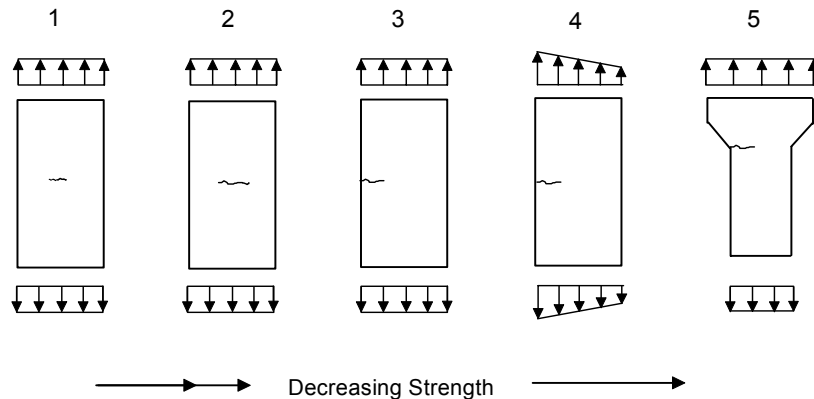


Figure 1 Five Different Cases of a Plate Containing a Crack

fracture mechanics parameters can be identified: *i*) crack length (Case 2); *ii*) crack location (at edge of plate in Case 3); *iii*) effect of bending (Case 4); and *iv*) presence of a stress concentration (Case 5). Of course, the result of any of these parameters in weakening the plate will depend on the actual circumstances. The effect can be significant, however. For instance, the consequence of a sharp stress concentration in combination with a crack (Case 5) could weaken a plate to less than one-half of its uncracked strength.

A magnified view of the area around a crack tip in an infinitely wide plate is shown in Fig. 2. This resembles closely the conditions of Case 1 when the crack length is small compared with the plate width. When a remote stress, σ , is applied, the crack opens a certain distance, d , and the stress that this cross-sectional area would have carried is diverted to the uncracked area of the plate. This diversion creates a high concentration of stress in the vicinity of the crack tip. For an elastic material, theoretically this stress is infinite at the crack tip: in real materials, plastic zones are formed since the strain exceeds the ability of the material to behave elastically. This process—whereby *i*) an applied load causes a crack to open, *ii*) the crack opening relieves crack surfaces of stress, and *iii*) crack tip plastic straining is created—is the fundamental mechanism that weakens structures containing cracks or crack-like discontinuities.

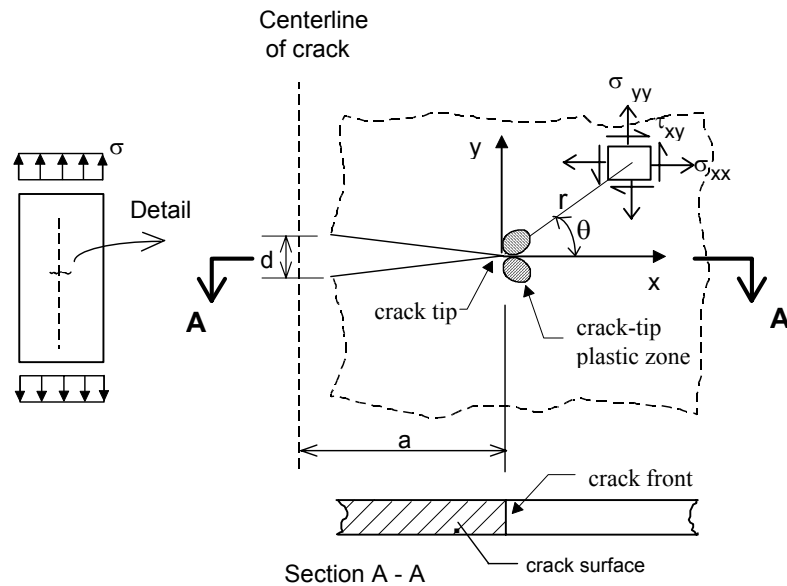


Figure 2 A Crack in an Infinitely Wide Plate

If plasticity is ignored, a description of the stress field near the crack tip can be obtained. Using special stress functions, a solution containing the coordinates r and θ is

developed. For the particular case of $\theta = 0$, that is, for the stress in the y-direction, the stress is

$$\sigma_{yy} = \frac{\sigma \sqrt{\pi a}}{\sqrt{2\pi r}} \quad (1)$$

provided that the crack length, a , is much larger than the distance from the crack tip, r . The numerator in Eq. (1) determines the gradient of the (theoretical) stresses as they rise to infinity when r approaches zero. This numerator is called the stress intensity factor, K . Thus:

$$K = \sigma \sqrt{\pi a} \quad (2)$$

The advantage of this model is that any combination of stress and crack length can be characterized by the single parameter K . Analytical solutions are available for other particular geometrical configurations and loading conditions; these are summarized in handbooks [10]. However, many practical cases cannot be solved analytically. In such instances, the following expression is used to approximate K :

$$K = W Y \sigma \sqrt{\pi a} \quad (3)$$

where Y is an expression that corrects for plate and crack geometry and W corrects for non-uniform local stress fields caused by the presence of factors such as residual stresses, stress concentrations, and stress gradients. Usually, such correction factors are determined using numerical methods. Here, also, solutions can be found in handbooks.

Equation 1 is based on linear-elastic material behavior and cannot account for yielding at the crack tip. Furthermore, stress redistribution due to plasticity alters the stress field outside the crack tip plastic zone. Nevertheless, if this zone is small, say less than 2% of the plate thickness, of the crack length, and of the uncracked ligament, then the stress intensity factor (K) approach is satisfactory.

These limitations are violated in many practical situations. For example, an elastic–plastic analysis may be required when stress concentrations cause localized plasticity. The most common analyses either use a parameter named J , which is an expression of the change in potential energy with respect to crack length, or use a parameter called the crack tip opening displacement (CTOD). Further description of elastic-plastic analyses is available elsewhere [9] and the American Society for Testing and Materials has produced standards for

determining these parameters experimentally. (See, for example, Ref. [11].) Occasionally, an equivalent K is calculated [3]:

$$\frac{K^2}{E} = J = \sigma_y \text{ CTOD} \quad (4)$$

where E is Young's Modulus and σ_y is the effective yield strength. When plate dimensions are large enough to restrict behavior to essentially two-dimensional straining (plane strain conditions), the material constant, E , is replaced by $E/(1-\nu^2)$, where ν is Poisson's ratio.

A further restriction on K exists for small crack lengths, where all of the approaches explained above lose their validity. When the size of the crack or initial discontinuity is of the order of grain size, micro-structural properties such as grain orientation influence crack growth [12]. Microstructural fracture mechanics models may then become necessary. These models are not yet well defined, and no generally accepted design rules are available. For the usual situation, when the crack length is greater than about five grain diameters, the models that assume an isotropic continuum, i.e., those employing K or J , are sufficiently accurate.

2.2. Fracture Limit State

The analysis tools available will indicate that fracture occurs when the crack parameter (i.e., K or J) exceeds a critical value, commonly referred to as the fracture toughness. The designer should choose a steel with a fracture toughness level that is sufficiently high for the intended application. The fracture toughness depends upon such factors as microstructure and composition of the material, service temperature, loading rate, plate thickness, and fabrication processes.

An accurate determination of the fracture toughness is complicated, especially in most structural engineering design situations. This is primarily due to the fact that, for most designs, plane strain conditions do not dominate; conditions of essentially two-dimensional stress (plane stress) have an influence, thereby disqualifying K as a model that characterizes combinations of stress and crack length. Elastic-plastic models are needed because the stress at fracture produces a plastic zone size that exceeds the limitations cited for the validity of K specified in Section 2.1.

Less sophisticated approaches are used for practical problems in structural engineering. The most widely used method for approximating the toughness quality of a steel is a procedure that was developed over 80 years ago, the Charpy impact test. In brief, this

method measures the energy absorbed by the rapid fracture of a small bar containing a machined notch. The bar is broken by a swinging pendulum and the absorbed energy is measured by the difference in swing height before and after fracture. The effect of temperature is examined by repeating the test using physically identical specimens that have been cooled to various temperatures. Several tests provide a relationship between absorbed energy and temperature for the steel under investigation.

The Charpy test, and many other similar procedures [9] provide only qualitative information because stress and crack length values cannot be assessed directly. However, correlation with fracture mechanics models are available for certain situations [8]. For example, Charpy impact data in the lower region of the energy vs. temperature response curve can be converted into dynamic plane-strain fracture toughness values, K_{I_d} , using an empirical formula.¹ If required, the K_{I_d} values then can be converted to static plane-strain fracture toughness values, K_{I_c} . In general, such correlations are valid only for steels of low to medium strength. Moreover, the toughness value where conditions change from plane strain to plane stress depends upon the yield strength and the thickness of the element. The location of this change cannot be correlated to Charpy results.

At a given temperature, a given material will always exhibit higher fracture toughness for plane stress conditions than for plane strain conditions in the elastic-plastic region. Therefore, K_{I_c} and K_{I_d} are conservative first estimates of the fracture toughness. Elastic-plastic analyses, which result in less conservatism, can be used when the design problem justifies increased complexity of work.

A critical crack length, a_{cr} , may be approximated by introducing the fracture toughness at the minimum service temperature and the maximum possible stress, σ , in Eq. 3. Fracture will not occur if the maximum size of the crack or crack-like discontinuity, a , is less than a_{cr} . Often, inspection technology influences this verification: a_{cr} is compared with the minimum verifiable crack length, a_0 . The engineer should ensure that the design configuration and the inspection equipment and procedures permit reliable detection of crack lengths less than a_{cr} .

In most modern steel structures, the likelihood of fracture shortly after erection has been completed is not high. Some problems may arise when severe weld discontinuities are present or when very thick plates are used or when the structure is in a very cold environment, but such situations are not common. Rational designs, which employ high-

¹The subscripts used here for K are explained in Example 1.

strength fine-grained steels and which use modern fabrication techniques, should provide high toughness and, consequently, large critical crack lengths, a_{cr} . At the same time, careful assembly and improvements in the technology of non-destructive inspection are reducing the minimum verifiable crack length, a_0 . As a result, the greatest risks of fracture in modern steel structures arise when sub-critical crack growth due to fatigue, corrosion, stress corrosion, etc. is possible. Predicting the occurrence of the fracture limit state is becoming more dependent upon the correct choice of the sub-critical crack-growth model than upon an accurate estimate of the fracture toughness of the detail. Crack growth due to fatigue is discussed in the next section.

2.3 Fatigue Limit State

Fatigue is the initiation and propagation of microscopic cracks into macro cracks by the repeated application of stresses. (As has already been noted, the initiation portion of fatigue life is essentially non-existent for fabricated steel structures.) In civil engineering practice, examination of the possibility of fatigue cracking must be a consideration for bridges, cranes, towers, off-shore platforms, and any such structure that is subjected to repeated loading. Although steel structures today use higher-toughness materials than was common in the past, and are thus more resistant to fracture than ever before, many structural elements remain susceptible to fatigue crack growth. Consequently, if the fracture limit state is reached, it is often the result of fatigue crack growth after many years of trouble-free service. Such an occurrence is covered by the definition of the fatigue limit state.

In addition to higher-toughness properties, development of low-alloy and fine-grain microstructures have increased the yield strengths of the steels used for construction. Consequently, higher service stresses have been allowed in recently built structures. Furthermore, welding is now used more often than formerly and this method of fastening leads to a lower fatigue life than would apply if the connection was made using rivets or bolts. Generally speaking, then, modern structures are more susceptible to fatigue cracking than were older structures. Furthermore, the number of old structures, for example railway bridges, that have exceeded their design fatigue life is growing exponentially. The combined effect of these trends is increasing the importance of fatigue strength evaluation.

All elements of a fabricated steel structure contain metallurgical or fabrication-related discontinuities, and most also include severe stress concentrators such as weld toes. Consequently, fatigue failure is often the result of slow crack growth from an existing discontinuity at a stress concentration. This growth can even begin before the structure is put

into service (the result of transportation of a girder, for example). A description of the fatigue crack growth phenomenon can be made on the basis of the fracture mechanics model described in Section 2.2.

The stress intensity factor K can be modified to represent fatigue crack growth by adapting Eq. 3 to account for repeated loading. For a constant stress range, $\Delta\sigma$ ($=\sigma_{\max} - \sigma_{\min}$), Eq. 3 becomes

$$\Delta K = W Y \Delta\sigma \sqrt{\pi a} \quad (5)$$

Equation 5 is related empirically to the crack-growth rate, da/dN , which is obtained from the slope of the curve of crack-growth measurements—see Fig. 3(a). This slope is used as the ordinate in a plot of this parameter against ΔK , using a double logarithmic representation—see Fig. 3(b). The values of ΔK are calculated using Eq. 5 for particular magnitudes of crack length, a . At very low growth rates, the curve for crack growth (in steel) becomes vertical, indicating a crack-growth threshold at ΔK_{th} , the threshold stress intensity factor. At higher values of ΔK , the curve straightens to a near-constant slope, and it becomes vertical again when the fracture toughness is approached at the maximum stress in the cycle.

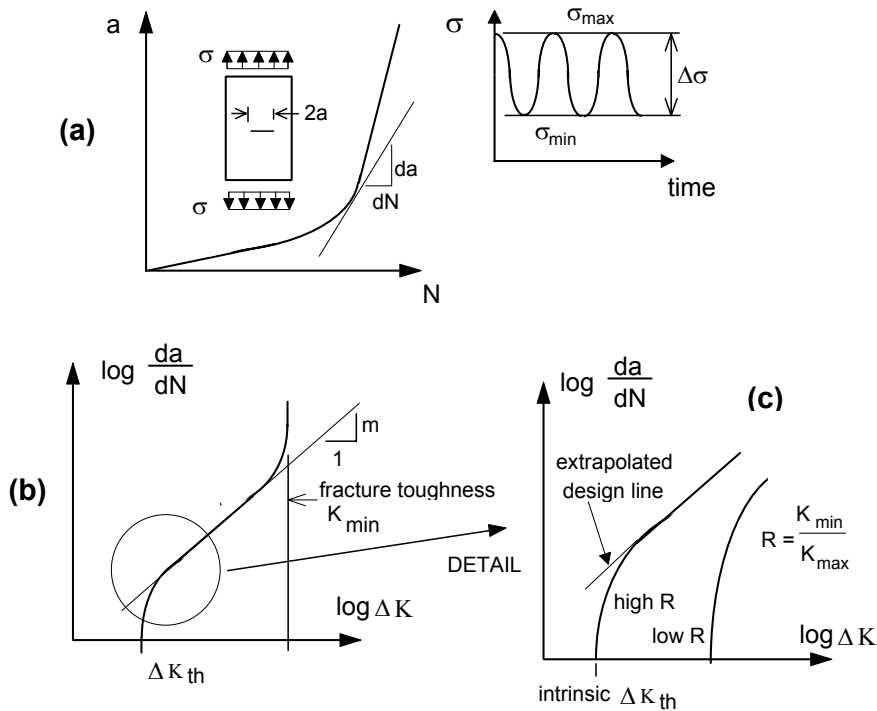


Figure 3 Stress-Intensity Factor and Fatigue Crack Growth. (a) Crack length vs. number of cycles; (b) Crack growth rate vs. stress intensity factor range; (c) Magnification of the lower portion of the curve in (b)

Material properties, stress level, and environment have greater influence in the end (vertical) portions of the curve than in the middle. In this center portion, which is of considerable engineering interest, the Paris equation is useful [13]:

$$\frac{da}{dN} = A \Delta K^m \quad (6)$$

where A and m are constants that are determined by means of regression analysis of test data. These constants are reliable when similar materials, loadings, and environments are compared. (The constants show up directly in the design specifications, as will be seen in Section 3.5.) Also, the regression analysis is dependent upon the domain of crack growth rates considered since the center portion of the curve in Fig. 3(b) is not perfectly straight.

Many structural applications involve repeated loading of over one million cycles: this requires a precise knowledge of slow crack growth rates near ΔK_{th} —see Fig. 3(c). Conservative assessments result when Eq. 6 is extrapolated into this region. The error resulting from the extrapolation is dependent upon the magnitude of the stress ratio, $R = \sigma_{min} / \sigma_{max}$. This ratio is often used to examine the effects of mean stress on crack growth.

When ΔK is much larger than ΔK_{th} , Eq. 6 can be integrated to calculate the crack propagation fatigue life, N :

$$N = \frac{1}{A} \int_{a_i}^{a_f} \frac{1}{\Delta K^m} da \quad (7)$$

where a_i and a_f are the initial and final crack lengths. These integration limits may take the values a_0 and a_{cr} , respectively, as defined in Section 2.2.

It was pointed out in Section 2.2 that small crack sizes and excessive plasticity may invalidate models that employ the stress intensity factor. This is equally true for fatigue applications: non-conservative calculations may result if so-called short crack behavior occurs [14]. Fortunately, such situations are less common when assessing the fatigue limit state. Usually, the stress intensity factor remains a useful characterizing parameter for conditions of fatigue crack growth since discontinuities are large and a high percentage of crack growth occurs under conditions where K is valid. Moreover, structural engineering applications have particular characteristics that reduce the occurrence of this anomalous behavior.

2.4 Fracture Mechanics used as a Qualitative Design Tool

Engineering designers rarely use fracture mechanics as a design tool. Older concepts, such as Charpy energy values for fracture toughness requirements and stress range models for fatigue assessments (see Section 3.4), are the most practical tools for evaluating many structures. Nevertheless, the concepts of fracture mechanics enable the designer to increase his qualitative understanding of structures containing crack-like discontinuities. Because more parameters are explicit in fracture mechanics analyses, designers can identify more easily those parameters that influence the strength of the structure. Some examples, covering the importance of discontinuities, parametric studies, and crack propagation behavior, are presented below. Guidelines for simple linear-elastic fracture mechanics models sufficient for most structural engineering designs are available in some design codes [15] and one illustration of the application of fracture mechanics analysis is given in Section 3.5.

The size of the discontinuity clearly influences the resistance of an element to fracture. For example, two trends are illustrated by the curves in Fig. 4(a). First, increasing the applied stress causes a decrease of the critical defect size. Second, an embedded discontinuity (such as an inclusion) is less serious than a surface discontinuity (such as a weld undercut). Fracture mechanics analysis clarifies the importance of discontinuities in fracture assessments. This has resulted in an increased emphasis on quality assurance guidelines and on detail designs that have small discontinuities.

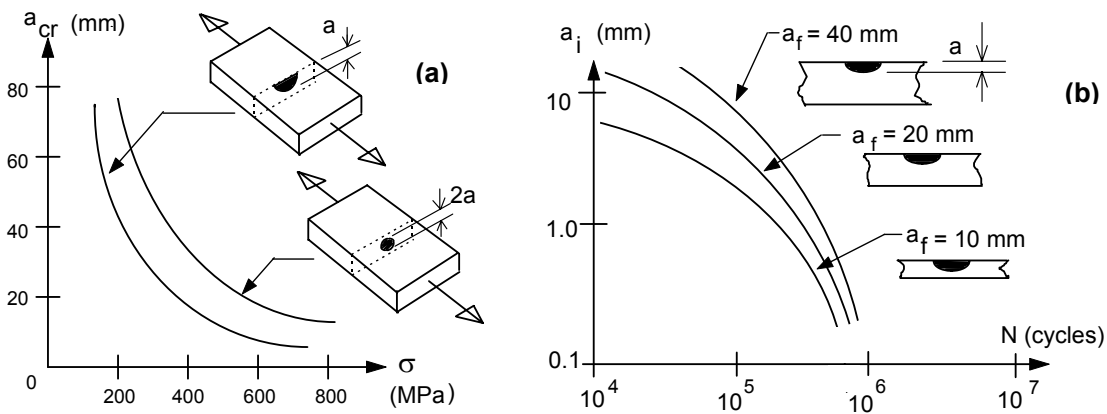


Figure 4 Examples of Studies that Examined the Significance of Discontinuities (a) Critical crack size vs. applied stress; (b) Effect of initial and final crack size on fatigue life

The effect of discontinuities is equally important when assessing the fatigue limit state. The integral in Eq. 7 has the limits a_i and a_f . Small variations in the magnitude of the

final crack size, a_f , may not significantly alter the resulting fatigue life. The initial crack size is far more important than the final crack size—see Fig. 4(b).

Fracture mechanics analysis facilitates recognition that any areas not welded become built-in cracks. Figure 5 shows an end plate welded to a beam. (The assembly will subsequently be bolted to a column flange, not shown.) Groove welding may not always be able to penetrate completely into the zone through which welding is intended. In the example, the flange groove weld will be difficult to complete in the vicinity of the web-to-flange junction. (However, provision of cope holes will give better access to the web-to-flange junction.) Design guidelines already recognize that flange fillet welds, an alternative to the groove welds shown, produce a detail of low fatigue strength because of the large unwelded areas (cracks).

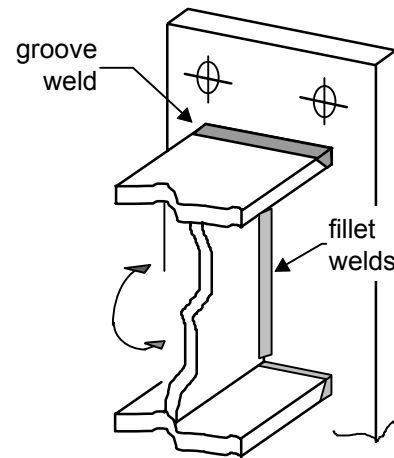


Figure 5 Unwelded Areas can become Built-In Cracks

A fatigue crack that starts at the surface of the material initially propagates very slowly into the plate thickness. The stress concentration, modeled by the parameter W in Eq. 5, affects the crack growth rate. Connections classified by specifications as falling into different fatigue strength categories may have different crack propagation characteristics for the same fatigue life—see Fig. 6.

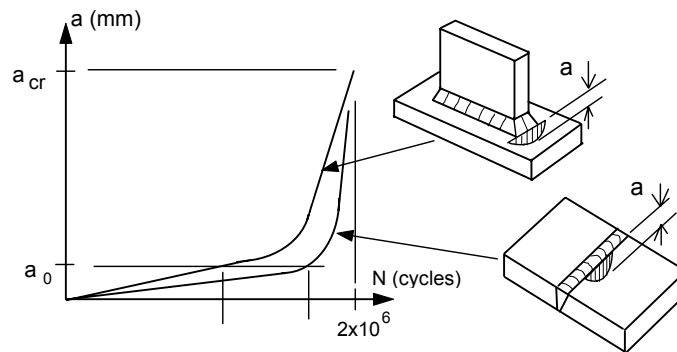


Figure 6 Comparison of Fatigue Crack Growth Behavior for Two Different Details Having the Same Fatigue Life

In this example (Fig. 6), the detail with lower-severity stress concentration (groove-welded plate) consumes a greater percentage of its total fatigue life during the propagation of

a crack to a size a_0 than does the detail with a higher-severity stress concentration (attachment detail). This means that a crack of a given size may be identified earlier at the attachment than at the groove weld. Other factors such as differences in inspection feasibility influence the exact timing of crack identification. Nevertheless, such crack growth behavior should be considered when establishing inspection intervals.

EXAMPLE 1

Crack loading modes are shown in Fig. 7. In structural engineering applications, Mode I, the crack opening mode, will almost always be the applicable condition. In order to distinguish among the various possible cases, the stress intensity factor K introduced in Section 2.1 is subscripted, e.g., K_I would be used for a Mode I case. The value of the stress intensity factor at which brittle fracture will occur is designated as K_{Ic} or as K_{Id} , depending upon whether the loading is essentially static (K_{Ic}) or is dynamic (K_{Id}).

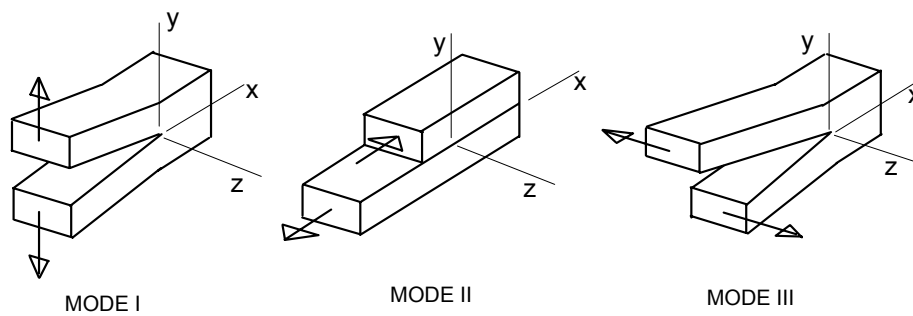


Figure 7 Basic Modes of Loading Involving Different Crack Surface Displacements

Published solutions for the expressions for the stress intensity factor are available for a wide variety of conditions [10]. Several common cases are shown in Fig. 8. (The term Q in part (b) is a correction for the presence of an elliptical surface flaw.)

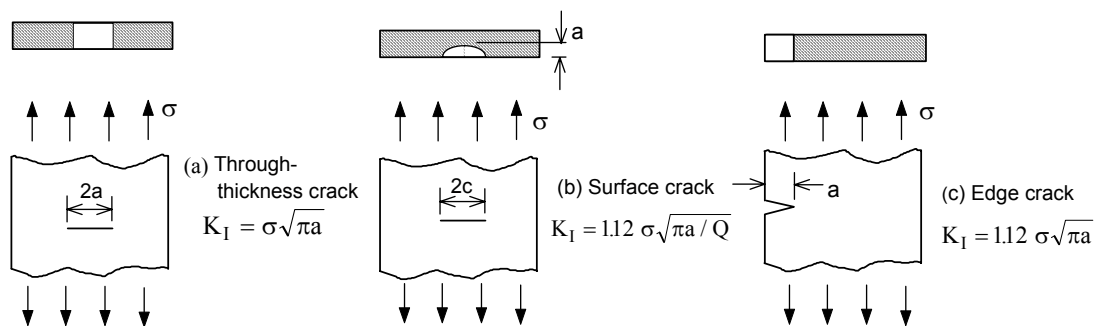


Figure 8 K_I Values for Various Crack Geometries (Infinitely Wide Plates)

Consider the element shown in Fig. 9, where a centrally located through-thickness crack is present in a plate that is loaded by a uniform tensile stress. (It is to be understood that the crack width is small relative to the plate width in the illustrations of Figs. 8 and 9. These illustrations are intended to depict the case of an "infinitely wide plate.")

Given: $\sigma_y = 550 \text{ MPa}$

$K_{IC} = 66 \text{ MPa m}^{1/2}$ (This information is provided by the supplier of the material and is related to the intended service temperature, loading rate, and the particular plate thickness.)

Design stress = 140 MPa

Question: (a) What is the flaw size at which brittle fracture might be expected?

Solution: It is given that the value of the critical stress intensity factor is $K_{IC} = 66 \text{ MPa m}^{1/2}$. From Fig. 8, the general expression for the stress intensity factor is $K_{IC} = \sigma \sqrt{\pi a}$. It is simply a matter of examining the situation $K_I \rightarrow K_{IC}$, or

$$\sigma \sqrt{\pi} \sqrt{a} = 66 \text{ MPa} \sqrt{\text{m}}$$

$$\text{Using } \sigma = 140 \text{ MPa and solving, } \sqrt{a} = 0.27 \sqrt{\text{m}}$$

$$a = 0.071 \text{ m} = 71 \text{ mm}$$

Thus, if the flaw size reaches $2a = 142 \text{ mm}$, failure by brittle fracture can occur.

Question: (b) If the design stress is increased to 310 MPa, what is the tolerable flaw size now?

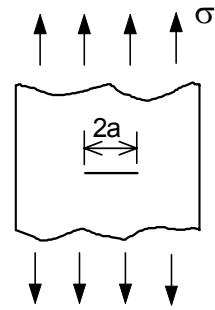
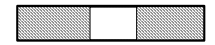
$$\text{Solution: } \sigma \sqrt{\pi} \sqrt{a} = 66 \text{ MPa} \sqrt{\text{m}}$$

$$310 \text{ MPa } \sqrt{\pi} \sqrt{a} = 66 \text{ MPa} \sqrt{\text{m}}$$

$$\text{Solving, } 2a = \text{flaw size} = 29 \text{ mm.}$$

Question: (c) Residual stress due to welding is present and it is estimated that the total stress (design stress + residual stress) is 500 MPa. What is the tolerable flaw size now?

$$\text{Solution: } \sigma \sqrt{\pi} \sqrt{a} = 66 \text{ MPa} \sqrt{\text{m}}$$



Through-thickness crack: $K_I = \sigma \sqrt{\pi a}$

Figure 9

$$500 \text{ MPa} \sqrt{\pi} \sqrt{a} = 66 \text{ MPa}\sqrt{\text{m}}$$

Solving, $2a = \text{flaw size} = 11 \text{ mm}$.

Comment: Often, it is not possible to superimpose stresses due to residual stresses because—

1. The distribution of residual stress is different from the applied stress. (Recall that the expression in Fig. 8 is valid only for a uniform, remote stress);
2. There is a stress concentration present. This requires that a correction factor for K be used on the applied loads, but not for the residual stresses;
3. There is a possibility of residual stress relaxation with crack growth. In such cases, the value of K for residual stresses should be calculated separately and then added to the K for the applied loads. Thus, superposition is applied at the level of K, the parameter that characterizes the stress field at the crack tip.

Chapter 3. Fatigue Strength Analysis

3.1 Introduction and Historical Background

Fatigue cracking was observed in railroad equipment over 120 years ago. Studies carried out at that time by Wöhler on railway rolling stock showed that stress concentrations and sharp angles in the axle configuration resulted in failures even though the stress in the material was well below its yield strength. The industrialization of society and the subsequent increased use of machinery and equipment led to other examples of failures resulting from fatigue cracking. As a result, studies into the phenomenon started in both Europe and in North America. For example, in North America the observation of cracks in railroad bridge truss hangers and in stringer end connection angles led to a number of laboratory investigations between 1930 and 1960.

Welded details were first examined in the 1930's when tests were carried out on welded steel details. These and later studies following World War II formed the basis for the early fatigue design specifications in North America. Fatigue cracks forming in steel bridges at a road test program conducted in the USA in the 1960's [16] became the genesis of the fatigue test program sponsored by the National Cooperative Highway Research Program (NCHRP) that began at Lehigh University in 1968. Prior to the NCHRP program, the fatigue design rules that existed for welded steel bridge components were based on small specimens and on a limited quantity of test data. This made it difficult to establish the significance of stress variables, detail type, types of steel, and quality of fabrication. The early provisions for fatigue life evaluation proved to be inadequate for a number of bridge details. This explains, in part, the relatively large number of cases of fatigue cracking in bridges that were designed prior to about 1975.

The approach taken by modern-day specifications for the fatigue design of fabricated steel structures is based primarily on work done in Great Britain [17] and in the USA [18–20] in the late 1960's and early 1970's. Although many other investigators have contributed to our understanding of the problem, both before and after the work cited, it was this research that identified the influence of residual stress on fatigue life. These studies also revealed the necessity to acknowledge that fabricated steel structures always contains cracks or crack-like discontinuities.

Fatigue can be defined as the initiation and propagation of microscopic cracks into macro cracks by the repeated application of stress. In terms of the fracture mechanics model

described in Chapter 2, an initial crack grows a small amount in size each time a load is applied. A good explanation of the crack growth mechanism has been provided by Broek [21]. Growth occurs at the crack front, which is initially sharp. Even at relatively low loads, there will be a high concentration of stress at the sharp front, and plastic deformation (slip on atomic planes) therefore occurs at the crack front. Continued slip results in a blunted crack tip, and the crack grows a minute amount during this process. Upon unloading, not necessarily to zero, the crack tip again becomes sharp. The process is repeated during each load cycle.

Figure 10 shows the fracture surfaces of a member that has an I-shaped cross-section. The web of the member, which was 10 mm thick, was fillet-welded to 13 mm thick flange plates. (The full thickness of the flange is not shown in Fig. 10). The profiles of the fillet welds are generally satisfactory and the flow lines of the weld show good penetration of the base metal. In this illustration, an internal flaw in the left-hand fillet weld grew under the repeated application of stress until the crack penetrated the outside surface of the weld. Since this was a laboratory specimen, at this point the beam was deliberately overloaded so that the remaining cross-section fractured and could be exposed.

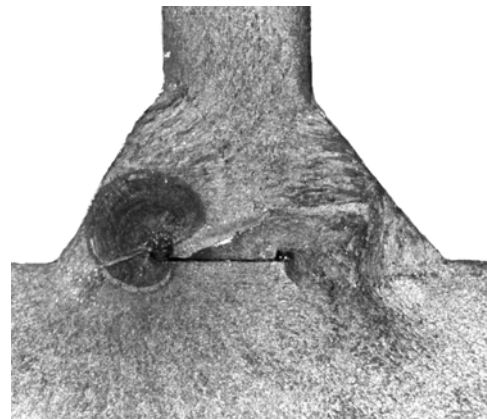


Figure 10 Fracture Surface of I-shaped Member

In the case illustrated in Fig. 10, the crack front eventually reached the exterior surface of the weld. Experience in the laboratory shows that as much as 80% of the fatigue life has been consumed by the time a fatigue crack emanating from an internal flaw reaches the surface and can be observed.

If the test that produced the specimen shown in Fig. 10 had not been terminated by the investigators, failure could have occurred in one of two ways. One possibility is that the fatigue crack grows to such an extent that the loss of cross-section means the load simply can no longer be carried by the uncracked portion of the beam. In this case, failure occurs by yielding of the remaining material, or, exceptionally, by instability if the crack growth produces a grossly unsymmetrical cross-section. The other way that the beam can fail is by brittle fracture. As discussed in Section 2.3, growth of a crack by fatigue can lead to brittle

fracture if the crack reaches a critical size according to the particular conditions of material toughness, temperature, and loading rate.

3.2 Sources of Flaws in Fabricated Steel Structures

The kinds of flaws that can occur in a fillet-welded detail are shown pictorially in Fig. 11. These include partial penetration and lack of fusion, porosity and inclusions (the fatigue crack shown in Fig. 10 started at a non-metallic inclusion), undercut or micro flaws at the weld toe, and cracking or inclusions around a weld repair or at start-stop locations or at arc strikes. Although the fabricator of the structure and those responsible for the fabrication inspection will attempt to minimize these defects, it is neither practical nor economically possible to eliminate them.

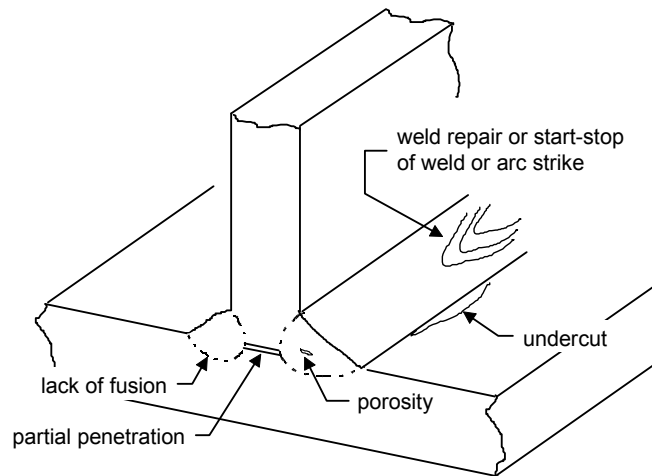


Figure 11 Flaws in a Fillet-Welded Detail

Test data on welded details have demonstrated that all fatigue cracks commence at some initial discontinuity in the weldment or at the weld periphery, and grow perpendicular to the applied tensile stresses. In a welded beam without attachments (simply two flange plates welded to a web), most laboratory fatigue cracks are observed to originate in the web-to-flange fillet welds at internal discontinuities such as porosity (gas pockets), incomplete fusion, or trapped slag. Figures 12 and 13 show fatigue cracks that have formed from porosity and entrapped slag in longitudinal submerged arc fillet welds. These discontinuities are always present to some degree, irrespective of the welding process and techniques used during fabrication.

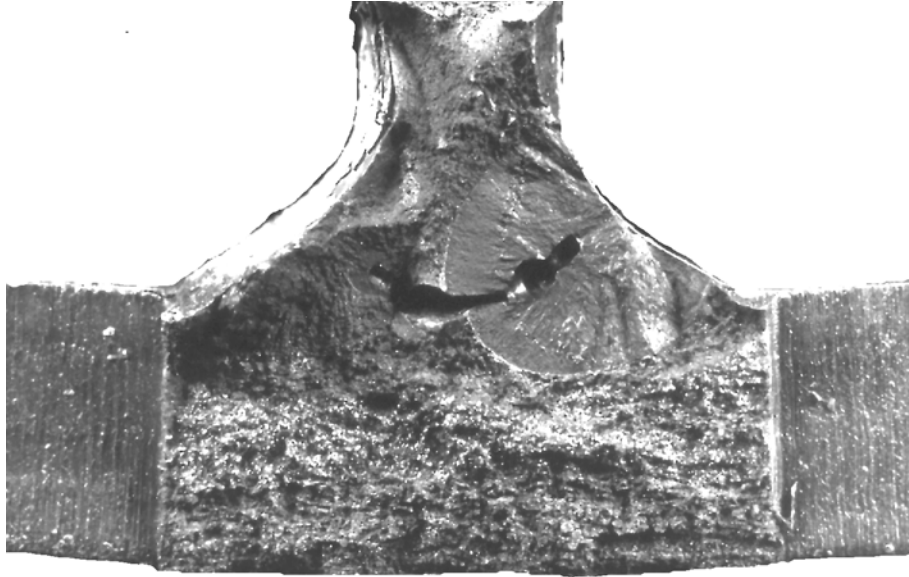


Figure 12 Fatigue Cracks Forming from Internal Porosity in Web-Flange Connection

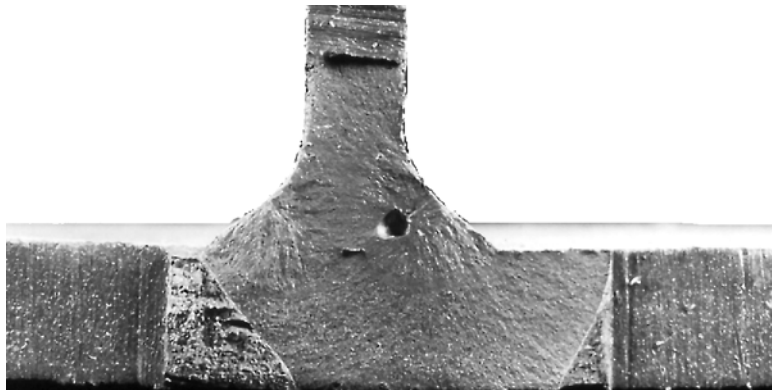
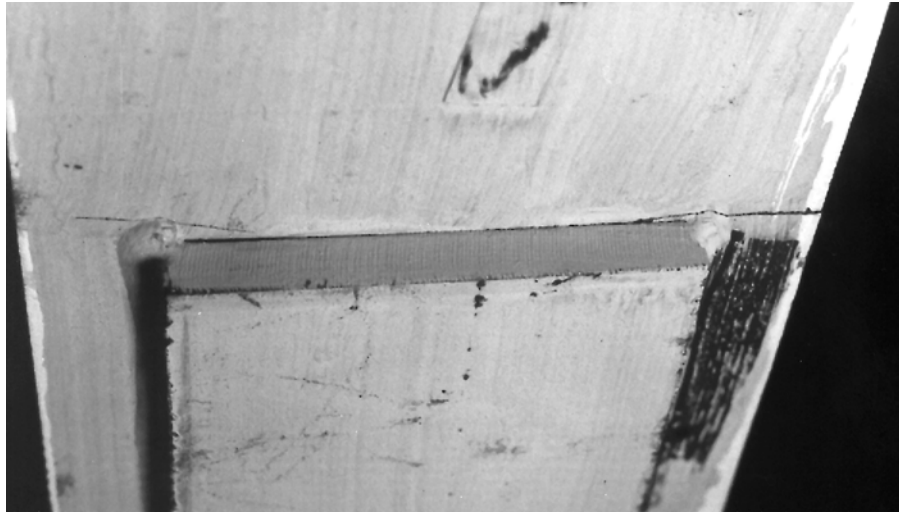
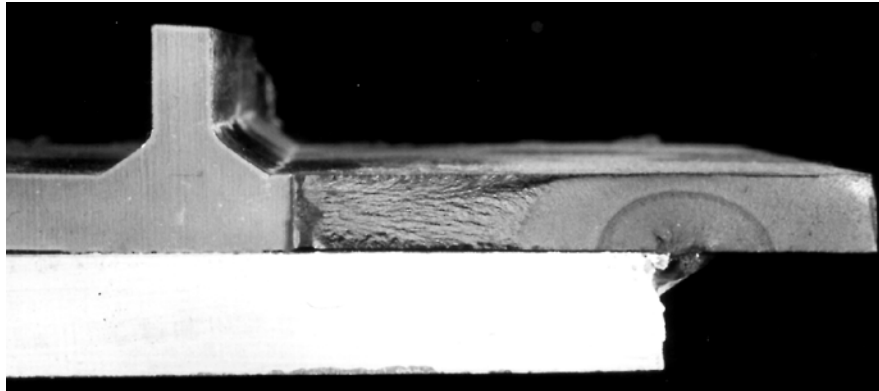


Figure 13 Fatigue Crack Enlarged to Three-Ended Crack From Internal Porosity

Attachments such as cover plates, gussets, stiffeners, and other components welded to a web or flange introduce a transverse weld periphery (toe), thus forming a line of elevated tension where fatigue cracking can start from small, sharp discontinuities. Figure 14 shows a fatigue crack that has formed at a cover plate fillet weld toe.



(a) Fatigue Crack at End of Cover Plate Fillet Weld Toe



(b) Crack Surface Showing Fatigue Crack Growth

Figure 14 Fatigue Cracking at Fillet Weld Toe

In some cases, a "defect" is an expected result of the type of fabrication process and has no effect on the life of the member. For instance, the partial penetration shown in Fig. 11 (which is also seen in the welded beam of Fig. 10) is a natural consequence of the fillet-welded connection: it is not expected that the two fillet welds will merge in the central region of the connection. Furthermore, since the crack represented by the lack of penetration is parallel to the direction of the (bending) stress field, a so-called Mode II crack (see Fig. 7), the crack will not open up under the application of stress and failure by fatigue is unlikely.

Consider a detail involving mechanical fasteners—an I-shaped beam with a cover plate fastened to the beam flange with bolts. The region between bolt lines could be described as a "flaw" or "crack," but, since the discontinuity is parallel to the stress field, the "crack" does not grow and therefore its presence does not affect the fatigue strength of the member.

The flaws that exist in all fabricated steel structures are a consequence of the manufacturing process of the steel itself and the normal fabrication processes. Flaws in rolled shapes arise from surface and edge imperfections, irregularities in mill scale, laminations, seams, inclusions, etc., and from mechanical notches due to handling, straightening, cutting, and shearing. In a rolled shape, fatigue crack growth can start from one of these sources. Comparatively, the "unaltered" rolled shape presents the most favorable fatigue life situation. However, there are not many practical cases in which a rolled shape does not have some kind of attachment, connection, or some other kind of alteration.

Mechanical details, in which holes are drilled or punched and forces are transferred by means of rivets or bolts, present a somewhat more severe fatigue life situation than the bare rolled shape. Drilled or sub-punched and reamed holes give some reduction in fatigue life as compared with an unaltered member, but the difference usually is not very great. If preloaded high-strength bolts are used, the disturbing effect of the hole is largely mitigated by the presence of the high local compressive stresses introduced by the bolt. Punched holes give a greater reduction in fatigue life than do drilled or sub-punched and reamed holes because of imperfections at the hole edge arising from the punching process. In this case, the crack usually starts at the edge of the hole.

Broadly speaking, any mechanical detail has a better fatigue life than does its equivalent welded detail. The types of flaws introduced when welding is used have already been discussed. In addition to the fact that more flaws will be present when welding is used, inspection for defects is more difficult than is the case when mechanically fastened details are used. Repairing defects in welded details is also difficult. Prohibiting the use of welded details in fatigue situations is not usually a practical option, however.

The task of the structural engineer is to be able to proportion those structural members that have a potential for failure by fatigue crack growth so that they have a sufficiently long life as compared with the design life of the structure. As will be seen, this will be done in the environment that some probability of failure must be accepted: in real terms, there is no structure that can be designed for zero probability of failure. The design will be carried out in the expectation that flaws will be present initially in all fabricated steel

structures and that all such members will contain residual stresses of relatively high magnitude. A concomitant feature is that in the design process it is possible to identify the size of flaws that are permissible and then to use this information as the basis for both initial inspection of the structure as well as on-going inspection. This latter feature is not yet well-developed in design specifications, and the usual procedure is to accept as permissible flaw sizes consistent with the specifications that accompany the fabrication processes, e.g., the welding specifications.

3.3 Basis for Design Rules

To those working in the research area, it was evident that the features that needed to be examined included the yield strength of the steel (reflected by the grade of steel), the number of cycles of load to which the member was subjected, some aspect of the stress itself, and the stress concentration present.

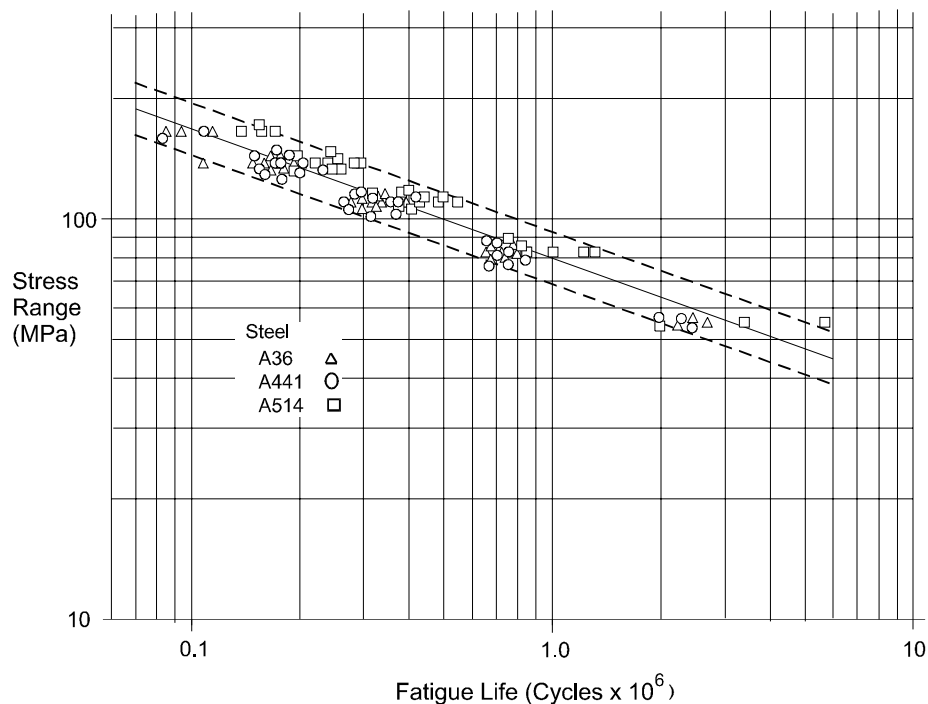


Figure 15 Effect of Grade of Steel on Fatigue Life of Beams with Transversely End-Welded Cover Plates

Figure 15 shows a plot of the stress feature versus the number of cycles to failure for a given detail (beams with transversely end-welded cover plates) for three different grades of steel. These particular steels represent the spectrum of steel strengths in use at the present time—from 250 to 690 MPa. Given that a certain amount of scatter is always present in results of this kind, it is evident that the yield strength of the steel does not have an important

influence on the results. Other information contained in this figure is significant and is typical of all fatigue strength tests results. First, the data plot as a straight line in this log-log representation. Second, the data are contained within a reasonably well-defined band about the mean. In Fig. 15, the dashed parallel lines plotted two standard deviations (measured relative to the horizontal axis) away from the mean line contain most of the test results. The degree of scatter in the results will have to be considered when a choice is made for a design life line. Customarily, this choice is made for the designer by the specification itself.

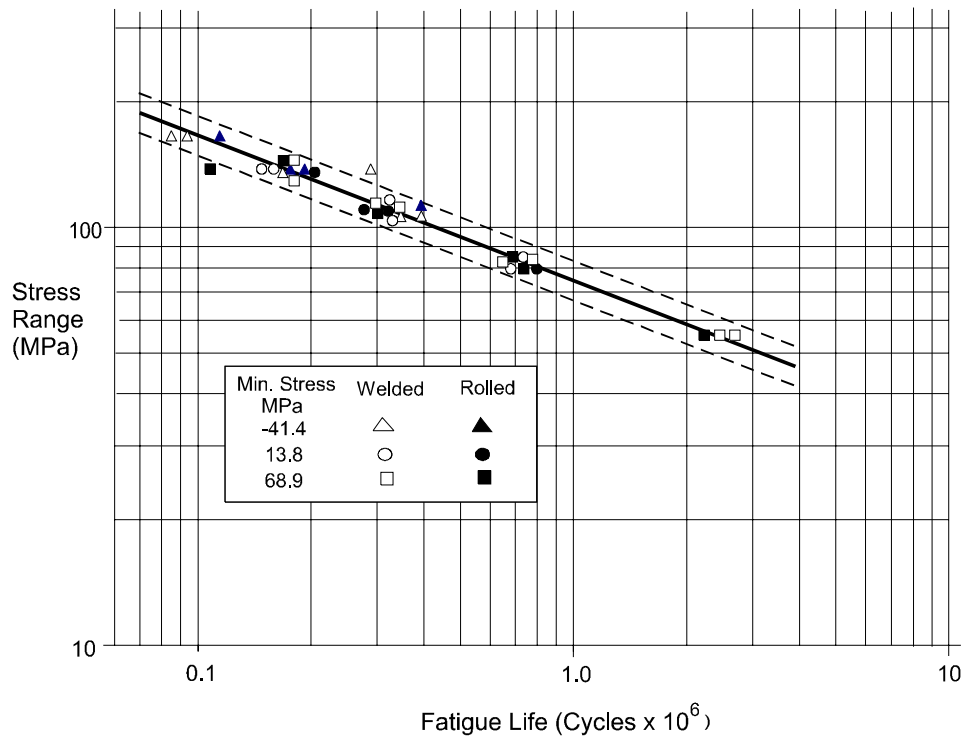


Figure 16 Effect of Stress Range and Minimum Stress on Fatigue Life for Welded End of Coverplated Beams

The way the stress feature should be represented is examined in the data contained in Fig. 16. Considering again the end-welded cover-plated beam (both as-rolled and three-plate welded beams are represented in Fig. 16, however), the effect of stress is introduced as the stress range, that is, the algebraic difference between the maximum stress and the minimum stress at the critical location ($\Delta\sigma_r = \sigma_{\max} - \sigma_{\min}$). The tests represented in Fig. 16 were done at values of minimum stress (σ_{\min}) equal to -41.4 MPa, 13.8 MPa, and 68.9 MPa, and, of course, a spectrum of stress range. Examine, for example, the data plotted for the stress range of 80 MPa. For this stress range, this means that the maximum stresses had to have been 38.6 MPa, 93.8 MPa, and 149 MPa, respectively, for the three values of minimum stress. It is obvious that the data are closely grouped and that the minimum stress *per se* does not

influence the results. As will be seen in Chapter 8, it is the presence of high levels of residual stress that dictates that stress range is the controlling stress parameter for a description of fatigue life, rather than maximum stress, minimum stress, or stress ratio (i.e., $\sigma_{\max}/\sigma_{\min}$).

In accordance with the ideas developed in Chapter 2, Basic Fracture Mechanics Concepts, it would be expected that stress intensity (K) should be represented in the fatigue life evaluation. For the usual level of design, this is not a practical solution, however, and a more expedient approach is taken. This is simply to arrange standard structural details into categories relative to their expected fatigue life. For example, illustrated in Fig. 17 are the fatigue life representations for two different categories—beams which have cover plates that include a weld across their ends and beams made up of three plates welded together, such as the beam illustrated by Fig. 10. Clearly, if the designer had one of the two types of members shown in Fig. 17, it would be possible to determine the fatigue life of that member.

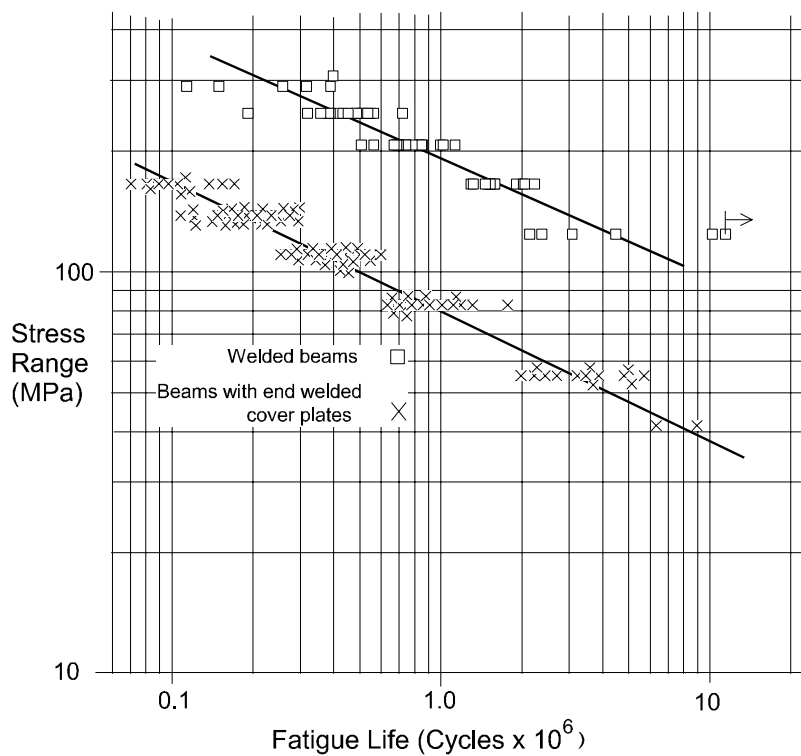


Figure 17 Fatigue Strength of Welded and Coverplated Beams

In summary, the fatigue life of a fabricated steel structure is determined by three factors. These are:

1. The number of cycles of loading to which the member is subjected;
2. the type of detail under examination; and
3. the stress range at the location of the detail.

It has been implicit in the discussion so far that the stresses, which are the driving force behind crack growth, are those corresponding to the loads on the structure. This is indeed an important case, and for this situation the stress range to be calculated is simply that corresponding to the nominal stress at the location of the detail. This is valid because selection of the detail itself implies inclusion of the stress concentration for that detail. There is another source of stresses in the structure that can produce crack growth, however. This is the stresses (really, strains) that are produced as a result of displacements. Displacement-induced fatigue cracking is at least as important as load-induced fatigue cracking, and it will be discussed in a separate section (Chapter 6).

3.4 Design Rules Given by the AASHTO Specification

The basis of the fatigue life rules given in all codes, standards, or specifications for the design of fabricated steel structures has been given in the preceding sections of this Chapter. Further elaboration will be required on a number of points, but it is appropriate to introduce next the rules given by one of the most-widely used standards, that of the American Association of State Highway and Transportation Officials (AASHTO)[2]. In this section, the fundamentals of the AASHTO rules will be introduced. The subject is more completely discussed in Chapter 5.

As in most contemporary standards, the AASHTO fatigue life rules reflect the two issues—fatigue cracking induced by stress and fatigue cracking induced by displacements within the structural system. Only the first has been explained so far, and the discussion in this section will continue to be limited to load-induced fatigue cracking. Displacement-induced fatigue cracking is presented in Chapter 6.

Figure 18 shows the fatigue life curves given in the AASHTO Specification. The plot shows stress range on the vertical axis and number of cycles on the horizontal axis for seven different Detail Categories. Both axes are logarithmic representations. Over some portion of the range, each Detail Category is a sloping straight line with a slope constant m equal to 3. Beyond a certain point, which depends on the Detail Category, the fatigue life line is horizontal. This feature will be discussed subsequently.

The information in Fig. 18 must be used in conjunction with information like that shown in Table 1 and Fig. 19, which give only a small portion of the relevant material in the AASHTO Specification.

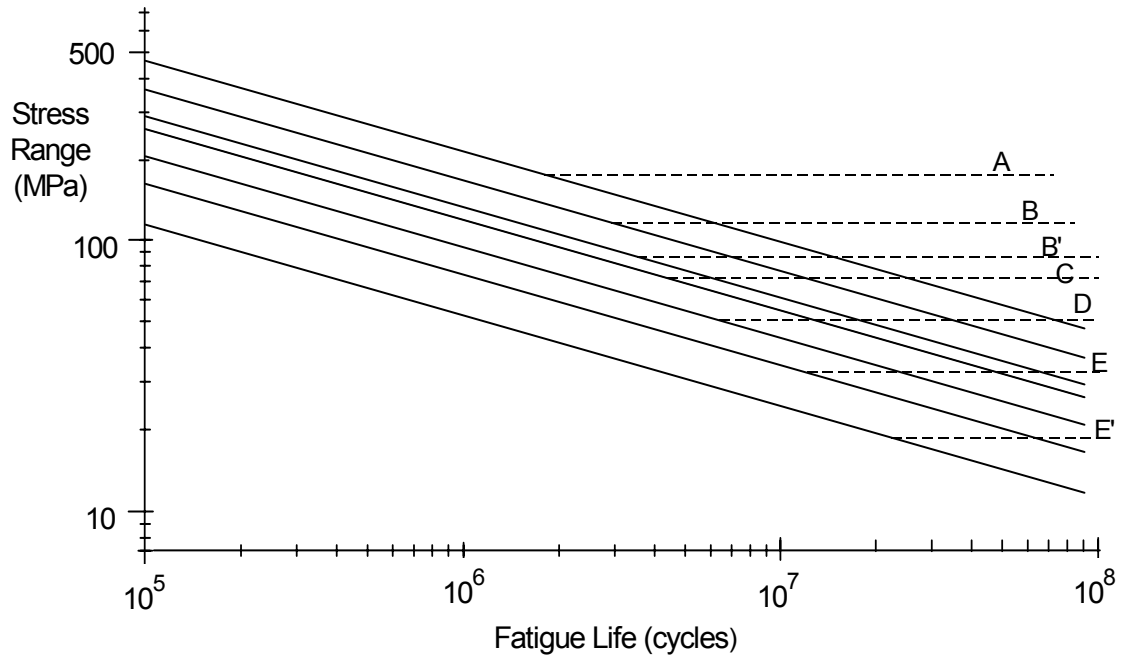


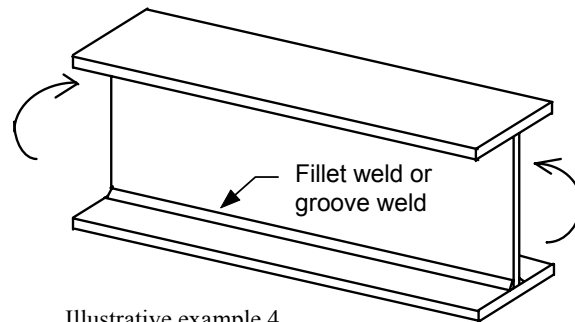
Figure 18 Fatigue Life According to the AASHTO Specification

General Condition	Situation	Detail Category	Illustrative Example (see Fig. 16 AASHTO)
Built-up Members	Base metal and weld metal in component, without attachments, connected by:		3, 4, 5, 7
	• continuous full penetration groove welds with backing bars removed, or	B	
	• continuous fillet welds parallel to the direction of applied stress	B	
	• continuous full-penetration groove welds with backing bars in place, or	B'	
	• continuous partial-penetration groove welds parallel to the direction of applied stress.	B'	
	etc.		
	etc.		

Table 1 Example of Fatigue Categories used in the AASHTO Specification

Table 1 must be used in conjunction with the type of information shown in Fig. 19, where one of the relatively large number of typical construction details classified by the specification is shown. Application of the information is straightforward. For example, suppose a designer proposes to use a beam made by joining three plates using continuous fillet welds parallel to the direction of stress, such as was shown in Fig. 10. According to Table 1 and Fig. 19, this is Detail Category B. If the number of cycles to which the beam will be subjected is, say, 2×10^6 , then the permissible range of stress for this detail is 120 MPa. This number was obtained using Fig. 18 to estimate the stress range corresponding to 2×10^6 cycles. Working out the equation of the line for this detail category, the "exact" value of the permissible stress range at 2×10^6 cycles is 125 MPa. As will be seen later, the AASHTO Specification provides information that allows the calculation of the permissible stress range corresponding to a given number of cycles.

The fatigue strength curves presented in the AASHTO Specification (Fig. 18) are those corresponding to the mean life of a detail, usually as obtained by physical testing, shifted horizontally to the left by two standard deviations. For reasonably large numbers of test data, the



Illustrative example 4 (refer to Table 1)

Figure 19 Illustrative Example for Table 1

corresponding confidence limit is estimated to be approximately 95%.

EXAMPLE 2

The overhead crane in a small manufacturing operation uses a simply-supported crane girder of 8 m span. The section used for the girder is to be made by fillet-welding three plates into an I-shape. The fillet welds will be continuous. The flange plates are 350 mm wide by 22 mm thick and the web plate is 306 mm by 14 mm. The moment of inertia of this section is $448 \times 10^6 \text{ mm}^4$. The main use of the crane will be to transport a 300 kN ladle from one end of the shop to the other. The crane travels in such a position that the crane girder receives a maximum 80% of the total load as a reactive force. It can be assumed that this force comes onto the girder as a single concentrated load. Information from the owner is that the crane will make no more than two trips per hour at this load level, this will be the only significant load, the work schedule will not exceed 10 hours per day five days per week, and the design life of the building is 40 years.

Is the fatigue life of this crane girder satisfactory? Use the AASHTO Specification.

Solution:

1. Number of stress cycles (equals number of load cycles, in this case) –

$$N = (2 \text{ cycles/hr.}) (10 \text{ hr./day}) (5 \text{ days/wk.}) (52 \text{ wk./yr.}) (40 \text{ yr.}) = 208\,000 \text{ cycles.}$$

2. Detail classification – According to the AASHTO Specification, this is Detail Category B.

From Fig. 18, read the Detail Category B line at $N = 208\,000$ cycles to find that the permissible stress range is approximately 300 MPa.

3. Calculate actual stress range –

$$\sigma_{\min} = 0$$

$$\sigma_{\max} \quad M = PL/4 = (300 \times 10^3 \text{ N} \times 0.8) (8\,000 \text{ mm})/4 = 480 \times 10^6 \text{ N mm}$$

$$\therefore \sigma_{\max} = M y / I = (480 \times 10^6 \text{ N mm}) (175 \text{ mm}) / (448 \times 10^6 \text{ mm}^4) = 188 \text{ MPa}$$

$$\text{Thus, } \Delta\sigma_r = 188 - 0 = 188 \text{ MPa.}$$

Since the actual range of stress (188 MPa) is less than the permissible range of stress for this detail (300 MPa), the situation is satisfactory.

Comments:

1. The number of stress cycles is not always equal to the number of load cycles. Designers should be alert for cases where a single passage of load produces more than one stress cycle, as could occur, for example, when a multiple axle vehicle traverses a member or when continuous beams are used.
2. Since stress due to dead load is always present in the member, the change in stress ($\Delta\sigma_r$) is always simply equal to the change in stress produced by the moving (i.e., live) loads.
3. Another way of looking at the problem is to compare the number of cycles that would be permitted at the actual stress range of 188 MPa with the number of cycles that actually occur. In this example, the number of cycles permitted by the AASHTO Specification for a stress range $\Delta\sigma_r = 188$ MPa is $N = 600\,000$ cycles, obtained from Fig. 18 or calculated as will be shown in Section 3.5.

3.5 Fracture Mechanics Analysis of Fatigue

In Chapter 2, *Basic Fracture Mechanics Concepts*, it was put forward that brittle fracture and fatigue are crack growth phenomenon that are characterized by the same parameter, K . As such, it should be possible to use the fracture mechanics method of analysis to deal with the fatigue strength problem.

The crack growth law was identified in Section 2.3 as

$$\frac{da}{dN} = A \Delta K^m \quad (6)$$

where a = crack length

N = number of cycles

A, m = numerical constants determined from regression analysis of test data

ΔK = change in stress intensity factor corresponding to a given change in stress range. In Section 2.3, this was also written (Eq. 5) as

$$\Delta K = W Y \Delta\sigma \sqrt{\pi a} \quad (5)$$

Integration of Eq. 6 gave the following expression for crack growth propagation (see also Section 2.3):

$$N = \frac{1}{A} \int_{a_i}^{a_f} \frac{1}{\Delta K^m} da \quad (7)$$

where a_i and a_f are the initial and final crack length, respectively. Making the substitution for ΔK , this becomes:

$$\begin{aligned} N &= \frac{1}{A} \int_{a_i}^{a_f} \frac{1}{\left[W Y \Delta \sigma \sqrt{\pi} \sqrt{a} \right]^m} da \\ &= \frac{1}{A} \Delta \sigma^{-m} (\sqrt{\pi})^{-m} \int_{a_i}^{a_f} \frac{1}{(W Y \sqrt{a})^m} da \end{aligned}$$

The terms $1/A$ and $(\sqrt{\pi})^{-m}$ are constants. Since the final crack size is always very large as compared to the initial crack size, any term appearing with the limit a_f can be neglected since the limit will appear with a negative power. The terms W and Y vary with the crack length, and of course the term \sqrt{a} also contains the crack length. However, for a given geometry and starting crack size, the term within the integral is also a constant. Designating the product of all of the constant terms as M and using the more common notation $\Delta \sigma_r$ instead of $\Delta \sigma$, the result can be written finally as

$$N = M \Delta \sigma_r^{-m} \quad (8)$$

or, alternatively, as

$$\log N = \log M - m \log \Delta \sigma_r \quad (9)$$

Equation 9 defines a sloping straight line on a plot of log stress range versus log number of cycles. This is precisely what is observed in the physical tests. See, for example, Figures 15, 16, and 17.

The AASHTO Specification provides values of the constant M in Eq. 8 for each fatigue category. These values, termed "A" in the AASHTO Specification, are listed in Table 2 for each fatigue Detail Category. Also shown in the table are the values of the stress range that identifies the horizontal portion of each curve, the so-called threshold stress. The AASHTO Specification uses $m = 3$ for all fatigue categories.

Application of Eq. 8 and 9 can be made in Example 2. In step 2 of the Solution, the permissible stress range for $N = 208\,000$ cycles for this Detail Category B now is calculated according to Eq. 8 as

$$\Delta \sigma_r = \left(\frac{M}{N} \right)^{1/3} = \left(\frac{39.3 \times 10^{11}}{208\,000} \right)^{1/3} = 266 \text{ MPa}$$

The value of M (39.3×10^{11}) was obtained from Table 2, where it is listed according to the Specification notation as "A." It should be obvious that it is much more expeditious to calculate values of fatigue life or permissible stress range than to try to read them from a log-log plot (Fig. 18).

In Comment 3 of Example 2, the number of cycles permitted for $\Delta\sigma_r = 188$ MPa had been estimated using Fig. 18 as 600 000. It now can be calculated (Eq. 8) as

$$N = M \Delta\sigma^{-3} = (39.3 \times 10^{11}) (188)^{-3} = 591\,000 \text{ cycles}$$

Table 2 Constants for use with Figure 18

Detail Category	Constant, A (MPa) ³	Threshold Stress (MPa)
A	82.0×10^{11}	165
B	39.3×10^{11}	110
B'	20.0×10^{11}	82.7
C	14.4×10^{11}	69.0
C'	14.4×10^{11}	82.7
D	7.21×10^{11}	48.3
E	3.61×10^{11}	31.0
E'	1.28×10^{11}	17.9

EXAMPLE 3

The beam whose failure surface is illustrated in Fig. 10 was one of a series of nine tested [22]. Using the test data¹, the regression line expressing the relationship between fatigue life and stress range was determined to be $\log N = 12.32 - 2.73 \log \Delta\sigma_r$. The flaws from which the cracks initiated were generally circular and the measured average size was 1.346 mm. Use fracture mechanics analysis to verify the experimentally obtained regression line.

¹ All the source data in this problem were expressed using U.S. Customary units. The necessary conversions have been made.

Solution:

It has been noted that the final size of the crack will not be influential in the result of Eq. 7. This means that the stress intensity modifiers W and Y in Eq. 5 can be taken as a constant. Calling the product $WY = C$, and substituting for ΔK in Eq. 7 gives

$$\begin{aligned} N &= \frac{1}{A} C^{-m} \Delta\sigma_r^{-m} \int_{a_i}^{a_f} a^{-m/2} da \\ &= \frac{1}{A} C^{-m} \Delta\sigma_r^{-m} \left. \frac{a^{1-m/2}}{1-m/2} \right|_{a_i}^{a_f} \end{aligned}$$

Calling $m/2 - 1 = q$, this can be written as

$$N = \frac{1}{A} C^{-m} \Delta\sigma_r^{-m} \frac{1}{q} \left(a_i^{-q} - a_f^{-q} \right)$$

Since the final crack size is always very large as compared with the initial crack size, the term a_f can be neglected because it appears with a negative power in this equation. Thus, the crack propagation equation can be further simplified to

$$N = \frac{1}{A} C^{-m} \Delta\sigma_r^{-m} \frac{1}{q} a_i^{-q}$$

Rolfe and Barsom [8] suggest that the constant of proportionality, A, in the crack growth equation (Eq. 6) can be taken as 2.18×10^{-13} for ferrite-pearlite steels. They also suggest the value of C in the stress intensity factor expression can be taken as $2.0/\sqrt{\pi}$ for a circular crack in a plate of infinite width, and that the term m can be taken as 3, i.e., $q = (m/2) - 1 = 0.5$. The combined multipliers of $\Delta\sigma_r$ are the term M in Eq. 8, and we can now solve for this value. Using the alternative form, Eq. 9, we solve for log M as –

$$\begin{aligned} \log M &= \log \left[\frac{1}{A} C^{-m} \frac{1}{q} a_i^{-q} \right] \\ &= \log \left[\frac{1}{2.13 \times 10^{-13}} \left(\frac{2}{\sqrt{\pi}} \right)^{-3} \frac{1}{0.5} (1.346)^{-0.5} \right] = 12.74 \end{aligned}$$

Thus, the equation of the fatigue strength line as obtained using the experimental data and a fracture mechanics analysis is

$$\log N = 12.74 - 3 \log \Delta\sigma_f$$

This is in good agreement with the fatigue strength line obtained from the experimental data exclusively, $\log N = 12.32 - 2.73 \log \Delta\sigma_f$.

Comments:

Obviously, this type of exercise is not directly useful to a designer since it requires knowledge of the type and size of flaw that is likely to result in fatigue crack growth and failure. However, the results of this analysis and others like it do identify that the behaviour observed in the laboratory can be substantiated by an analytical prediction—the fracture mechanics analysis. It gives confidence in the prediction of cases not tested experimentally when those predictions are based on presumption of reasonable starting flaw sizes and shapes.

Chapter 4. Fatigue Assessment Procedures for Variable Stress Ranges

In all of the discussion so far, it has been implicitly assumed that the stress range at the detail under investigation is unique and that counting or predicting the number of cycles is straightforward. As might be anticipated, things are not simple in either of these categories: fatigue loading is usually quite complex. The designer has to deal with the reality that stress ranges of different magnitude take place at the detail and that these stress ranges are applied for varying numbers of cycles. Methods for dealing with these problems are outlined in this Chapter.

4.1 Cumulative Fatigue Damage

In this section, a method is presented that accounts for the damage that results when fatigue loading is not applied at a constant harmonic amplitude. Although both linear and non-linear damage theories are available, the one that is customarily used in civil engineering practice is a linear theory that is easy to understand and apply and which gives satisfactory results. This is the linear damage rule first proposed by Palmgren in 1924 and further developed by Miner in 1945 [23]. It is known as the Palmgren-Miner rule, and it assumes simply that the damage fraction that results from any particular stress range level is a linear function of the number of cycles that takes place at the stress range. The total damage from all stress range levels that are applied to the detail is, of course, the sum of all such occurrences. This can be written in equation form as:

$$\sum \frac{n_i}{N_i} = 1 \quad (10)$$

where n_i = number of cycles that take place at stress range level i

N_i = number of cycles that would cause failure at stress range level i .

The rule is obviously very simple. It has two major shortcomings [23]: it does not consider sequence effects and it is independent of the average stress in the cycle. To at least some degree, both of these factors are not consistent with observed behavior. However, when residual stresses are high and when plasticity is restricted (usually the case in structural engineering applications), it is known that these factors have only a small influence. Moreover, the approach gives reasonable correlation with test data and it has the considerable advantage that it is easy to use. The AASHTO Specification [2] advises that the Palmgren-Miner rule can be used to account for cumulative damage. It should also be noted that the term "failure" in these definitions is not intended to be taken literally. It is to be

interpreted as the permissible fatigue life, that is, the value represented by the mean life less two standard deviations on the log stress range vs. log number of cycles plot.

EXAMPLE 4

The beam of Example 2 was designed, fabricated, and erected when the owner decided that, in addition to the loads that had already been stipulated, it will be necessary for the crane to be able to accommodate one trip per hour at a load level of 350 kN. (See Example 2 for all other details.) Is the fatigue life of this crane girder still satisfactory? Use the AASHTO Specification.

Solution:

1. According to Example 2, the number of cycles at the old load level was 208 000 ($= n_1$)
2. According to Example 2, the number of cycles to failure at the old load level was 588 000 ($= N_1$)

3. Number of cycles at the new load level is –

$$N = (1 \text{ cycle/hr.}) (10 \text{ hr./day}) (5 \text{ days/week}) (52 \text{ weeks/yr.}) (40 \text{ yr.}) \\ = 104\,000 \text{ cycles } (= n_2).$$

4. Number of cycles to failure at the new load level –

In Example 2, the stress range under the 300 kN loading was found to be 188 MPa. The stress range for the 350 kN load can be calculated by proportion as $(350/300) (188 \text{ MPa}) = 219 \text{ MPa}$.

The detail that is under examination, the built-up beam composed of three plates joined by continuous fillet welds, is a Category B detail according to the AASHTO specification. Recalling that the AASHTO designation A of Table 2 is equivalent to the constant M in Eq. 8, this means that the value of this constant is 39.3×10^{11} . Thus, in Eq. 8, using $m = 3$ this becomes:

$$N = M \Delta\sigma^{-3}$$

$$N = (39.3 \times 10^{11}) (219)^{-3} = 374\,162 \text{ cycles } (= N_2)$$

Finally, checking Eq. 10:

$$\sum \frac{n_i}{N_i} = 1 \text{ or,}$$

$$\frac{n_1}{N_1} + \frac{n_2}{N_2} = \frac{208\,000}{588\,000} + \frac{104\,000}{374\,162} = 0.35 + 0.28 = 0.63$$

Since the total effect ("damage") of the two different stress ranges is less than 1.0, the crane girder is still satisfactory under the new loading condition.

It is often convenient to express the Miner-Palmgren cumulative fatigue damage rule (Eq. 10) in terms of an equivalent stress range. We wish to calculate an equivalent constant amplitude stress range, $\Delta\sigma_e$, that will display the same amount of damage as actually produced by the variable amplitude stress ranges. Thus, using the Palmgren-Miner statement of damage (Eq. 10), it is required that

$$\sum \frac{n_i}{N_i} = \frac{\sum n_i}{N_e} \quad (11)$$

In Eq. 11, the left hand side represents the damage under the variable amplitude stress cycles, for which the terms were defined under Eq. 10. The right hand side expresses the damage under the constant amplitude equivalent stress range, i.e., $\Delta\sigma_e$. Each of N_i and N_e correspond to the number of cycles to failure—one for the variable amplitude stress ranges and the other for the equivalent, constant amplitude, stress range.

Equation 8, which expressed the failure condition in a general way, can now be applied to Eq. 11. Thus, $N_i = M \Delta\sigma_i^{-m}$ applies to the left hand side of Eq. 11 and $N_e = M \Delta\sigma_e^{-m}$ applies to the right hand side. Making the substitutions—

$$\sum \frac{n_i}{M \Delta\sigma_i^{-m}} = \frac{\sum n_i}{M \Delta\sigma_e^{-m}}$$

The term M is a constant and can be eliminated from the equation. Then, solving for the equivalent stress range

$$\Delta\sigma_e^m = \sum \frac{n_i \Delta\sigma_i^m}{\sum n_i} \quad (12)$$

Calling $n_i/\sum n_i = \gamma_i$, that is, γ_i is the fraction that any particular portion of the stress range is of the total number of cycles, then Eq. 12 is written as

$$\Delta\sigma_e^m = \sum \gamma_i \Delta\sigma_i^m$$

Finally, solving for the equivalent stress range, we have

$$\Delta\sigma_e = \left[\sum \gamma_i \Delta\sigma_i^m \right]^{1/m} \quad (13)$$

In some specifications, for example the rules provided by the American Railway Engineering Association (AREA) [24], the equivalent stress range (S_{Re}) is written as

$$S_{Re} = \left[\sum \gamma_i S_{Ri}^3 \right]^{1/3} \quad (14)$$

where the symbol S_{Ri} is used to indicate the stress range, $\Delta\sigma_i$. It should be clear by inspection that Equation 14 is identical to Eq. 13, given that $m = 3$.

EXAMPLE 5

Use the equivalent stress method to determine the percentage of life that has been expended by the loading applied to the beam of Example 4.

Solution:

All of the necessary data are available in the solutions to Examples 2 and 4. In summary, these are –

$$n_1 = 208\,000 \text{ cycles}$$

$$n_2 = 104\,000 \text{ cycles}$$

$$\Delta\sigma_1 = 188 \text{ MPa}$$

$$\Delta\sigma_2 = 219 \text{ MPa}$$

$$N = 208\,000 + 104\,000 = 312\,000 \text{ cycles, and}$$

$$\gamma_1 = \frac{208\,000}{312\,000} = 0.67 \quad \gamma_2 = \frac{104\,000}{312\,000} = 0.33$$

Now, using the expression given by Eq. 14 to calculate the equivalent stress range –

$$S_{re} = S_{rMiner} = \left[\sum \gamma_i S_{Ri}^3 \right]^{1/3} = \left[(0.67 \times 188^3) + (0.33 \times 219^3) \right]^{1/3} = 199.5 \text{ MPa}$$

For this Detail Category B and the equivalent stress range of 199.5 MPa, the number of cycles to failure can be calculated (Eq. 8) as –

$$N = M \Delta\sigma^{-3} = (39.3 \times 10^{11} \times 199.5^{-3}) = 494\,953 \text{ cycles}$$

Since the actual number of cycles is 312 000, the percentage of life expended is $(312\,000/494\,953) 100\% = 63.0\%$.

Comments:

The same result was also seen in the solution to Example 4, where the Miner's summation was 0.63. Whether the solution proceeds by the method shown in Example 4 (Miner's summation) or by that shown in Example 5 (equivalent stress range method) is simply a matter of choice.

EXAMPLE 6

A stress range histogram has been obtained from field measurement of stresses on a certain simple-span girder bridge. This was obtained from a sample of 2064 truck crossing events. The total truck traffic that is estimated to have taken place since the opening of the bridge is 35×10^6 cycles. It can be assumed that each passage of a truck causes one stress range at any given detail. (This information is taken from Reference [25]).

The critical detail on this bridge, and the one for which the stress history is given, is that at the end of a partial length coverplate. The thickness of the flange of the girder is 25 mm and the coverplate is attached to the girder flange by fillet welds.

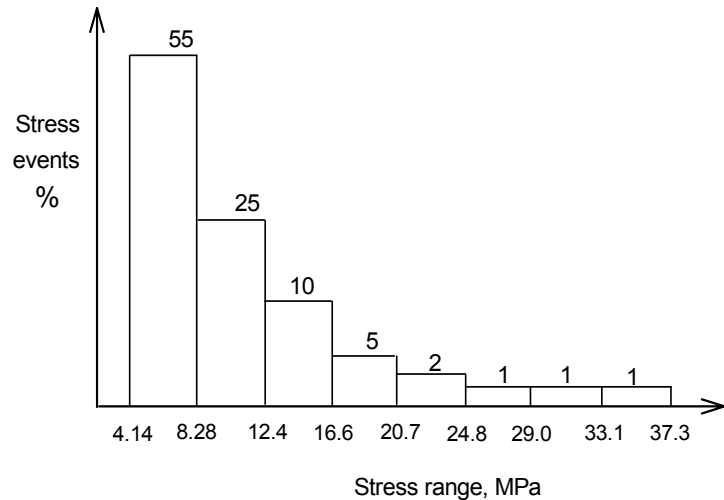


Figure 20 Example 6

a) Is fatigue cracking possible at this detail?

b) Calculate how much of the fatigue life of this detail has been used up. Use each of the two possible approaches (i.e., direct application of the Miner summation and use of a calculated equivalent stress range).

Use the AASHTO Specification in the solution of this problem.

Solution:

According to the AASHTO specification, this is a Detail Category E' (Consult the specification: this information is not contained within this document.)

(a) According to Fig. 20, the maximum stress range recorded is 37.3 MPa. The threshold stress for an E' detail is 17.9 MPa, which can be read from Fig. 18 or obtained directly from Table 2. Since the actual stress is greater than the minimum stress above which crack growth is possible, this indicates that fatigue cracking is possible in this girder.

(b) In order to calculate the fatigue life expended, it is suggested that the average stress in each range be used.

The results of the calculations necessary to determine the remaining fatigue life are given in Table 3. Sample calculations for the first row are shown following the table.

Table 3 Example 6

$\Delta\sigma_i$ average MPa	n_i cycles x 10^6	N_i cycles x 10^6	$\frac{n_i}{N_i}$	$\gamma_i = \frac{n_i}{35 \times 10^6}$	$\gamma_i \Delta\sigma_i^3$
6.21	19.25	534	0.04	0.55	131.7
10.3	8.75	117	0.07	0.25	273.2
14.5	3.5	42.0	0.08	0.10	304.9
18.6	1.75	19.9	0.09	0.05	321.7
22.7	0.70	10.9	0.06	0.02	233.9
26.9	0.35	6.57	0.05	0.01	194.6
31.0	0.35	4.30	0.08	0.01	297.9
35.2	0.35	2.93	0.12	0.01	436.1

$$\sum \frac{n_i}{N_i} = 0.60 \qquad \sum \gamma_i \Delta\sigma_i^3 = 2194$$

Sample calculations for the first four items of Row 1 of the Table:

$$\Delta\sigma_1 = (4.14 + 8.28) / 2 = 6.21 \text{ MPa} \quad (\text{Refer to the stresses given in Fig. 20})$$

$$n_1 = (55\%) (35 \times 10^6 \text{ cycles}) = 19.25 \times 10^6 \text{ cycles}$$

$$N_1 = M \Delta\sigma_r^{-3} \quad (\text{Eq. 8})$$

$$= (1.28 \times 10^{11}) (6.21)^{-3} = 534 \times 10^6 \text{ cycles} \quad (M \equiv A \text{ from Table 2})$$

$$\frac{n_1}{N_1} = \frac{19.25}{535} = 0.04$$

Since the Miner summation for all the events in this loading history is 0.60, this means that 60% of the fatigue life of this detail has been expended.

Now, determine the fatigue life expended by calculating an equivalent stress range. The information necessary for substitution into Eq. 13 has been generated in the last two columns of Table 3 and recall also that $\sum n_i = 35 \times 10^6$ cycles in this example.

$$\Delta\sigma_e = \left[\sum \gamma_i \Delta\sigma_i^m \right]^{1/m} \quad (\text{Eq. 13})$$

$$= (2194)^{1/3} = 13.0 \text{ MPa}$$

Next, calculate the number of cycles that can be sustained by a Detail Category E' for an equivalent stress range of 13.0 MPa. Using Eq. 8, and where we will substitute $\Delta\sigma_e = 13.0$ MPa for the term $\Delta\sigma_r$:

$$N = M \Delta\sigma_r^{-3}$$

$$= (1.28 \times 10^{11}) (13.0)^{-3} = 58.3 \times 10^6 \text{ cycles}$$

Since the number of cycles that can be sustained by the Category E' detail is 58.3×10^6 cycles and the actual number of cycles is 35×10^6 cycles, the fatigue life expended is $35.0/58.3 = 0.60$. This is the same as the value calculated using the Miner summation.

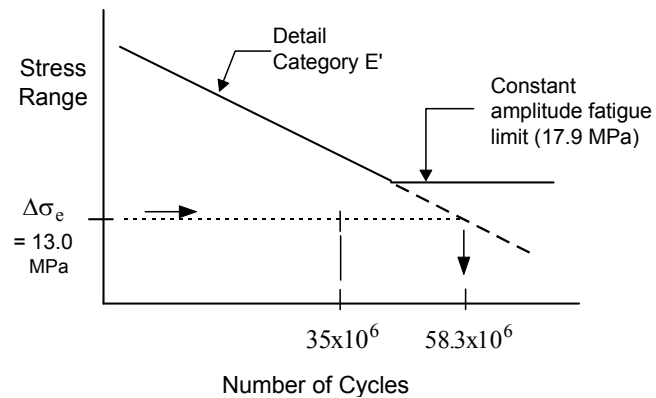


Figure 21 Example 6

Comments:

Figure 21 displays the equivalent stress range calculation graphically. Note that in this example the equivalent stress range falls below the constant amplitude fatigue limit. The calculation proceeds on the basis that all cycles are damaging, that is, the extension of the sloping fatigue life line is used. There is a discussion of this issue in Section 4.3.

4.2 Analysis of Stress Histories

Situations often arise where the applied loads create stress levels and stress counts (number of cycles at a given stress level) that are much more complicated than those given in Example 4. For example, if the crane in Example 4 is carried by a continuous beam over

several intermediate supports, more than one stress cycle is applied per trip at a given location. This results because loading adjacent spans causes stress cycles in addition to the cycle created when the crane passes directly over the location under examination. For this more general case, one trip is termed a loading event and the stress variation at a given point in the structure during such an event is called a stress history.

Very complicated stress histories can be caused by loading events such as the passage of a truck over a bridge or a wave hitting an offshore oil platform. Furthermore, the occurrence of a loading event brings about different stresses within different elements in a structure, and, in addition, the number of cycles per loading event may be related to the type and location of the element under consideration. Many different stress histories may need to be evaluated for a complete fatigue assessment of a complex structure.

In fields other than civil engineering, elaborate stress measurements are often taken on actual structures subjected to service loading in order to overcome uncertainties associated with calculated values of stresses in elements. However, it is rare that such measurements are carried out on civil engineering structures, usually because of the cost. Consequently, civil engineers generally resort to stress analysis using load models and dynamic magnification factors that are provided in codes and standards.

Figure 22 shows the stress history at a certain location in a member as a moving load passes across a structure. Shown are the maximum live load stress, the minimum live load stress, and the dead load stress. In any trace of stress versus time there is one absolute maximum live load stress and one absolute minimum live load stress, of course. The stress range between these two extremes is shown on the figure. (It is noteworthy that the stress range is independent of the dead load stress, and it has already been indicated (Section 3.3) that stress range is the dominant stress-related feature of fatigue life determination.) However, there can be other "local" maximum and minimum live load stresses. The question is, how is the element under examination for fatigue life influenced by these other stress excursions?

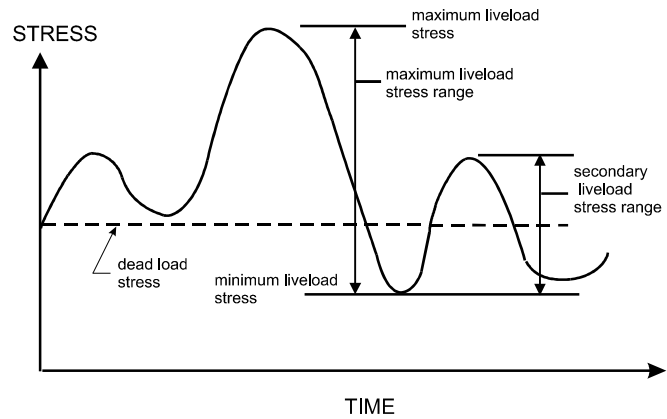


Figure 22 Typical Stress vs. Time Variation Under a Moving Load

One method of interpreting the type of stress history shown in Fig. 22 is to simply use the maximum live load stress range shown in the figure. However, as the "minor" stress ranges increase in value, their influence becomes important at some point. Methods that are used for counting stress ranges include the reservoir method, the rainflow method, the peak count, and the mean-crossing peak count method. The reservoir and rainflow methods are the ones most commonly used in civil engineering applications [26, 27]. Generally, rainflow counting is more suited to computer analyses of long stress histories, whereas the reservoir method is most convenient for graphical analyses of short histories. The results obtained by these two methods are the same.

The plot shown in Fig. 23 (a) is an example of stress variation in an element subjected to a loading event. Typically, simple analyses result in stress histories having fewer peaks than shown in this figure, whereas actual stress measurements usually reveal more

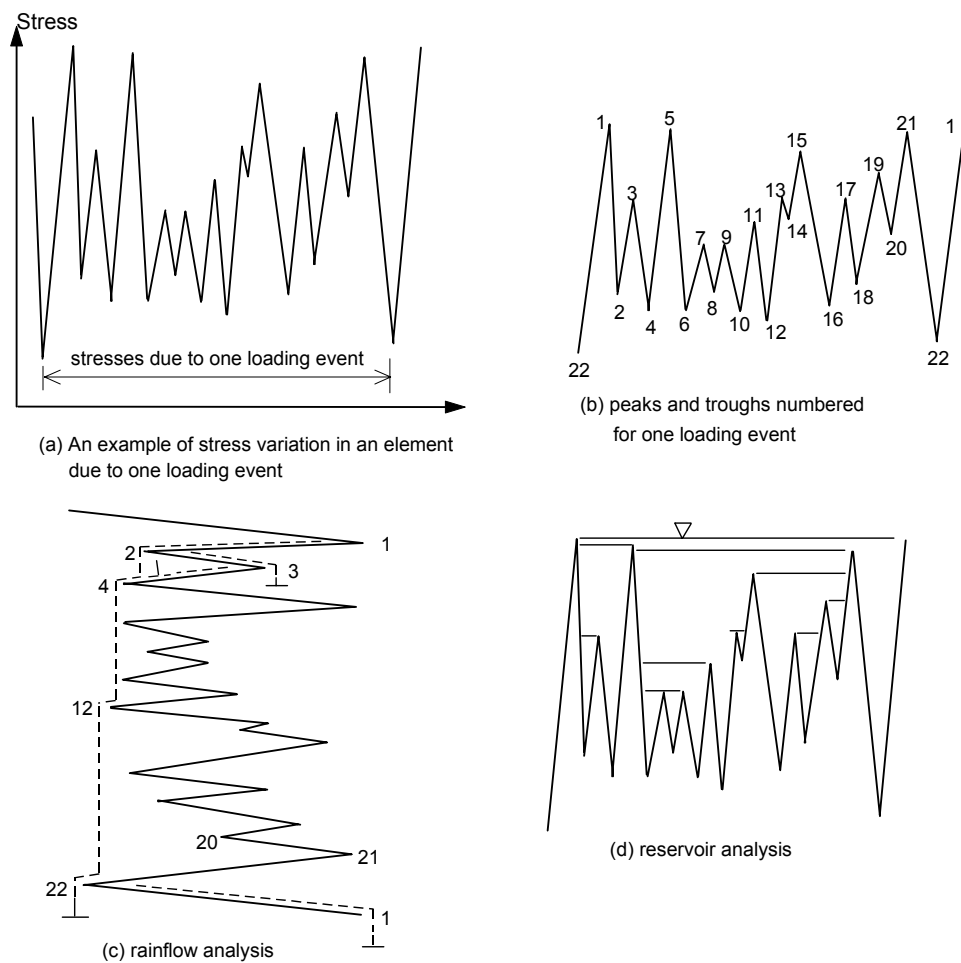


Figure 23 Analysis of Stress Histories

complex stress histories.

The information shown in Fig. 23 (a) cannot be used directly in the Palmgren-Miner rule, Eq. 10, without application of a stress counting method in order to tabulate values for the number of cycles, n_j , for different stress range levels. As already indicated, the most widely used are the so-called rainflow counting method and the reservoir methods. Peaks and troughs for one loading event are numbered in Fig. 23 (b) and this history is rotated 90 degrees in Fig. 23 (c) in order to perform the rainflow analysis.

The rainflow method is named for its analogy of rain drops flowing down a pagoda roof. The following rules apply to rainflow counting:

1. A drop flows left from the upper side of a peak or right from the upper side of a trough and onto subsequent "roofs" unless the surface receiving the drop is formed by a peak that is more positive for left flow or a trough that is more negative for right flow. For example, a drop flows left from point 1 off points 2, 4 and 12 until it stops at the end of the loading event at point 22 since no peak is encountered that is more positive than point 1. On the other hand, a drop flows right from point 2 off point 3 and stops since it encounters a surface formed by a trough (point 4) that is more negative than point 2.
2. The path of a drop cannot cross the path of a drop that has fallen from above. For example, a drop flowing left from point 3 stops at the horizontal position of point 2 because a path coming from point 2 is encountered.
3. The horizontal movement of a raindrop, measured in units of stress from its originating peak to its stop position is counted as one half of a cycle in the stress spectrum.

The reservoir method, so-named because of its analogy of water contained in reservoirs formed by peaks and drained successively out of troughs, is shown in Fig. 23 (d). To start, imagine that the area bounded by the highest peak in the loading event forms a reservoir of water contained by it and the same peak in a following, identical, loading event. Using the numbering shown in part (b) of Fig. 23, this is point 1. Next, drain water from the reservoir out of the lowest trough in the spectrum, point 22 in Fig. 23 (b). Water caught between other peaks forms smaller reservoirs. Drain water successively out of the lowest troughs in the loading event until all reservoirs have been drained. The vertical distance, measured in stress units, between a high water level and the drain (trough) that lowers it is counted as one full cycle in the stress spectrum.

The rainflow and reservoir methods give identical results provided that rainflow counting begins with the highest peak in the loading event, as is shown in Fig. 23.

EXAMPLE 7

The values of the peaks for the stress history shown in Fig. 23 are given below. Apply (a) rainflow counting and (b) reservoir counting in order to identify the stress ranges in the stress spectrum. Finally, (c) evaluate the effects of one million loading events of this stress history acting on a beam that uses a continuous partial penetration groove weld to connect the flanges to the web.

The given data are –

Peak / Trough No.	Stress (MPa)
1	93
2	18
3	55
4	10
5	85
6	10
7	37
8	18
9	37
10	10
11	46
12	6
13	55
14	46
15	74
16	8
17	55
18	18
19	65
20	39
21	83
22	0

Solution: (a) Rainflow counting:

From Peak or Trough No.	To Horizontal Distance of Point No.	Half Cycle (MPa)
1	22	93
2	3	37
3	2	37
4	5	75
5	6	75
6	11	36
7	10	27
8	9	19
9	8	19
10	9	27
11	10	36
12	21	77
13	14	9
14	13	9
15	16	66
16	15	66
17	18	37
18	17	37
19	20	26
20	19	26
21	12	77
22	1	93

Solution: (b) Reservoir counting method:

Drain from Trough No.	Water Level at Peak	Stress Range (MPa)
22	1	93
12	21	77
4	5	75
16	15	66
2	3	37
18	17	37
10	11	36
6	7	27
20	19	26
8	9	19
14	13	9

Note that these stress ranges are the same as were determined in part a) using the rainflow counting method (where half-cycles are reported).

Solution: (c) Cumulative damage using the Palmgren-Miner rule:

According to Table 1 this is an AASHTO Detail Category B'. Table 2 indicates that the fatigue life constant for use in Eq. 8 is 20.0×10^{11} . (The reader should review Example 8 relative to this part of the problem after Section 4.3 has been studied.)

Stress Range $\Delta\sigma$ (MPa)	Fatigue Resistance $N = 20.0 \times 10^{11} (\Delta\sigma)^{-3}$	Damage Due to 1×10^6 Loading Events, n_i/N
93	2 486 000	0.402
77	4 381 000	0.228
75	4 740 000	0.211
66	6 957 000	0.144
37 (twice)	39 484 000	0.051
36	42 867 000	0.025
27	101 610 000	0.010
25	128 000 000	0.008
19	291 588 000	0.003
9	2.7×10^9	0.000

Damage summation: $\sum n_i/N = 1.08 \geq 1.0$

Comments:

This analysis indicates that the fatigue evaluation has failed, meaning that the element may not withstand one million loading events. At this point, the designer has several remedial possibilities. In order of importance these are:

1. A better design detail should be investigated. Often, fatigue problems can be traced to poor initial design detail choices. In this example, the use of continuous fillet welding rather than continuous partial penetration groove welding would increase the fatigue strength of this element by about 25% according to the AASHTO rules since the fatigue category changes from Detail B to Detail B'. If this change could be made, in this example the damage summation would be 0.55, a substantial reduction, and the detail would then pass the fatigue evaluation.

2. Measures that reduce stresses due to dynamic loading should be studied. Such measures could involve employing continuous construction, avoiding short members near application of loads, reducing the number of expansion joints, improving road surfaces on road bridges, and improving three-dimensional load-carrying capacity.
3. A more detailed fatigue analysis could be carried out. This is covered next, in Section 4.3.
4. Only as a nearly-last resort, the thickness of the member could be increased in order to lower the stresses. Note that, if this is done, the fatigue strength may also decrease; see Section 8.4.

4.3 Fatigue Limits

In Fig. 24 a given stress range spectrum (distribution of stress ranges at a particular structural element) is shown for three possible cases. Case 1 refers to the situation where all cycles are above the constant amplitude fatigue limit (CAFL). For Case 2, the same distribution of stress ranges is located such that there are stress ranges both above and below the CAFL. In Case 3, all stress ranges in the spectrum are below the CAFL.

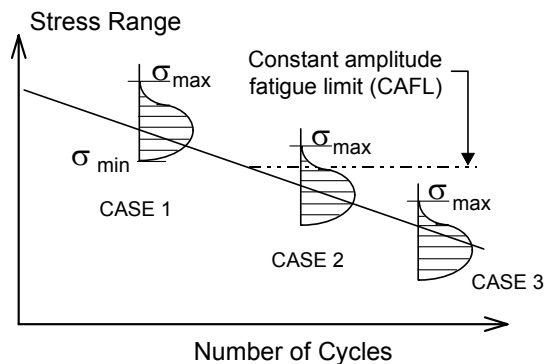


Figure 24 Three Cases of Variable Amplitude Stress Spectra

The constant amplitude fatigue limit is simply that stress range level below which there will be no fatigue crack growth under the condition of constant amplitude loading. In laboratory testing, constant amplitude loading is the procedure most often used, primarily because it is the easiest situation to create. Some real fatigue life cases will correspond to this. For example, a machine part that is loaded in the same way for all of its operating cycles corresponds to the constant amplitude loading case. On the other hand, civil engineering applications such as bridges and offshore structures would hardly ever be loaded in constant amplitude fatigue. Rather, as we have already seen (Section 4.2), the stress ranges that actually act on a structural detail correspond to a case of variable amplitude fatigue. We have seen that the use of an effective stress range (Eq. 13 or 14) is a way of expressing the variable amplitude stress ranges as an equivalent constant amplitude stress range. The

question remains: does constant amplitude loading fairly represent variable amplitude loading?

Studies done on the fatigue life of cover-plated beams (AASHTO Detail Category E') [28] showed that constant amplitude tests and variable amplitude tests (done at the equivalent constant amplitude stress range) gave comparable results up to at least one million test cycles. There are fewer data (from any sources) for stress ranges in the order of ten million cycles upward. However, it appears that the maximum stress *per se* must also be considered at these long lives.

For Case 1 shown in Fig. 24, all of the stress cycles in the spectrum contribute to fatigue crack growth and must be considered in any fatigue life evaluation. This is how the discussion and examples have been treated so far. Case 3 is also clearcut: because none of the stress cycles in the spectrum are above the constant amplitude fatigue limit, no fatigue assessment is required. (However, if a stress range in a spectrum that resulted from another loading event does exceed the CAFL, then Case 3 spectra should be considered in the same way as Case 2 spectra.)

Case 2 spectra are most often associated with situations where long fatigue lives are required. For example, structures such as bridges, offshore platforms, chimneys, and overhead highway signs are often subjected to millions of loading events. It is difficult to guarantee that values of all stress ranges will remain less than the value for the CAFL throughout the service life of the structure.

Two options are possible for the analysis of Case 2 spectra. First, it can be assumed, conservatively, that all cycles contribute to crack propagation in the element from the first cycle of fatigue loading. This is equivalent to assuming that the value for the fatigue threshold stress intensity factor is zero. For this option, analysis proceeds in a fashion identical to the analysis required for Case 1. In other words, all stress ranges in the spectrum are assumed to contribute to fatigue crack growth. The analyses in Examples 5, 6, and 7 adopted this option. In effect, this option assumes that the fatigue strength curve continues below the CAFL with a slope constant of 3.

The second option for analysis of Case 2 spectra is based on the more logical assumption that not all cycles in the spectrum will contribute immediately to crack propagation. This assumption is equivalent to admitting the presence of a non-zero value for the fatigue threshold stress intensity factor. As crack propagation proceeds, more and more

cycles in the spectrum will exceed the threshold stress intensity factor range until all cycles in the spectrum contribute to crack propagation at a certain crack length.

International opinion as to how the analysis should proceed in the Case 2 second option is not unanimous. This is due to a lack of test data at sufficiently long fatigue lives so as to be able to verify proposed analysis methods. Furthermore, fracture mechanics analyses are hindered by difficulties in estimating values for the threshold stress intensity factor under conditions of high tensile residual stress that vary with crack length. European practice, e.g., the ECCS rules [15], allow the use of a slope constant, m , of 5 for stress ranges below the CAFL.¹ However, recent work indicates that this may be unsafe for stress spectra applied to large beams with welded longitudinal attachments [29]. Nevertheless, test data for all other cases investigated indicate that use of the slope constant of 5 is acceptable. It remains to be seen whether the best rule is the first option or the second option qualified by a provision for exceptional cases. More research and testing is needed.

The second limit discussed in this Section, the cut-off limit, is used to discard small stress cycles from the stress spectrum. Small cycles in the spectrum do not contribute significantly to fatigue damage: it is considered that by the time cracks grow to a length where these stresses would induce stress intensity factor ranges greater than the threshold stress intensity factor range, the vast majority of fatigue life has been expended.

The importance of the cut-off limit is greatest when automatic stress measuring equipment is used to measure stress ranges. This equipment is capable of measuring several thousand small cycles per loading event. When the number of small stress cycles (having values less than half of the CAFL) is greater than two orders of magnitude more than the number of large cycles, the Palmgren-Miner damage summation can produce an excessively conservative evaluation. The Eurocode rules suggest a cut-off limit at the stress level that corresponds to the intersection of the fatigue strength curve ($m = 5$) with one hundred million cycles.

EXAMPLE 8

Part (c) of Example 7 required calculation of the cumulative damage for a given stress spectrum. The Palmgren-Miner rule was used, and implicit in the solution was that all cycles

¹ The fatigue life rules in ECCS and in the more recent Eurocode [46] are nearly identical. They are similar in many major respects to those in the AASHTO Specification. However, a significant difference is that the number of cycles at which the CAFL is taken to occur is a constant (5 million cycles) for all detail categories in the European standards, whereas in the AASHTO rules the number of cycles at which the CAFL starts varies with the detail category. The AASHTO approach is more consistent with the experimental evidence.

of the spectrum produce fatigue crack growth. Establish whether the situation is Case 1, 2, or 3 according to the terminology introduced in this Section.

Solution:

The detail given in Example 7 is an AASHTO Detail Category B'. Table 2 indicates that the threshold stress for Category B' is 82.7 MPa. (The term *threshold stress* is synonymous with CAFL.) According to the information given in Example 7, the maximum stress in the spectrum is 93 MPa, and the minimum stress in the spectrum is 0 ksi.

Since the maximum stress (93 MPa) is greater than the CAFL (82.7 MPa), this means that the stress spectrum does not correspond to Case 3 (see Fig. 24). Since the minimum stress (zero) is less than the CAFL, the stress spectrum is not Case 1. Thus, the stress spectrum is identified as Case 2, that is, the range of stresses within the spectrum straddles the CAFL.

Comments:

The calculations carried out in Part (c) of Example 7 counted all stress cycles as damaging. As pointed out earlier in Section 4.3, this is equivalent to assuming that the sloping straight line of the Detail B' category extends downward indefinitely at a slope constant $m = 3$ on the log-log plot.

Chapter 5 Fatigue Design According to the American Association of State Highway and Transportation Officials Specification (AASHTO)

5.1 Introduction

The discussion in the first four chapters of this document has centered around concepts of fatigue crack growth and how to treat design tasks that are linked to load-induced crack growth. Distortion-induced fatigue crack growth is also an important consideration; this is the subject of Chapter 6. The examples thus far have deliberately been kept simple, so that the instructive points made could be developed in the mind of the reader.

In this chapter, the rules of the American Association of State Highway and Transportation Officials (AASHTO) Specification [2] that reflect load-induced fatigue are examined. Chapter 6 will contain observations arising out of the AASHTO Specification that relate to distortion-induced fatigue.

5.2 Redundancy and Toughness

Users of previous editions of the AASHTO Specification (e.g., 15th Edition, 1992) will be aware that the concept of structural redundancy has been dropped in the fatigue design rules of the 1994 Edition. In those earlier specifications, permissible stress ranges were set forth for both redundant and non-redundant members. The stress range values for non-redundant members were fixed, as a matter of engineering judgment, at 80% of the values for redundant members. The rationale for this was that the consequences of failure were greater in the former, and therefore they should be designed more conservatively. This was a reasonable position, but, at the same time, greater fracture toughness was also specified for non-redundant members. This constituted a double penalty, and therefore the distinction of fatigue design with respect to non-redundant members and redundant members has been dropped from the current (1994) edition of the Specification. (The distinction for fracture toughness has been maintained, however. The relevant term used in that part of the specification is "fracture-critical.")

Even though the differentiation between non-redundant and redundant members is no longer part of load-induced fatigue design, it is still instructive to examine the issue. Whenever possible, and if economical, the designer should use details and concepts that introduce "redundancy."

The 1992 AASHTO definition of a non-redundant member was that it was a member whose tension failure would result in collapse of part, or all, of a structure.¹ The statement was interpreted in a variety of ways, however. For example, continuous bridges that consist of just two parallel girders would generally be regarded by designers as non-redundant. The assumption is simply that such a bridge would fail catastrophically if one girder fractured. Although this seems a reasonable position, it is contrary to experience with actual structures. For example, the two-girder Lafayette Street Bridge in St. Paul, Minnesota carried traffic without difficulty for several months even though a girder had fractured near the center span inflection point [20]. Similarly, the I-79 bridge across the Ohio River near Pittsburgh carried traffic even though a crack was present that extended all the way up to the top flange [20]. (It is not known how long the situation existed. However, traffic was carried without incident in this condition for at least a few hours, between the time the crack was observed by the crew on a passing tugboat and when traffic on the bridge was stopped.) In both of these structures, their lateral bracing systems participated in carrying the load because the cracked plate girder behaved like a torsionally stiff box.

There are at least three types of redundancy: only the first one listed is accepted by some owners, however.

1. Statical redundancy (i.e., a statically indeterminate structure). A continuous girder bridge is statically redundant.
2. Multiple load paths, usually as identified in the principal cross-section. This implies that there are at least three parallel load-carrying components such as girder elements.
3. Internal member (cross-section) redundancy. Beams or truss members in which the cross-sectional components are fastened with rivets or bolts are considered to be redundant internally. The severing of one component by a fatigue crack may not lead to catastrophic failure since the other components are still intact. Of course, instability due to the non-symmetry of the cracked cross-section might be a consideration in some cases. However, generally it is not until a fatigue crack starts in second component that collapse becomes a concern.

The concept that multiple unwelded components of a beam, truss, or arch member

¹ Obviously, tension failure could be the failure of a tension member, but it was intended that the definition include the concept of the tension failure of a portion of the cross-section, e.g., the tension region of a beam in bending.

builds in crack arresters and therefore improves performance has been documented. For example, recent research has shown that the multi-component riveted members, which have a component fatigue category of D, can sometimes be evaluated as Category C provided that the fasteners are tight and in good condition [30]. However, the design specification does not yet make this distinction. Good practice sometimes goes beyond the minimum requirements, even though a perceived detailing improvement may not produce an advantage in terms of the specification.

The redundancy in the case of statical indeterminacy is identified as a routine part of the structural analysis. It is obvious that a statically indeterminate structure will be less likely to suffer catastrophic collapse in the event of significant cracking due to fatigue. However, the degree to which this vulnerability might exist can only be established with the aid of an extensive, three-dimensional computer analysis. Sometimes, owners are receptive to demonstration of redundancy by this means. The objective is usually to show that a more economical structure is also redundant, e.g., that a three-girder redesign alternative is comparable to a four-girder design. This requires design skill and good details.

Although a redundant system receives no benefit in the AASHTO Specification as compared with a non-redundant system, good design practice incorporates as much redundancy as can be justified economically.

Because of the possibility of fatigue crack formation, fracture toughness is also a matter of concern in bridge structures. It is possible that fatigue crack growth can lead to conditions that will trigger brittle fracture, a highly undesirable situation. Use of a steel that has a good level of fracture toughness and avoidance of details that create triaxial stress conditions are important to achieving the desired fatigue life and preventing premature fracture. In addition, tough steels promote stable crack extension, which is a desirable feature for fatigue crack inspection.

The goal is to avoid brittle fracture, which is a type of catastrophic failure. Low fracture toughness bridge steels can result in brittle fracture under normal service loads when cracks or crack-like geometric conditions develop. Bridge steels are strain rate sensitive, which means that the loading rate from traffic is not as severe as the dynamic rate associated with the standard Charpy V-notch impact test commonly used to provide qualitative information about the steel material. Fracture toughness is also dependent upon temperature. As the temperature decreases, fracture toughness also decreases. Although fracture

mechanics provides a useful analysis tool to relate crack size and stress level to the material fracture toughness characteristics, an accurate determination of fracture susceptibility for structural engineering design is complicated. This is primarily because the model characterizing combinations of stress and crack size results in plasticity levels such that the elastic stress model becomes invalid.

Nevertheless, the Charpy V-notch tests can provide a useful means of screening out materials that would be susceptible to brittle fracture at small crack sizes, thereby preventing achievement of adequate fatigue resistance.

5.3 Fatigue Design in the AASHTO Specification

In the material presented so far, it has been established that the fatigue life of a structural steel component can be described in terms of just three elements. These are the stress range that is acting on the detail under examination, the number of cycles to which the detail is subjected, and a description of the fatigue life inherent in the detail.

The AASHTO rules were first introduced in Section 3.4, where the elements of the design requirements were outlined so that examples could be carried out. In this section, more information concerning the fatigue provisions in the AASHTO rules will be provided.

5.3.1 Fatigue Load and Frequency

The basis of the load to be used for the fatigue design of bridges according to the AASHTO Specification is the so-called *Design Truck*. The Design Truck consists of three axles. In order, these are one axle of 35 kN load followed by two of 145 kN load each. The axle spacing between the 35 kN load and the first 145 kN load is 4.3 m and the spacing between the two 145 kN axles is a variable quantity that can range between 4.3 and 9.0 m. The Design Truck is a loading that applies to many different design cases. For fatigue, there are two unique features that are applied to the Design Truck. One is that the axle spacing between the two 145 kN axles is fixed at 9.0 m. The other feature is that the axle loads to be used for calculation of the fatigue stress ranges are to be taken as 0.75 times the axle loads of the Design Truck. This reflects the observation that the large number of truck passages associated with the fatigue strength examination are commensurate with lighter trucks than the Design Truck. These, and other related details, are in Article 3.6.1.2.2 of the Specification.

The stress range at the particular detail under examination for fatigue strength is to be

evaluated according to the loading described, including also the dynamic load allowance stipulated in Article 3.6.2 of the Specification. For consideration of fatigue, the dynamic load allowance is designated simply as a 15% increase in the stress range calculated using the Design Truck, modified as described above.

In general, each detail must satisfy the requirement that

$$\gamma(\Delta f) \leq (\Delta F)_n \quad (15)$$

where Δf = the live load stress range due to passage of the fatigue load. (In this document so far, this has been designated $\Delta\sigma_r$)

$(\Delta F)_n$ = the nominal fatigue resistance

γ = the load factor for the fatigue load combination. The value $\gamma = 0.75$ is to be used for the fatigue case, as discussed above.

As we have already seen, the nominal fatigue resistance is linked to the number of stress ranges that will be imposed. According to the AASHTO Specification, the loading is to be taken as the single-lane average daily truck traffic, $ADTT_{SL}$. Unless better information is available, this quantity is to be calculated as:

$$ADTT_{SL} = p \times ADTT \quad (16)$$

where $ADTT$ = the number of trucks per day in one direction, averaged over the design life
 $ADTT_{SL}$ = the number of trucks per day in a single lane, averaged over the design life

p = a factor reflecting the number of lanes available to trucks. If only one lane is available to trucks, $p = 1$; if two lanes are available then $p = 0.85$; if three or more lanes are available, then $p = 0.80$.

The Specification provides other information regarding the loading. For instance, the designer is advised that the average daily traffic (ADT), which includes all cars and trucks, is physically limited to about 20 000 vehicles per lane per day. The fraction of truck traffic in this total is estimated to be about 20% for rural interstate highways, 15% for urban interstate or "other" rural highways, and 10% for "other" urban conditions. If site-specific information is not available, the usual situation, these values can be used to generate the frequency of loading of the Design Truck.

5.3.2 Fatigue Resistance

Each detail must satisfy the requirement that the calculated stress range, termed Δf in the Specification, be equal to or less than the nominal resistance identified in the Specification, $(\Delta F)_n$. As just discussed, the calculated stress range is that arising from application of the fatigue Design Truck, including impact. The subscript n in the expression for nominal resistance simply identifies that there must be a linkage with number of cycles—the fatigue resistance is a function of the number of cycles of the stress range.

The nominal fatigue resistance is to be taken as:

$$(\Delta F)_n = \left(\frac{A}{N} \right)^{1/3} \quad (17)$$

where A is the constant listed in Table 2 ($\equiv M$ in Eq. 8) and

$$N = (365) (75) n (\text{ADTT})_{\text{SL}} \quad (18)$$

The constant A in Eq. 17, which is equivalent to the term M in Eq. 8, reflects the severity of the detail, according to the Detail Categories identified in Fig. 18 and Table 2. Given that the term $(\Delta F)_n$ is simply the value of the term $\Delta \sigma_r$ at its permissible value for the given number of cycles, it can be seen that Eq. 17 is identical to Eq. 8. Equation 8 is the fatigue life expression that was developed from a fracture mechanics approach. Thus, the AASHTO requirement for fatigue life (Eq. 17) is consistent with the fatigue life of a given detail as described on a theoretical basis and incorporating the results of physical testing by the inclusion of the term A in Eq. 17.

Equation 18 is the number of cycles of stress range expected to be imposed on the structure in a design life of 75 years. (At the option of the designer, another number can be used in place of 75.) The term n is included in Eq. 18 as a way of acknowledging that more than one stress cycle can result from a single passage of the fatigue Design Truck. Primarily, this is as a result of the vibrations set up in the structure as the truck moves across. Values of n are tabulated for 10 different cases in Table 6.6.1.2.5–2 of the Specification. For a simple span girder, for example, $n = 1.0$ is to be used for spans less than 12 m and $n = 2.0$ is to be used for spans greater than 12 m. For cantilever girders, $n = 5.0$ must be used. (This high number reflects the susceptibility of cantilevers to vibration under moving loads.) The AASHTO Table can be consulted for other cases.

The AASHTO Specification rules provide that, in addition to Eq. 17, the following

requirement must also be met—

$$(\Delta F)_n \geq \frac{1}{2}(\Delta F)_{TH} \quad (19)$$

where $(\Delta F)_{TH}$ is the constant amplitude fatigue threshold stress. (This has been referred to elsewhere in this document as the constant amplitude fatigue limit, CAFL.)

Viewing Equations 17 and 19 together, the latter says that the sloping straight line represented by Eq. 17 need not extend below a horizontal straight line at the value of one-half the constant amplitude fatigue limit. According to Figure 18, it would appear that the constant amplitude fatigue limit itself should be used. However, the requirement reflects the fact that the stress ranges calculated according to the AASHTO rules are a simplified depiction of the actual stress ranges that can take place. In particular, there can be occasional stress ranges that are considerably greater than the calculated, nominal stress ranges. If even a small number of these stress ranges exceed the CAFL, fatigue crack growth will take place. The check using Eq. 19 determines whether or not the maximum stress range in the random variable cycle exceeds the CAFL. It is assumed that the maximum stress range, $\Delta\sigma_{max}$, is twice as great as the nominal stress range calculated from the fatigue truck, which represents the effective stress range, $\Delta\sigma_e$. This is reflected in Eq. 19.

Figure 25 illustrates these points concerning the AASHTO rules. The AASHTO permissible fatigue life line is the sloping solid straight line shown in Fig. 25, followed by the dashed sloping straight line, and then by the dashed horizontal straight line. Also shown

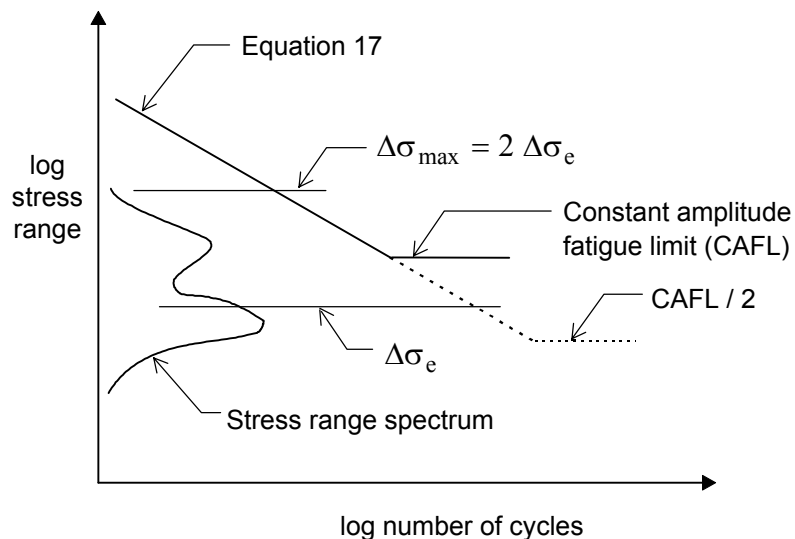


Figure 25 AASHTO Fatigue Limits

in the figure is a hypothetical random variable stress spectrum, plotted on the ordinate. Shown is the equivalent stress range for the spectrum, $\Delta\sigma_e$, which in this case intercepts Eq. 17 below the CAFL. We note, however, that the maximum stress range in the spectrum is above the CAFL, i.e., fatigue crack growth will occur. The spectrum shown has been given the unique relationship wherein $\Delta\sigma_{\max} = 2 \Delta\sigma_e$. If it is visualized that the stress spectrum is moved down to a level such that $\Delta\sigma_e$ is just below the level CAFL/2, then it is apparent that the maximum stress in the spectrum is just below the CAFL. Thus, if the check of Eq. 19 indicates that $\Delta\sigma_e$ is below the value CAFL/2, then all cycles are below the fatigue limit and no fatigue cracking will occur.

The AASHTO rules point out (Article 6.6.1.2.1) that the force effect for the fatigue design of a steel bridge shall be the live load stress range. This is consistent with the discussion so far in this document. However, it is recognized that fatigue cracks will not grow if the stress range is entirely compressive, an observation supported by both field and laboratory experience². Accordingly, a further provision in Article 6.6.1.2.1 allows the designer to identify those regions where only a compressive stress range is expected and to therefore eliminate them from further consideration. In accordance with the discussion just concluded, it is again necessary to assume that the live load stress range can be as high as twice that calculated using the AASHTO fatigue Design Truck. Thus, the statement in Article 6.6.1.2.1 that allows the designer to reduce the areas of a bridge requiring examination for fatigue is:

"In regions where the unfactored permanent loads produce compression, fatigue shall be considered only if this compressive stress is less than twice the maximum tensile live load stress resulting from the fatigue load..."

5.4 Summary of AASHTO Requirements

- Determine the number of design cycles. Use the AASHTO recommendations, or load survey information, or information provided by the owner.
- Identify the Detail Category for each component of the structure that could be sensitive to fatigue.
- Calculate the stress range at the details of interest.
- Determine the permissible stress range for the detail under examination and its

² In practice, it is often difficult to ensure that stresses will always remain in compression, especially when fit-up stresses, stresses due to temperature changes, and stresses due to foundation settlement may be present.

number of stress range cycles. (Engineering judgment should be exercised: some details can be eliminated from examination on the basis of comparison with others of similar stress range and number of cycles.)

- If the actual stress range at the detail exceeds the permissible value, modify the design and repeat the assessment.

5.5 Design Example

The following design example will be used to elaborate the fatigue requirements of the AASHTO Specification. The problem is derived from *Design Example 2* of Reference [31]. In that example, the 1977 AASHTO Specification rules were used and the details were laid out in US Customary units. Because the illustration that follows includes calculation of the stresses and other design aspects that are not a central part of this document, reference will be made from time to time to the specific articles of the Specification. This will enable the reader to use that source for more information.

EXAMPLE 9

Design Information:

Two-span continuous girder bridge, 42.7 m spans, girder spacing at 2440 mm c/c, four parallel girders

Rural interstate highway, two lanes of traffic in same direction

Unshored composite construction (positive moment region only)

Concrete slab: $f'_c = 20.7$ MPa, modular ratio $E_s/E_c = 10$

Reinforced concrete slab, 203 mm thick, plus a 12 mm thick integral wearing surface

Welded plate girder, ASTM A588 steel, $F_y = 345$ MPa.

Design Assumptions:

For purposes of this example, assume that the given section (Fig. 26 and Table 4) is satisfactory for non-cyclic loading and that all steel meets the fracture toughness requirements. Of course, both of these issues would be a normal part of the design procedure.

Concrete over Field Section 1 (see Fig. 26) always acts compositely with steel girder. Concrete over Field Section 2 never acts compositely with steel girder (i.e., no shear studs).

Problem: Investigate the suitability of an interior girder with respect to fatigue.

Solution:

Cross-Section Properties.

Table 4 lists the dimensions of the steel plate girder and the section properties calculated from those dimensions. Sufficient information is given such that interested readers can confirm the calculations if desired. These section properties are used subsequently to calculate stress ranges. In a similar fashion, Table 5 lists the section properties of the composite cross-section. For these calculations, it is necessary to identify the effective flange width of the composite cross-section. This is obtained using Article 4.6.2.6.1 of the AASHTO Specification, where, for an interior girder, the effective slab width is the least of —

$$\begin{aligned} &0.25 \times \text{effective span length (to point of permanent load inflection)} \\ &= 0.25 \times 30\,000 = 7\,470 \text{ mm} \end{aligned}$$

$$\begin{aligned} &\text{or, } 12 \times \text{average thickness of slab} + \text{greater of web thickness or } 0.5 \times \text{top flange width} \\ &= (12 \times 203.2) + (0.5 \times 304.8) = 2\,590 \text{ mm} \end{aligned}$$

$$\text{or, the average spacing of adjacent beams} = 2\,440 \text{ mm} \quad \textit{Governs}$$

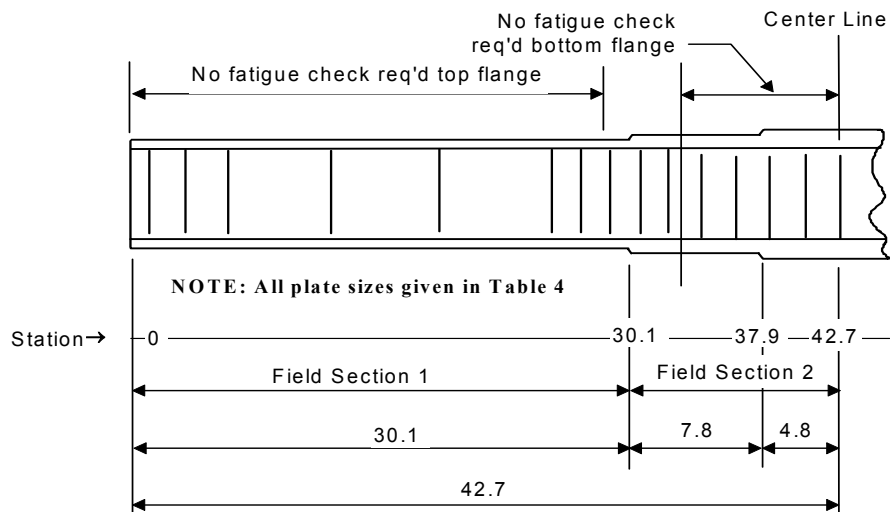
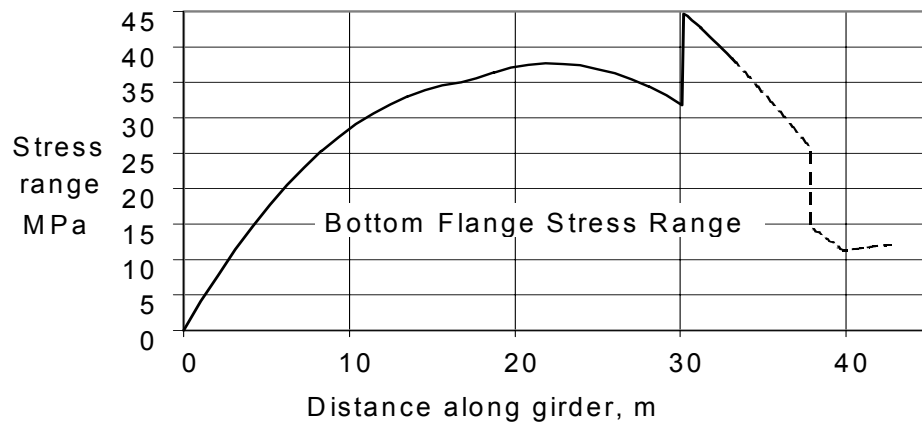
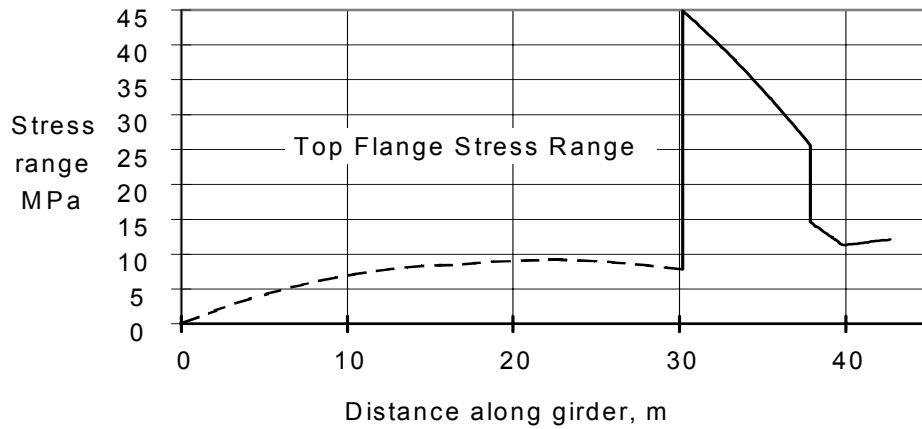


Figure 26 Plate Girder Details and Stress Range Diagrams

TABLE 4 –Properties of Steel Section

Plate Girder Only				
	END	MIDDLE	CENTER	Notes:
Web				END refers to Field Section 1
h (mm)	1524	1524	1524	
w (mm)	11.11	11.11	11.11	
A_w (mm ²)	16 932	16 932	16 932	
Top Flange				MIDDLE refers to the portion of Field Section 2 that is away from the pier
b (mm)	304.8	381.0	609.6	
t (mm)	15.88	25.40	31.75	
A_f (mm ²)	4 839	9 677	19 355	
Bottom Flange				CENTER refers to the portion of Field Section 2 that is over the pier
b (mm)	457.2	381.0	609.6	
t (mm)	23.81	25.40	31.75	
A_f (mm ²)	10 887	9 677	19 355	
Neutral Axis (x-x)	(from web centerline, +ve up)			
A_{total} (mm ²)	32 657	36 286	55 641	
Top Flange: $A\bar{y}$ (mm ³)	3 725 497	747 082	15 055 615	
Bottom Flange: $A\bar{y}$ (mm ³)	-8 425 575	-7 497 082	-15 055 615	
$\Sigma A\bar{y}$ (mm ³)	-4 700 079	0	0	
\bar{y} (mm)	-143.9	0.0	0.0	
Moment of Inertia (x-x)				
Web: $wh^3/12$ (x10 ⁶ mm ⁴)	3 277	3 277	3 277	(web, about own axis)
Web: $A_w(\bar{y})^2$ (x10 ⁶ mm ⁴)	350.7	0.0	0.0	(web, about girder centroid)
TF: $A_f(h/2 - \bar{y})^2$ (x10 ⁶ mm ⁴)	3 971	5 619	11 238	(top flange, about girder centroid)
BF: $A_f(h/2 + \bar{y})^2$ (x10 ⁶ mm ⁴)	4 159	5 619	11 238	(bottom flange, about girder centroid)
ΣI_x (x10 ⁶ mm ⁴)	11 758	14 515	25 754	

TABLE 5 – Properties of Composite Section

Composite Section		
Composite Section	Note: Composite action develops in End Section (Field Section 1) only	
Modular ratio $n (= E_c / E_s)$	10	
Concrete Thickness (mm)	203.2	
Effective Concrete Width (mm)	2 438	
Effective Concrete Area (mm ²)	495 402	
Equivalent Area of Steel (mm ²)	49 540	
Composite Neutral Axis (x-x)	(measured from neutral axis of steel girder, +ve up)	
A_{total} (mm ²)	82 198	
Concrete: $A\bar{y}$ (mm ³)	50 699 188	
Steel Girder: $A\bar{y}$ (mm ³)	0	
$\Sigma A\bar{y}$ (mm ³)	50 699 188	
\bar{y} (mm)	616.8	(from neutral axis of steel girder alone, +ve up)
or \bar{y} (mm)	472.9	(from web centerline, +ve up)
or \bar{y} (mm)	-406.6	(from centroid of concrete slab, +ve up)
Composite Moment of Inertia (x-x)		
Girder: (x10 ⁶ mm ⁴)	11 758	
Girder: $A_{girder}(\bar{y})^2$ (x10 ⁶ mm ⁴)	12 424	
Concrete: (x10 ⁶ mm ⁴)	170.5	
Concrete, $A_{equiv}(\bar{y})^2$ (x10 ⁶ mm ⁴)	8 190	
ΣI_x (x10 ⁶ mm ⁴)	32 543	

Number of Load Cycles

According to Eq. 16 (which is Eq. 3.6.1.4.2–1 of the AASHTO Specification), the number of trucks per day in a single lane is

$$ADTT_{SL} = p \times ADTT$$

where $p = 0.85$ (AASHTO Table 3.5.1.4.2–1) since in this bridge two lanes are available to trucks. The average daily truck traffic (ADTT) will be taken as 20% (rural interstate highway) of the physical limit of 20 000 vehicles per lane per day. Thus,

$$ADTT_{SL} = p \times ADTT = 0.85 \times (0.20 \times 20\,000) = 3\,400 \text{ trucks / lane / day}$$

According to Eq. 18 (AASHTO 6.6.1.2.5–2), the number of stress cycles is then—

$$N = (365) (75) n (ADTT)_{SL} , \text{ or}$$

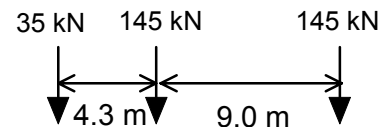
$$N = (365) (75) n (3\,400) = 93.075 \times 10^6 n \text{ cycles / lane over an assumed 75-year life.}$$

In this expression, the term n reflects the number of stress cycles for a given truck passage. According to AASHTO Table 6.6.1.2.5–2, for a continuous span bridge of 42.7 m the value is $n = 1.5$ for details located within $L/10 = 4.3$ m, or $n = 1.0$ otherwise. (In fact, the Table simply differentiates as "near interior support" or "elsewhere." However, Commentary to the Table suggests that $L/10$ can be used to define locations near the interior support. In this example, and since the two spans are of equal length, details within 4.3 m on each side of the interior support can be categorized as "interior.")

Finally, it can be concluded that for locations within 4.3 m of the interior support, $N = 93.075 \times 10^6 n \text{ cycles / lane} = 93.075 \times 10^6 \times 1.5 = 139.6 \times 10^6$, say, 140×10^6 cycles / lane, and for all other locations $N = 93.075 \times 10^6 n \text{ cycles / lane}$, say, 93×10^6 cycles / lane.

Load Assumptions and Calculations

The Fatigue Design Truck is the Design Truck (as shown in the sketch), multiplied by the load factor of 0.75 (AASHTO Table 3.4.1–1), and applying an impact allowance of 0.15 (AASHTO Article 3.6.2.1).



The load distribution factor (i.e., the fraction of a truck in a given lane that accrues to an interior girder) will be taken as 0.40. This is obtained from Article 3.6.1.4.3b and from

Article 4.6.2.2.2b. In the calculation of the load distribution factor, the longitudinal stiffness of the slab–girder system is involved. According to Article 4.6.2.2.2b, this term, K_g , can be taken as unity for the purpose of a preliminary analysis. Using this value, the load distribution factor is 0.398, say 0.40. The "exact" analysis, obtained using the section properties of Field Section 1, gives a load distribution value of 0.408. Obviously, in this problem these results are sufficiently close to one another that either could be used. Furthermore, in a so-called exact analysis, the section properties at the location where the fatigue truck is placed on the influence line for moment at a given detail should be used. This will vary, depending upon which detail is being examined. Considering the level of confidence likely in the load distribution factor calculation, these refinements seem unwarranted.

Calculation of Stress Ranges

It was pointed out earlier in this Chapter (Section 5.3.2) that fatigue need be considered only when the dead load stresses (unfactored load) are compressive and are less than twice the live load tensile stresses. It is advantageous for the designer to take advantage of this provision in order that the bridge length over which fatigue needs to be examined is reduced.

In this example, the dead load of the steel section is estimated to be 2.5 kN/m for Field Section 1 and 3.0 kN/m for Field Section 2. The initial dead load (unfactored) due to the concrete slab and girder self-weight, applied to the girder alone, is 12.40 kN/m. The additional dead load, including wearing surface, applied to the composite section, is 5.84 kN/m (unfactored). These values are used in conjunction with the fatigue live load to calculate the stresses in the top and the bottom flanges of the steel section. In accordance with AASHTO Article 6.6.1.2.1, this examination establishes that no fatigue check is required between bridge stations 0 and 29.1 m for the top flange and between stations 33.3 m and 42.7 m for the bottom flange. (The centerline of the two-span structure is bridge station 42.7 m).

Figure 26 shows the live load tensile stress range for the top and bottom flanges of the steel section. The regions that do not have to be examined for fatigue are shown as broken lines in this figure. This information can now be used to evaluate the fatigue life of the various details. (Space does not permit tabulation of the stress ranges at discrete locations, but this would be available to the designer, of course.)

Fatigue Life Assessment of Flange to Web Weld

A continuous fillet weld is used to join the flange to the web. According to AASHTO Fig. 6.6.1.2.3-1 and Table 6.6.1.2.3-1, this is Detail Category B. For Category B, the fatigue life constant is $A = 39.3 \times 10^{11} \text{ MPa}^3$ (Table 6.6.1.2.5-1) and the constant amplitude fatigue threshold is 110 MPa (Table 6.6.1.2.5-1). Therefore, the fatigue strength according to Eq. 17 (AASHTO Eq. 6.6.1.2.5-5) is first calculated as

$$(\Delta F)_n = \left(\frac{A}{N} \right)^{1/3} = \left(\frac{39.3 \times 10^{11}}{N} \right)^{1/3}$$

It has already been established that for locations within 4.3 m of the interior support (Sta. 38.4 m), $N = 140 \times 10^6$ cycles. Everywhere else, $N = 93 \times 10^6$ cycles should be used. Substitution of these values gives $(\Delta F)_n = 30.4 \text{ MPa}$ when $N = 140 \times 10^6$ cycles and $(\Delta F)_n = 34.8 \text{ MPa}$ when $N = 93 \times 10^6$ cycles.

Application of Eq. 19 also says that the permissible stress range need not be less than one-half of the constant amplitude fatigue threshold, however. In this case, the value is $110 \text{ MPa}/2 = 55 \text{ MPa}$. This governs in both cases since it is larger than both 30.4 MPa and 34.8 MPa. (An alternative way to think of Eq. 19 would be to multiply the calculated stress by a factor of 2, which then provides the estimated maximum stress range. This should be less than the CAFL.)

The actual stress range for the top flange in the region Sta. 29.1 to 38.4 m is 44.9 MPa (see Fig. 26). The actual stress range for the bottom flange in the region Sta. 33.3 to 42.7 m is also 44.9 MPa. Since the actual range of stress for this detail is less than the permissible value of 55 MPa, the flange-to-web fillet weld detail is satisfactory with respect to fatigue.

Comment: Details of Category A or B are seldom critical with respect to fatigue. With experience, it should be possible to eliminate most cases by inspection. In fact, AASHTO Article 6.6.1.2.3, which is the introductory statement setting out the fatigue requirements, refers only to components and details with fatigue resistance less than or equal to Detail Category C.

Fatigue Life Assessment of Flange Plate Splices

Figure 26 shows that the girder flange plates must be spliced at Stations 30.1 and 37.9 m. Both these locations are located in the regions wherein $N = 93 \times 10^6$ cycles. The plates change in both width and thickness at each location. The detail category is dependent upon

just how these transitions are made. If it is assumed that the transition slopes are not greater than 1:2.5 and that the groove weld reinforcement is not removed, then Detail Category C is applicable. According to the AASHTO rules, the fatigue life constant is $14.4 \times 10^{11} \text{ MPa}^3$ and the constant amplitude fatigue threshold stress range is 69 MPa for this category. Thus, the fatigue strength is the greater of $69/2 = 34.5 \text{ MPa}$ or

$$(\Delta F)_n = \left(\frac{A}{N} \right)^{1/3} = \left(\frac{14.4 \times 10^{11}}{93 \times 10^6} \right)^{1/3} = 24.9 \text{ MPa}$$

At Sta. 30.1 m, the maximum tensile stress range is 31.8 MPa (bottom flange) and at Sta. 37.9 the stress range is 25.6 MPa (either top or bottom flange). Both of these values are less than the permissible value of 34.5 MPa. The groove weld at the transition in flange plate sizes is therefore satisfactory in fatigue.

Fatigue Life Assessment of Transverse Stiffeners

Transverse stiffeners are present in a girder in order to stiffen the web and assist in carrying the shear forces. If this is their only function, they will be welded or bolted to the web and fitted tight against the underside of the compression flange. For economy, especially in the fitting process, these transverse stiffeners will be cut short of the tension flange (Fig. 27). When transverse stiffeners are present, it is common practice to use them as the connecting plate for diaphragms or cross-frames. If this is the case, then the stiffener must be welded or bolted to each flange of the girder. Often, the stiffeners are also used for the connection of lateral bracing. Once again, the transverse stiffener must be connected to both flanges if it is used to receive lateral bracing. Information on these requirements is contained in AASHTO Article 6.6.1.3 and Article 6.10.8.1.1.

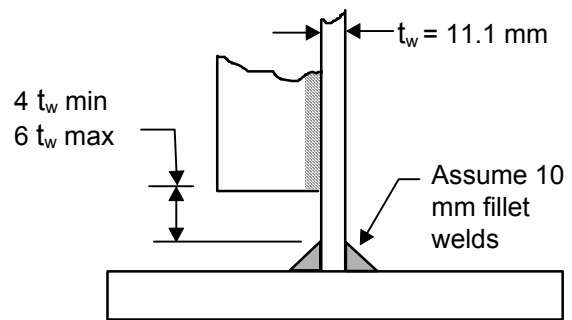


Figure 27 Stiffener Detail

It will be assumed in this example that some of the transverse stiffeners will have diaphragms or cross-frames connected to them and some will not. This is a realistic circumstance for most bridges. Later in the example there will also be a discussion about the connection of lateral bracing members to the transverse stiffeners.

When the stiffener will not to be fitted to both flanges, then the end in the tension flange

region must be cut short of the flange-to-web weld a distance not less than four times the web thickness and not more than six times the web thickness. (AASHTO Article 6.10.8.1.1.) This requirement relates to distortion-based fatigue and is discussed in Chapter 6.

According to Fig. 27, and assuming that the flange to web weld will be 10 mm, the maximum gap ($6 t_w$) will require that the end of the stiffener be $(6 \times 11.1) + 10 = 77$ mm from the nearer side of the flange. This information is required in order to be able to calculate the stress at the toe of the stiffener-to-web fillet weld.

In accordance with AASHTO Fig. 6.6.1.2.3–1 and Table 6.6.1.2.3–1, the fillet weld at the end of a transverse stiffener is a Category C' detail. The fatigue life constant is $14.4 \times 10^{11} \text{ MPa}^3$ and the constant amplitude threshold stress limit is 82.7 MPa. Thus, the fatigue strength of this detail is the greater of $82.7 / 2 = 41.3$ MPa or

$$(\Delta F)_n = \left(\frac{A}{N} \right)^{1/3} = \left(\frac{14.4 \times 10^{11}}{N} \right)^{1/3}$$

When $N = 93 \times 10^6$ cycles, the result is $(\Delta F)_n = 24.9$ MPa and when $N = 140 \times 10^6$ cycles $(\Delta F)_n = 21.8$ MPa. For both these regions, then, the permissible stress range is 41.3 MPa. In Field Section 1, the maximum tensile stress range in the bottom flange is 37.7 MPa (Fig. 26). Figure 28 shows the stress gradient at the detail in this region. The stress range at the critical location is calculated as $(1159/1260) \times 37.7 \text{ MPa} = 34.7$ MPa. Since the permissible stress in this region is 41.3 MPa, the transverse stiffeners in Field Section 1 are satisfactory with respect to fatigue. It should also be obvious, with experience, that in this example the stress range at the critical location in the transverse stiffener need not have been calculated. The stress range at the level of the bottom flange (37.7 MPa) is already less than the permissible stress range (41.3 MPa).

In Field Section 2, the permissible stress range is again calculated as 41.3 MPa (see calculation above). The actual stress range in this zone is a maximum of 44.9 MPa (Fig. 26). A calculation of the stress range at the extremity of the stiffener (similar to the calculation illustrated in Fig. 28) will identify that the stress range at this location is 41.3 MPa. As it happens, this is identical to the permissible stress range. Thus, any transverse stiffener in Field Section 2 that does not extend to the tension flange is satisfactory with respect to fatigue.

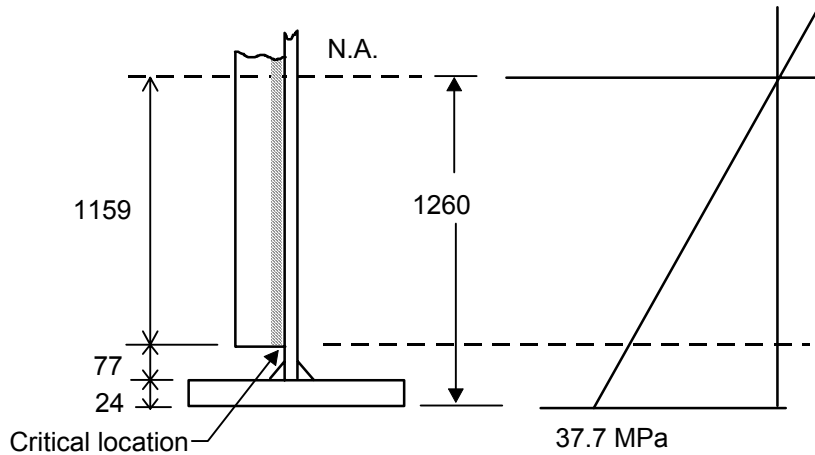


Figure 28 Stress Gradient at Transverse Stiffener

Undoubtedly, some transverse stiffeners will have to extend from flange to flange and be fastened to those flanges. This is because diaphragms will be present, and the most convenient way of attaching them to the girders is to use the transverse stiffeners. Thus, these stiffeners will extend all the way to the flange and be welded to it. (Bolting is also a possibility, if desired.) This is a Category C' detail, just as was the stiffener welded only to the web. Accordingly, the permissible stress range is 41.3 MPa, as calculated for the stiffeners that stopped short of the flange. In Field Section 1 the maximum stress range is 37.7 MPa for the tension flange and in Field Section 2 the maximum stress range is 44.9 MPa. By inspection, the condition in Field Section 1 is satisfactory. In Field Section 2, the stress range at the end of the stiffener (i.e., at the level of the inner surface of the flange) will be $\left[\frac{1260 - 24}{1260} \right] \times 44.9 \text{ MPa} = 44.0 \text{ MPa}$. See Fig. 27. Since the permissible stress range is only 41.3 MPa, this means that the detail is not satisfactory. The designer can either accept the small amount of underdesign (about 6%) or ensure that this type of transverse stiffener is not located anywhere in the region of Field Section 2 where the flange stress exceeds $41.3 \text{ MPa} / \left[\frac{1260 - 24}{1260} \right] = 42.1 \text{ MPa}$. According to Fig. 26, this will be only a very short portion of the girder to the right of bridge station 30.1 m. Review of the calculated stress (not given in the example) reveals that the stress range has decreased to 42.1 MPa at bridge station 31.4 m.

Fatigue Life Assessment of Lateral Bracing Attachment

Lateral bracing can be attached to the girder in different ways. A horizontal plate can be fastened to the web or to the flange by welding or by bolting. The lateral bracing members

are then bolted (usual case) or welded to this connection plate. (In the AASHTO Specification, this is referred to as a "lateral connection plate.") If transverse stiffeners are present and the lateral connection plate is to be located within the web depth, then it must be attached to the stiffener when on the same side of the girder as the stiffener or centered on the stiffener otherwise. (AASHTO Article 6.6.1.3.2). Although the use of lateral connection plates within the web depth and centered on transverse stiffeners is a detail that has been widely used in the past, it will be seen that it presents a number of difficulties related to fatigue.

The fatigue category for this type of detail will depend upon the length of the plate (in the direction of stress), the treatment of the weld ends (no treatment, transition radius on the weld, or transition radius and welds ground smooth), and the thickness of the plate.

For the example girder, try a square plate that is less than 25 mm thick, and no special finishing of the weld. According to AASHTO Table 6.6.1.2.3-1, this will be Category E when the plate length is greater than either 12 times the plate thickness or 100 mm. It is likely that the connection plate will have to be longer than either of these values for proper attachment of the bracing members.

Category E is a severe fatigue detail. The fatigue life constant is $3.61 \times 10^{11} \text{ MPa}^3$ and the constant amplitude threshold stress limit is 31.0 MPa. Thus, the permissible fatigue stress is the greater of $31.0/2 = 15.5 \text{ MPa}$ or

$$(\Delta F)_n = \left(\frac{A}{N} \right)^{1/3} = \left(\frac{3.61 \times 10^{11}}{N} \right)^{1/3}$$

When $N = 93 \times 10^6$ cycles, the result is $(\Delta F)_n = 15.7 \text{ MPa}$ and when $N = 140 \times 10^6$ cycles $(\Delta F)_n = 13.7 \text{ MPa}$. For convenience, simply take 15.5 MPa as the permissible fatigue stress in both regions.

In Field Section 1, the stress gradient diagram is that shown in Fig. 28. In order to not exceed the permissible stress of 15.5 MPa, a calculation will show that the horizontal plate must be located 735 mm from the bottom. This is not a practical solution; the lateral bracing should be much closer to the plane of the lower flange. Try a similar detail except that there will be a transition radius $>50 \text{ mm}$ at the end of the plate and the welds ends will be ground smooth. According to Table 6.6.1.2.3-1 the lateral connection plate is now a Category D detail. The fatigue life constant is $7.21 \times 10^{11} \text{ MPa}^3$ and the constant amplitude threshold stress limit is

48.3 MPa. Calculation will show that the criterion $48.3 \text{ MPa}/2 = 24.1 \text{ MPa}$ will govern throughout. The necessary location of the horizontal plate is now 455 mm above the bottom of the girder. Although this is a considerable improvement over the previous condition, it still places the connection plate a considerable distance from the lower flange. Furthermore, in this girder it is inevitable that some connection plates will have to be placed around the transverse stiffeners. The situation is shown in Fig. 29. Although the extreme ends of the horizontal plate could have a radius and the welds ground, the interior "ends" of the plate near the transverse stiffener could not receive this treatment. Thus, the condition reverts to that of a square plate.

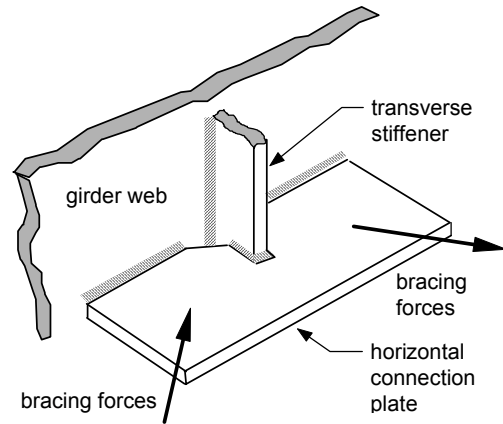


Figure 29 Transverse Stiffener and Horizontal Connection Plate

The type of lateral bracing attachment plate that attaches to a transverse stiffener must also meet a distortion-based fatigue requirement. This topic is discussed in Chapter 6 and the fatigue design of this lateral bracing attachment is completed in Example 11.

All things taken into account, the designer should consider simply attaching the horizontal connection plate to the lower flange. According to AASHTO Fig. 6.6.2.3–1 and Table 6.6.2.3–1, if the horizontal connection plate is made the same thickness as the flange plate, a transition radius of between 150 and 600 mm is used at the ends, and the welds ground smooth, then this is a Category B detail. The fatigue life constant is $39.3 \times 10^{11} \text{ MPa}^3$ and the constant amplitude threshold stress limit is 110 MPa. Thus, the permissible stress range for this detail is the greater of $110/2 = 55.0 \text{ MPa}$ or

$$(\Delta F)_n = \left(\frac{A}{N}\right)^{1/3} = \left(\frac{39.3 \times 10^{11}}{N}\right)^{1/3}$$

When $N = 93 \times 10^6$ cycles, the result is $(\Delta F)_n = 34.8 \text{ MPa}$ and when $N = 140 \times 10^6$ cycles $(\Delta F)_n = 30.4 \text{ MPa}$. For both these regions, then, the permissible stress range is 55.0 MPa. In the bottom flange, the maximum tensile stress range is 37.7 MPa in Field Section 1 and 45.0 MPa in Field Section 2 (Fig. 26). Thus, this connection detail is satisfactory for use anywhere along the length of the girder. A high-strength bolted connection is also a possibility. It is likewise a Category B and the connection would be much simpler than the

welded one. However, the effect of the bolt holes on the strength of the flanges would have to be taken into account.

Fatigue Life Assessment of the Shear Studs

In this girder, Field Section 1 is composite and will therefore have shear studs. Field Section 2 is non-composite and so no studs will be present. Positive bending moment predominates in Field Section 1. However, as Figure 26 identifies, there is also a region of positive stress range (which results from loading in the opposite span). The examination of dead load stress plus two times the live load stress identifies that the region from Sta. 0 to 29.1 is always in compression, however, and so no fatigue check is required. This leaves the region between Sta. 29.1 and 30.1 m (end of Field Section 1) in which a fatigue check is required for the studs. Studs are a Detail Category C (AASHTO Table 6.6.1.2.3-1), which has a relatively high fatigue life. The largest stress range in the short portion of the girder that must be checked is only 8.1 MPa (Fig. 26). It will be taken by engineering judgment that the studs are satisfactory in fatigue.

Fatigue Life Assessment of Bolted Splice

Figure 26 implies that the girder is spliced at Sta. 30.1 m, i.e., at the junction of Field Section 1 and Field Section 2. The actual splice will likely be made just to the left of that location, however, in order that filler plates will not be required for the flange splice plates. The actual location of the center of the splice will depend upon the length of the splice plates required for the flanges. Assume that the splice will be centered at Sta. 29.0. From inspection of Fig. 26, the bottom flange stress range controls the design. The detailed calculations show that the stress range in the bottom flange is 33.2 MPa at location 29.0 m.

The AASHTO Specification designates Category B for bolted connections that are slip-critical. The stress is to be calculated on the gross cross-section, which is the value 33.2 MPa cited above. The splice is located in the region wherein $N = 93 \times 10^6$ cycles.

The flange-to-web weld was also a Category B, and the calculations done earlier for that detail identified that the permissible stress range is 55 MPa. Since this is greater than the actual stress range, the bolted splice will be satisfactory with respect to fatigue.

This example has dealt with the major elements of fatigue life assessment for the welded plate girder. As the details are completed, the designer should be alert for other situations that require a fatigue life assessment.

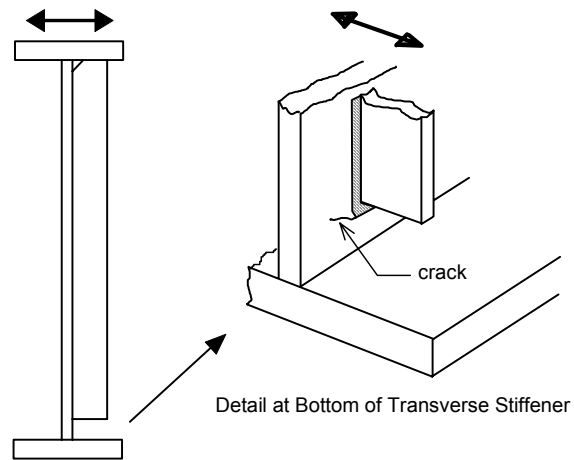
Chapter 6 Distortion-Induced Fatigue Cracking

6.1 Introduction

Most of the topics so far have discussed the effect of stresses acting on pre-existing flaws, cracks, and geometrical discontinuities with respect to fatigue lives of fabricated steel elements. The assumption has been that these stresses can be calculated, usually at an elementary level. The loads used are the same as those associated with the strength design of the members. In many instances, however, fatigue crack growth results from the imposition of deformations, not loads. Although it is possible in some of these cases to calculate a stress range, this is usually performed after the fact and requires that field measurements be made. Designers are not likely to be able to identify the need for such calculations in the course of their work. As will be seen, this type of fatigue crack growth results from the imposition of relatively small deformations, usually out-of-plane, in local regions of a member. These deformations are not anticipated in the design process. The main defense against this source of cracking is proper detailing, and this, in turn, is dependent on experience.

6.2 Examples of Distortion-Induced Cracking

An example of the phenomenon is illustrated in Fig. 30. Standard practice for many years was to cut transverse stiffeners short of the bottom (tension) flange so as to avoid a severe detail for fatigue if the stiffener is welded to the flange at that location¹. (There are also practical reasons for cutting the stiffener short: the stiffener will have to be made to a precise length if it is to extend from flange to flange.) The height of the gap between the end of the stiffener and the girder flange is usually quite small. If lateral movement of the top flange relative to the bottom flange takes place, large strains are imposed in the gap region because of the significant change in stiffness between the stiffened and unstiffened (gap)



Girder and Transverse Stiffener

Fig. 30 Fatigue Cracking from Out-of-Plane Movement

¹ Experience gained over the past 20 years has shown that, in fact, the fatigue life of the detail is independent of whether the stiffener terminates in the web or is extended down to the flange. This is reflected in current specifications. The only difference, then, is the effect of the stress gradient.

regions of the web. Typically, the strains that are produced are so large [32] that it may take relatively few cycles for a crack to propagate. The flange movement could be the consequence of transverse forces in a skew bridge, but it could even be due to shipping and handling.

The detail in Fig. 30 shows the crack emanating from the weld toe at the bottom of the stiffener. Often, the crack will also extend across the toe of the fillet weld at the underside of the stiffener and for some distance into the web. Up to this stage, the crack is more or less parallel to the direction of the main stress field that the girder will experience in service. Thus, if the source of the displacement-induced fatigue can be identified and eliminated, then further growth of the crack is unlikely. However, if crack growth has gone on for some time, the crack may have turned upwards or downwards in the web and thus be aligned in the most unfavorable orientation with respect to service load stresses.

The detail just described (Fig. 30) has been the source of many fatigue cracks in the past. New designs accommodate the situation in different ways, reducing the possibility of fatigue crack growth that is induced in this manner.

Another illustration of a case in which out-of-plane movement can produce fatigue cracks is shown in Fig. 31, where a floor beam is attached to a vertical connection plate that is welded to the web of a girder. Under the passage of traffic, the floor beam will rotate as shown. As this rotation occurs, the bottom flange of the floor beam lengthens and the top flange shortens. Lengthening of the bottom flange will not be restrained because it is pushing into the web of the girder, which is flexible in this out-of-plane direction. However, because the top flange of the girder is restrained by the deck slab, shortening of the top flange of the floor beam can only be accommodated by deformation within the gap at the top of the connection plate. This type of deformation is shown (exaggerated) in the detail in Fig. 31.

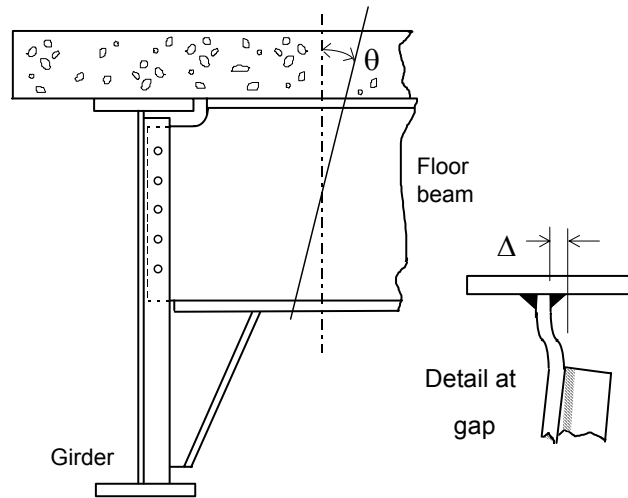


Fig. 31 Floor Beam-to-Girder Connection

The behavior illustrated in Fig. 31 has been confirmed by field measurements taken by Fisher [32]. Moreover, the field study showed that each passage of an axle caused a significant stress range at the top of the connection plate. In this situation, fatigue cracks could develop either at the weld at the top of the connection plate or at the web-to-flange fillet weld of the girder, or both. The residual tensile stress in this small gap will tend to be very high because of the proximity of the two welds. It can be expected that fatigue cracks could occur under relatively few cycles of load, although of course the fatigue life will depend largely upon the deformation, Δ , that actually takes place as a result of the rotation of the floorbeam.

EXAMPLE 10

Given:

Figure 31 illustrated a floor beam to girder connection where out-of-plane cracking could occur. The detail is repeated here, as Fig. 32. The web plate thickness is $t = 12$ mm, the length of the gap is $L = 15$ mm, and a measurement of the displacement of the gap shows that $\Delta = 0.004$ mm. What is the fatigue life of this detail?

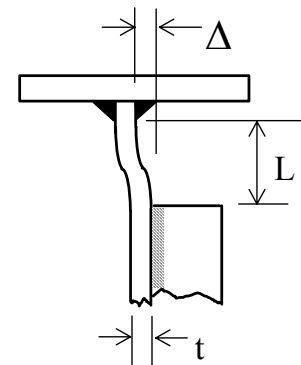


Fig. 32 Example 10

Solution:

According to the AASHTO Specification, the web-to-flange fillet weld is a Detail Category B for the in-plane bending stresses ("continuous fillet weld parallel to the direction of applied stress"). However, the weld is Category C when the out-of-plane displacement depicted in Fig. 32 takes place ("fillet-welded connection with weld normal to the direction of stress"). The fillet weld that is used to attach the connection plate to the web is a Detail Category C' ("transverse stiffener to web weld"). For the out-of-plane displacement under examination, the stress range at the web-to-flange weld and at the stiffener-to-web weld will be identical. Therefore, Category C' will govern the design.

Application of the moment-area principle, or reference to a design handbook, will show that the moment at the end of a fixed ended beam when it is displaced transversely an amount Δ at one end is

$$M = \frac{6 EI \Delta}{L^2}$$

Thus, the stress is
$$\sigma = \frac{M y}{I} = \left(\frac{6 E I \Delta}{L^2} \right) \left(\frac{t}{2} \right) \left(\frac{1}{I} \right) = \frac{3 E \Delta t}{L^2}$$

Since the displacement Δ varies each time the floorbeam rotates, the stress so calculated is really the stress range, $\Delta\sigma$. Thus, solving for $\Delta\sigma$ ($\equiv \sigma$) and using the specific values given:

$$\Delta\sigma = \frac{(3) (200\,000 \text{ MPa}) (0.004 \text{ mm}) (12 \text{ mm})}{(15 \text{ mm})^2} = 128 \text{ MPa}$$

The number of cycles that a Detail Category C' can sustain a for stress range of 128 MPa can now be calculated. From Table 2, the constant amplitude fatigue limit (threshold stress) is 82.7 MPa for a Detail Category C' and the value of the fatigue life constant is $14.4 \times 10^{11} \text{ MPa}^3$. Because the actual stress range is greater than the CAFL/2 = 41.4 MPa, the fatigue life is calculated according to Eq. 8:

$$N = M \Delta\sigma^{-3} = (14.4 \times 10^{11}) (128)^{-3} = 687 \times 10^3 \text{ cycles}$$

Comment:

This example shows that even a very small amount of out-of-plane displacement can have a significant effect on fatigue life.

6.3 Further Examples of Distortion-Induced Cracking

The distortion-induced fatigue conditions that can be present in fabricated steel members was introduced in Section 6.2 and used in Example 10. Section 6.3 provides more general comments and gives further examples for bridge structures.

6.3.1 Web Gaps in Multiple Girder and Girder Floor Beam Bridges

Diaphragms and cross-frames in multibeam bridges are used to provide torsional stiffness to the structure. The diaphragms or cross-frames are connected to the longitudinal members by means of transverse connection plates, and this often provides fatigue conditions similar to the floor beam-to-girder connection plate discussed in Section 6.2. The connection is usually made to transverse stiffeners that are welded to the girder web. In the past, it was customary that no connection be provided between the stiffener and the tension flange because this would adversely affect the fatigue detail category of the girder. Sometimes these stiffeners were not attached to either flange. Since adjacent beams deflect differing amounts under traffic, the differential vertical movement produces an out-of-plane deformation in the

web gap at the stiffener ends if they are not attached to the beam flange. The magnitude of this out-of-plane movement depends on the girder spacing, amount of bridge skew, and type of diaphragm or cross-frame.

Various types of diaphragms are used, ranging from rolled sections to simple X-bracing made of angles. Figure 33 shows the underside of a multiple girder bridge that has an X-type cross-frame bracing system. In the web gap, cracking developed in the negative moment region (i.e., top flange in tension) of this continuous span structure. This cracking is illustrated in Fig. 34, which is a view along the length of the bracing toward the girder and its transverse stiffener. The transverse stiffener to which the X-bracing is attached was not welded to the top (tension) flange for the reasons described earlier. This permitted out-of-plane displacement to occur in the web gap and, consequently, cracks formed along the web-to-flange fillet weld and at the top of the connection plate.



Fig. 33 X-Bracing and Girders



Fig. 34 Fatigue Cracks in Web Gap of Diaphragm Connection Plate

One of the earliest and most common sources of fatigue cracks in welded bridges is the cracking in the web gaps at the ends of floor beam connection plates. (See also Section 6.2.) These cracks have occurred in the web gap near the end reactions when the floor beam connection plate was not welded to the bottom (tension) flange. However, the most extensive cracking is observed in the negative moment regions of continuous girder bridges where the connection plate is not welded to the top (tension) flange of the girder. One such case is illustrated in Fig. 35. The view is toward the web of the girder. Cracking is seen along the fillet weld toe at the web-to-flange weld (horizontal crack) and at the top of the stiffener (vertical crack). The illustration shows that the floor beam has been bolted to the transverse stiffener and that the top of the stiffener has a small corner clip where it reaches the top of the girder web. The clip is provided so that the stiffener clears the girder web-to-flange fillet weld. Thus, even though the stiffener extends to the underside of the girder flange, it is not fastened to the flange and the presence of the stiffener clip creates the gap in which deformation was concentrated.



Fig. 35 Fatigue Cracks at Floor Beam Connection Plate Web Gap

6.3.2 Web Gaps in Box Girder Bridges

Internal diaphragms in various types of box girder structures are a source of web gap cracking as a result of cross-section distortion. This type of cracking has been seen both in continuous and simple span spread box girder structures.

An example of this type of cracking is shown in Fig. 36. The structure is an elevated, curved continuous span structure. Two curved steel box girders with internal diaphragms support the reinforced concrete deck. Fatigue cracking occurred in the top web gaps (negative moment region) near the piers and in the bottom web gaps (positive moment region) at the diaphragm locations. In both cases, the cracking was the result of out-of-plane movement in the web gap. This resulted from the box girder distortion and the resultant diaphragm forces.

The cracking that occurred at the top web gap is shown in Fig. 36. The photograph, which was taken inside the girder, shows the (sloping) girder web in the left-hand portion of the figure, a transverse connection plate welded at right angles to it, and a gusset plate (horizontal) that formed part of the lateral bracing used for shipping and construction. The gusset plate is about 80 mm below the top of the connection plate and there is a small gap between the top of the transverse connection plate and the underside of the girder flange. (The photograph shows that a loose plate has been placed in this gap above the connection plate. It was later fastened in place in order to prevent further movement of the girder web in



this region.)

Fig. 36 Web Gap Cracking at Box Girder Diaphragm Connection Plate

Fatigue cracking has also been observed in the bottom web gaps at the locations of internal diaphragms in simple span steel box girders. An example of this type of cracking is shown in Fig. 37. These cracks are also the result of out-of-plane distortion in the web gap. The web gap displacement results primarily from torsional distortion of the box girder when eccentric loads are applied to the structure.

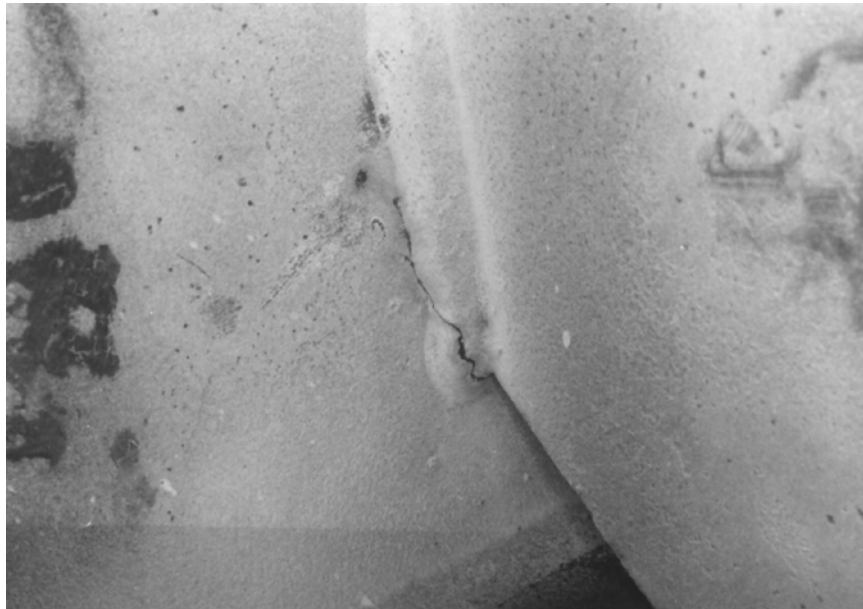


Fig. 37 Web Gap Cracking at End of Transverse Connection Plate

6.3.3 Long Span Structures

A number of tied arch structures have been built in which the floor beams are framed into the arch tie girder with web shear connections alone. No direct connection is provided between the floor beam flange and the tie girder. In older structures, the floor beam end connections were riveted. In such instances, the double angles are riveted to the floor beam web and the outstanding angle legs are riveted to the tie girder. In more recent arch design, a transverse welded connection plate on the tie girder webs is utilized. If this is the case, then the floor beams are bolted to the welded transverse connection plate.

Cracks have been observed in the floor beams of structures with either riveted end connections or welded transverse connection plates. The cracks form in the floor beam web along the web-to-flange connection at the floor beam web gap. This gap is present between the end of the connection angles or at the end of the welded connection plates. The cracks extend parallel to the floor beam flange along the length of the web gap and then begin to turn and propagate toward the bottom flange. Figure 38 shows a crack in the web gap of the floor beam just above the end connection to the tie girder. The photograph also shows a drilled hole at the left-hand end of the crack. As will be discussed in Chapter 8, this is often an effective way of stopping the further growth of a crack.

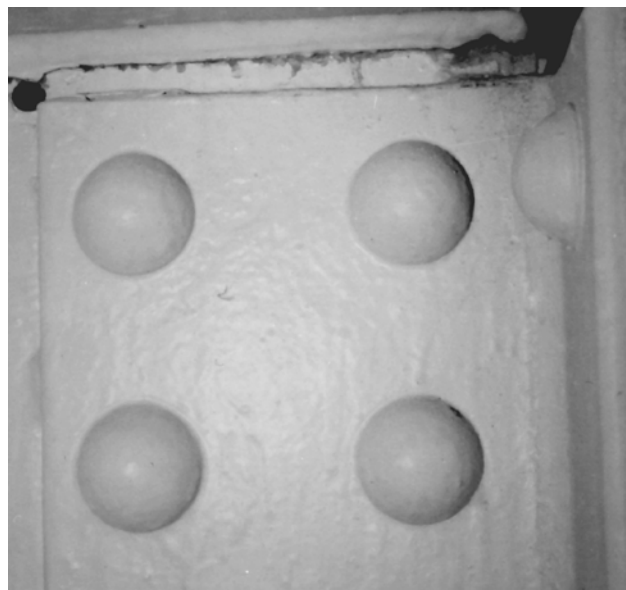


Fig. 38 Floor Beam Web Gap Crack at End Connection to a Tie Girder

Similar cracks have been observed in long span trusses where floor beams are connected to the bottom chord panel points.

Cracks have also developed in box tie girders at internal diaphragms. The fatigue cracking occurred in tie girder web gaps (created by internal diaphragms) at the floor beam locations as a result of the web gap out-of-plane distortion. The web gap distortion is the result of the bending of the floor beams and the relative movement between the two tie girders. This creates diaphragm forces that torsionally deform the tie girders.

6.3.4 Coped Beam Connections

In order to facilitate the easy connection of one flexural member to another, the flange of one of the members is often cut back, as is illustrated in Fig. 39 (The detail shown was used extensively in the past in through-girder railway spans.) In other cases, the flanges may simply be narrowed: this is called a "blocked" beam. Fatigue cracking at coped beam locations is not so much related to distortion-induced fatigue as it is illustrative of cracking at a location where the calculated stress is zero.

In the case of coped beams, either the top or bottom flange, or both, may be coped. The cope is generally made by flame-cutting the material, and experience shows that workmanship is often unsatisfactory. The radius of the cope may be small and the cutting done unevenly. In addition to the potential for fatigue cracking created by such workmanship, the flame-cutting process can leave a region of hardened and brittle material adjacent to the cut.

The coped end of the beam is at a location of theoretical zero stress since the connection must necessarily be one that does not transmit moment and the shear force is carried by the web. Nevertheless, the region of the cope will have stresses due to bending because of the restraint at the connection. There are many examples of fatigue cracking at cope locations [20], and the best solution in the case of new designs is to avoid copes entirely. If copes must be included, execution of the work and inspection must be of a high standard. Specific information on the fatigue life of a coped beam can be found in Reference 34.

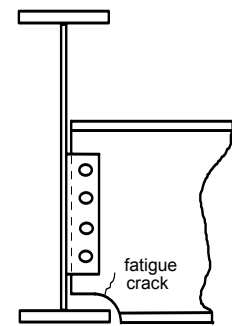


Figure 39 Bottom Flange of Floorbeam Coped at Connection to Girder

6.3.5 Connections for Lateral Bracing

The connection of lateral bracing to girders should be done as close to the plane of the bottom flange as possible. (In this discussion, it is assumed that the top flange will be braced by the deck.) Sometimes, the connection between the lateral bracing system and the girder will be to a horizontal plate welded to the girder web. (In the AASHTO Specification, this is termed a "lateral connection plate.") If transverse stiffeners are present, usually the case, the arrangement will be as shown in Fig. 40.

In the illustration, the horizontal connection plate is fitted around the vertical transverse stiffener and welded to it where they are in contact. In other arrangements, the vertical stiffener passes clear through a slot in the horizontal plate without attachment at that location. In either event, it is highly likely that a gap will be left in the region shown in order to avoid intersection of the horizontal and vertical welds. Consequently, as the bracing forces push into and pull on the web at this location, the web will rotate about a vertical axis formed by the back of the vertical stiffener and the plane of the web. Because the web is very flexible in the out-of-plane direction, this causes large strains in the web in the gap region when the lateral connection plate is not attached to the transverse stiffener. The region is also a zone of high residual stresses because of the proximity of the vertical and horizontal welds. Lack of fusion in the weld or other micro-defects can also be anticipated at the weld terminations. Taken all together, these conditions mean that the type of detail shown is very susceptible to fatigue crack growth [25, 33].

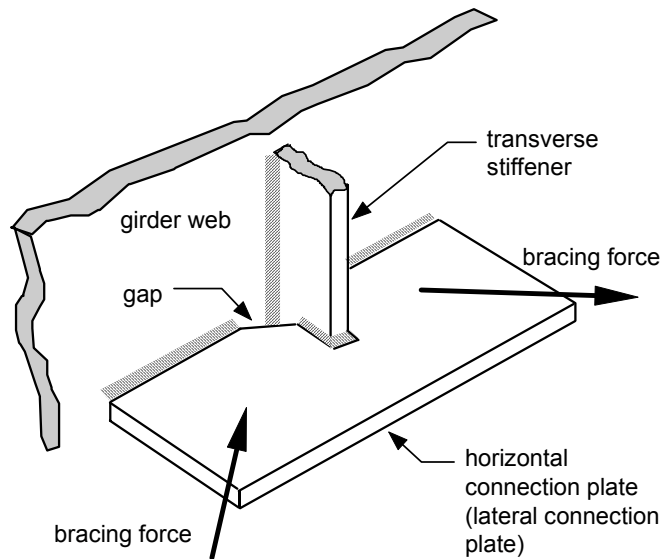


Fig. 40 Connection of Lateral Connection Plate

6.3.6 Other Examples

Many end connections are designed as "simple," that is, it is assumed that no moment is transmitted. However, even simple connections do carry some moment, and this means

that the connection elements will deform under the moment. End rotation at web framing angles causes the angles to deform and load the rivets, bolts, or welds in ways not contemplated by the design. If the loading is cyclic, fatigue cracks may develop in the angles themselves or in the bolts, rivets, or welds. In the cases of the mechanical fasteners, prying forces develop that may cause fatigue cracking under the heads or nuts.

Another example of distortion concentrated in a small space is when a beam or girder flange is loaded directly. The most obvious example of this is the case of railway beams or girders. Particularly in older bridges, it was common to place the ties directly on the top flange of the flexural members in the floor system. Thus, a stringer flange, for example, can be rotated as traffic passes over the structure. If the flange is too flexible in this direction, cracking can occur at the web-to-flange junction.

6.4 AASHTO Specification Requirements Relating to Distortion-Induced Fatigue

Based on the discussion and examples thus far in this Chapter, it can easily be appreciated that it is difficult for a specification or design standard to provide very much in the way of explicit rules relating to distortion-induced fatigue. The AASHTO design specification provides a separate section on distortion-induced fatigue (Article 6.6.1.3). It contains a general statement that stresses the importance of proper connection of transverse components to longitudinal (i.e., main) components. Sub-sections then offer specific information relating to transverse connection plates (Article 6.6.1.3.1), lateral connection plates (Article 6.6.1.3.2), and orthotropic decks (Article 6.6.1.3.3).

Article 6.6.1.3.3 simply directs the reader to Article 9.8.3.7, which gives detailing requirements for orthotropic decks. Those requirements are mainly a reflection of good practice and experience derived from this type of deck construction. The articles relating to connection plates provide rules for this important topic of girder detailing. As has already been illustrated in this Chapter, cracking resulting from improper detailing of connection plates is a significant source of fatigue cracking in bridges. Example 11 will illustrate some of the features of this section. Article 6.6.1.3 also alerts the user to the possibility of fatigue cracking as a result of excessive out-of-plane flexing of a girder web. This will be illustrated in Example 12.

6.5 Design Examples

EXAMPLE 11

Given:

In Example 9 (Chapter 5), a lateral connection plate was examined for its load-induced fatigue life. (See "Fatigue Life Assessment of Lateral Bracing Attachment" in that example.) One possible solution was to center a horizontal plate around a transverse stiffener, as shown in Fig. 29. According to Example 9, the plate had to be located 455 mm above the bottom of the girder in order to meet the requirements of the load-induced stresses. Is this arrangement satisfactory with respect to distortion-induced fatigue?

Solution:

The AASHTO requirements for distortion-induced fatigue of a lateral connection plate are given in Article 6.6.1.3.2. If the connection plate is not attached to the flange, the preferable solution, then in the case of a stiffened web it should be attached not less than one-half the flange width above or below the flange. This minimum distance requirement is to ensure that distortion-induced fatigue cracking does not take place in the web between the lateral connection plate and the flange. The maximum flange width in this girder is 609.6 mm (see Example 9, Table 4). Thus, the AASHTO requirement is that the horizontal connection plate be at least 305 mm above the flange. The distance identified as satisfactory for load-induced fatigue, 455 mm, therefore is satisfactory also for distortion-induced fatigue.

Comment: Recall that this stiffener arrangement was not the preferred solution, however. See Example 9.

EXAMPLE 12

Given:

Does the web of the girder used in Example 9 (Chapter 5) meet the AASHTO distortion-related fatigue requirements for webs?

Solution:

The possibility of fatigue due to web flexing is first cited in AASHTO Article 6.6.1.3, but this simply refers the reader to Article 6.10.4. The requirements for the case of flexure, Article 6.10.4.3, are given only for girder webs that have no longitudinal stiffeners. (If longitudinal stiffeners are present, it is considered that web flexing will not occur to any significant extent.)

For flexural stresses, if

$$\frac{2D_c}{t_w} < 5.76 \sqrt{\frac{E}{F_{yc}}}, \quad \text{then it is required that } f_{cd} \leq R_h F_{yc}$$

In these expressions, D_c is the depth of the web in compression, t_w is the web thickness, E is the modulus of elasticity of steel, F_{ys} is the yield strength in the compression flange, and f_{cd} is the maximum compressive stress, due to the fatigue load, in the compression flange. The term R_h is a flange stress reduction factor. For homogeneous girders, its value is unity.

(The AASHTO Article 6.10.4.3 actually gives a three-part rule, of which only the governing one for this example has been presented here.)

The expression on the right-hand side of the first inequality is equivalent to the allowable web slenderness given in the allowable stress design provisions of the 1992 AASHTO allowable stress design specification. In other words, when this requirement is met the web is stocky enough that it will remain elastic under working loads. Note that the requirement deals with stress, not stress range as is done generally for fatigue life checks. According to Article 6.10.4.2, the flexural stress resulting from the fatigue load is to be taken as twice the calculated value. This is consistent with the requirements explained in Section 5.3.2.

The depth of the web in compression will be greatest in Field Section 2, where the girder is non-composite. According to Table 4, $D_c = 1524/2 = 762$ mm and $t_w = 11.1$ mm. The yield strength of the compression flange material is 345 MPa. Thus—

$$\frac{2 \times 762}{11.1} < 5.76 \sqrt{\frac{200\,000}{345}} \quad \text{or,} \quad 137 < 139$$

Since the inequality requirement is met for the quantities associated with this girder, then the compressive stress (resulting from the fatigue load) in the flange can be as large as the yield strength of the flange. Recall, however, that the compressive stress is to be taken as twice that calculated for the fatigue load.

In this girder, calculations show that the maximum compressive stress in the compression flange due to two times the fatigue load is 149 MPa. Since this is less than the permissible (345 MPa), fatigue cracking due to web flexing is not a concern.

Comments:

1. An experienced designer would probably recognize that this girder has a relatively stocky web and that flexural web buckling leading to fatigue is unlikely. Based on the

calculations already done, it will be concluded here, without calculation, that fatigue resulting web buckling due to shear will likewise not be a concern. The AASHTO rule for this case is presented in Article 10.6.4.4.

2. It should be recalled that the possibility of fatigue cracking due to web flexing was also the subject of Section 6.3.5. In that case, the web flexing was local—the region in the vicinity of a transverse stiffener and a horizontal connection plate was under examination.

6.6 Summary

Out-of-plane distortion that is concentrated in small web gaps remains a large source of fatigue cracking in bridge structures. It develops in nearly every type of bridge structure including trusses, suspension bridges, plate girders, box girders and tied arches. It is fortunate that most of the cracks that develop from local distortion lie in planes parallel to the load-induced stresses. In addition, since stress intensities around distortion-induced cracks may decrease with increasing crack length, cracks can slow, and even stop, once a certain flexibility has been provided. As a result, distortion-induced cracks have not caused significant numbers of fractured flanges or hampered the load-carrying capability of the bridge member in which they form.

Chapter 7 Inspection and Repair of Fatigue Cracks

7.1 Introduction

It is the responsibility of the engineer to evaluate the fatigue life of an existing structure, and then, if necessary, to advise on a protocol for inspection. If the inspection reveals that cracking is present, then the responsibility will extend to recommendations for remedial action. The previous chapters have given the scientific foundation for the fatigue life evaluation. This chapter provides recommendations directed toward helping the engineer devise a plan for inspection and then to decide what to do if a crack is discovered. Ideally, decisions should be based upon a scientific understanding of crack propagation, combined with knowledge gained through practical experience of examining steel structures and dealing with cracks found in those structures. Often, when a crack is found in a steel structure more careful inspection will reveal additional cracks in similar elements. If no action is taken to eliminate the cause of cracking, more cracks usually appear at other locations. For these reasons, the discovery of a crack should be taken seriously by the inspection team and reported immediately to the engineer responsible for the structure. Quick fixes, carried out by untrained personnel, often worsen the problem.

7.2 Protocol for Fatigue Crack Investigation

Based on the forgoing, a reasonable protocol for fatigue crack investigation is as follows:

- Carry out a remaining fatigue life analysis based on load-induced fatigue. If this analysis identifies details that have little or no remaining fatigue life, these locations are then candidates for an examination when a physical inspection of the structure is carried out.

The principles of the remaining fatigue life assessment have been covered in earlier chapters of this document. For important structures, it may be appropriate to carry out field measurement of strains. This will provide a better estimate of load-induced stresses. Global strains calculated using the conventional methods of analysis are usually conservative. At the same time, local strains are often not even identified by the traditional methods of structural analysis.

- Use the shop drawings of the members that make up the structure to help identify those details that are susceptible to distortion-induced fatigue.

- If a physical inspection of the structure is indicated, this should be carried out by trained personnel. (Methods of inspection are discussed later in this chapter.)
- If cracks are located, consider appropriate repair methods and advise on inspection procedures subsequent to the repairs.

7.3 Identifying the Causes of Cracking

Cracks in a structure may be identified as a result of an examination that starts with fatigue life assessment, as described in Section 7.2, but they may simply be seen in a routine inspection of the structure. The first decision that must be made following the discovery of cracks is whether the structure is safe in its existing condition. The examination at this point can lead to one of several options.

- The structure is deemed to be unsafe for the intended use and it must be shut down.
- The structure is deemed to be safe providing that load levels are reduced.
- Because of redundancy, the structure is deemed to be safe at existing load levels even though cracks have been identified. It is possible that, although remedial action is not required, continued monitoring of the structure is indicated.

In those instances where the structure is not shut down for use, an attempt should be made to determine the causes of cracking before any corrective action is taken. Although this course of action seems obvious, often it is not followed in practice. Fatigue crack growth mechanisms are activated by factors such as large numbers of stress ranges, severe stress concentrations, dynamic magnification (impact), out-of-plane displacements, corrosion damage, inappropriate fabrication procedures, bad welding processes, and large defects. Frequently, more than one factor contributes to a critical situation. It is important that the repairs account for the causes of the cracking.

The parameters that effect the stress ranges at a given location can be difficult to quantify. For example, the effect of truck passages over a worn expansion joint at the end of a bridge may be impossible to evaluate without strain gauge measurements. Stress ranges brought about by temperature changes and other types of deformation-induced stresses (sometimes called secondary stresses) present similar problems. Occasionally, signs of high stresses, such as wear marks on contact surfaces or visible out-of-plane movement, indicate that the structure is subjected to high stress ranges. Often, the most accurate evaluation possible can not do more than provide a list of candidate factors ordered according to their importance. In some instances, examination of a crack segment removed from the structure can assist a specialist in the determination of the most probable causes. See reference [25].

Knowledge of stress ranges is usually related to the accuracy of estimates of the number of fatigue cycles applied to the structure. If possible, this information should be checked against recommendations for fatigue strength in the design specification in order to determine whether cracking would be expected under such circumstances. Note that if cracking is visible, it may be assumed that there is no remaining fatigue life at that location, and therefore a check can be performed using standard relationships between stress range and total fatigue life. The reason for making such a check is that if fatigue cracking cannot be explained in this way, all sources of fatigue loading may not have been identified. The fact that the structure has survived without fatigue failure for a given period may be the only piece of information available that is completely certain.

When fatigue loading information and code recommendations cannot explain fatigue cracking, other factors not covered by fatigue strength curves—such as large defects due to poor fabrication methods, out-of-plane movements, and the effects of corrosion—may have influenced cracking. Special requirements exist for the fabrication of steel structures subjected to fatigue loading. For example, eccentricities due to fit-up that may be acceptable for some structures might weaken a structure subjected to fatigue loading. The structure should be examined for evidence of large eccentricities, corrosion damage, and fabrication-induced discontinuities. Note that lack of weld penetration which is oriented transversely to the direction of fatigue loading is equivalent to an initial crack. (See Figure 5.) These discontinuities are the result of poor fabrication and quality control.

7.4 Cracking at Low Fatigue Strength Details and Defects

Frequently, cracking in welded bridge structures is the result of *i*) flaws that escaped detection, *ii*) the use of details more severe than assumed in the design, or *iii*) secondary and displacement-induced stresses. (Except for secondary and displacement-induced stresses, comparable conditions do not develop in riveted and bolted bridge structures.) Most critical cracks exist in tension areas. When details are located in compression stress regions and no possibility of stress reversal exists, there is a reduced fatigue risk. Under these conditions, crack growth will be confined to the residual tensile stress zone of the detail unless out-of-plane deformations occur.

It is appropriate to examine further some low fatigue strength details that have been or are being used in steel bridges. Those design details that fall into AASHTO Category E or E' are particularly susceptible to fatigue crack growth in steel bridges. The lowest fatigue rating, Category E', is seen in cover-plated beam bridges that have flange thickness greater than 20 mm. Although the use of cover-plated steel beams has almost disappeared from use

in new structures because of its low fatigue rating, many existing bridges have these beams. However, details that are equivalent to the cover-plated beam continue to be used. These include certain longitudinally or transversely loaded groove-welded or fillet-welded gusset plates or other attachments.

Figure 41 shows the bottom flange of a rolled steel shape to which a cover plate has been attached by welding. A fatigue crack is present in the rolled section. It started at the toe of the fillet weld at the location of the cover plate termination. In addition to the usual conditions of potential crack growth at the toe of a fillet weld, there will be a significant stress concentration at this location of abrupt change in cross-section. In this case where a transverse end weld is present, it is likely that multiple initiation sites are present. They eventually link together as the small individual cracks grow and coalesce to form a single large crack. Even if the transverse weld were not present, fatigue cracking from the termination of the longitudinal welds (or the longitudinal weld end returns) is highly likely.



Figure 41 Fatigue Crack at End of Cover Plate

Another low fatigue strength detail is the welded web gusset plate, such as the one illustrated in Fig. 42. These are particularly susceptible to crack growth when they are adjacent, but not attached, to transverse stiffeners and connection plates. In the figure, the horizontal gusset plate is the dark area at the top of the photo. A transverse (vertical) web stiffener passes through a rectangular hole in the gusset plate. A fatigue crack is seen emanating from the fillet weld region near the junction of the rectangular hole and the girder web. As the crack moves downward, it is intercepted by a retrofitted hole intended to stop the crack from moving into the lower flange of the girder.

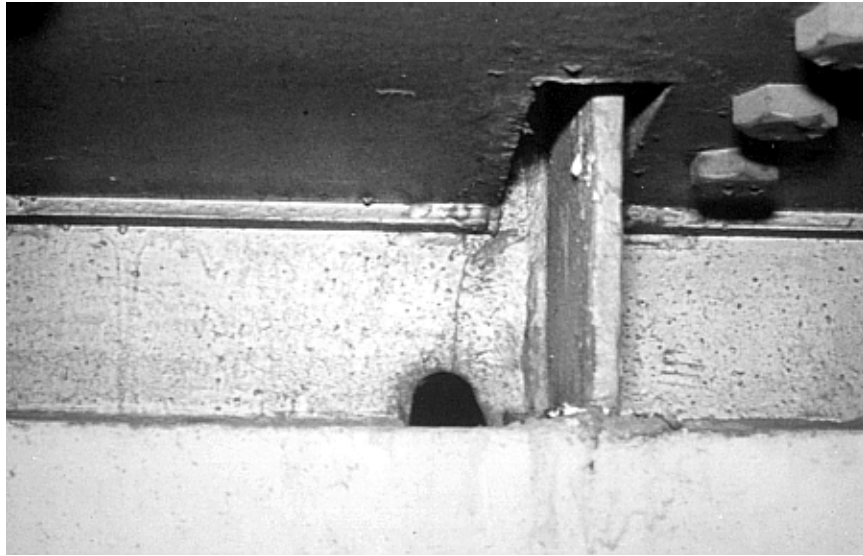


Figure 42 Fatigue Crack at Web Gusset

The fatigue crack shown in Fig. 42 was the result of combined cyclic stresses—those from the expected in-plane stress and those from the unexpected out-of-plane stress in the web gap. The latter stress develops from the lateral forces that cause the gusset plate to twist and deform the web gap. This phenomenon was discussed earlier: see Section 6.3.5.

The use of low fatigue strength details such as cover-plated beams and welded web and flange gusset plates should be avoided on bridge structures that will experience large numbers of stress cycles during their design life. If cover plates are used on high volume bridges, they should extend full length of the girder.

There are several other Category E or E' details that are susceptible to fatigue cracking at weld terminations. Typical of these structures and cracking is the small crack shown in Fig. 43. It originated at the end of a longitudinal fillet weld that was used to attach a 0.9 m long lateral connection plate to the underside of the floor beam flange. (The longitudinal weld is located at the junction of the top side of the connection plate and the edge of the flange. In Fig. 43, the edge of the floor beam flange is the element with the descriptive marking "FB 28 S.") The cracks were small, and it was possible to retrofit these details by grinding and peening the weld terminations.

Large initial defects and cracks that result from poor quality welds are a primary source of fatigue crack growth. In many cases, however, it is not appreciated that the welding of so-called secondary members or attachments must meet the same weld quality criteria and nondestructive test requirements as for main members. Even though the secondary member does not carry calculated stress, its welded connection to a stress-carrying member means



Figure 43 Fatigue Crack at Lateral Gusset Plate Welded to Floor Beam Web

that stress concentrations, initial defects, and so on directly influence the fatigue life of the main member. An example of a detail this category is a splice in a longitudinal girder web stiffener. The longitudinal stiffener fulfills its purpose without carrying significant stress. If the welding of the stiffener to the web is not expected to meet high quality control and inspection requirements because it is a secondary attachment, fatigue cracking can be the result.

The girder web shown in Fig. 44 is the fascia girder of a nine-girder four-span bridge on an Interstate highway [20]. The bridge was approximately nine years old when the fatigue crack was discovered. The fracture initiated at an unfused groove weld that was used to join sections of the longitudinal stiffener. It grew both upward (to about the mid-depth of the girder) and downward. The lower end of the crack had penetrated the bottom flange of the girder. A second crack was discovered later in the same girder. It had also started from an unfused groove weld in the longitudinal stiffener,



Figure 44 Crack in Girder Web from Splice in Longitudinal Stiffener

but had only severed the stiffener and not yet penetrated the web when it was discovered.

A condition related to that just described occurs when backing bars are used to make a groove weld between transverse stiffeners and a lateral gusset plate. Lack-of-fusion often exists adjacent to the girder web in the transverse groove welds. If the transverse welds intersect the longitudinal welds, they provide a path for a crack to enter the girder web.



Figure 45 Lack-of-Fusion Defect Adjacent to Backing Bar at Gusset Stiffener Weld

Cracks that develop in the web at lateral connection plates generally start at the location of intersecting welds. The horizontal gusset plate used to connect diaphragm and lateral bracing members to a longitudinal girder is often slotted to fit around a transverse stiffener. In the U.S., one of the first structures to exhibit this cracking was the Lafayette Street Bridge over the Mississippi River at St. Paul, Minnesota [20]. Figure 45 shows the junction of the horizontal gusset plate (foreground) with girder web (right-hand side of photo) and the vertical transverse stiffener. The connection between the horizontal gusset plate and the vertical stiffener was made using a groove weld founded on a backup bar. However, the groove weld did not penetrate to the backup bar, particularly near the girder web. This meant that there was a significant lack of fusion in a plane perpendicular to the main stress field in the girder. Since this weld also intersected both the vertical weld attaching the stiffener to the web and the longitudinal weld attaching the gusset to the web, a path was provided into the girder web. Examination of the fracture surface showed that a brittle fracture occurred after the fatigue crack propagated into the web. The final condition of the girder was that the crack had completely severed the lower flange and had stopped

about 150 mm above the horizontal stiffener, which itself was about 150 mm above the flange.

7.5 Methods for Inspection for Fatigue Cracking

In Section 7.2, it was stressed that it is desirable that any inspection for fatigue cracking be preceded (if possible) by an analysis of the structure and by identification of details prone to out-of-plane cracking. Inspection is usually a difficult and expensive process, and these preliminary steps will help to focus the inspection on the high-risk regions of a structure. A knowledge of where cracking is likely to occur in a detail that has been identified as prone to fatigue damage is likewise an important adjunct to the inspection process itself. Clearly, the goal is that the inspector be able to concentrate on those details that are candidates for cracking and thereby be able to direct resources to the locations where fatigue cracking is likely to occur. It is unusual to be able to inspect every part of a given structure for fatigue cracking: time and money do not permit this except in the case of specialized structures.

The next step is to identify the inspection methods that are both appropriate for the expected manifestation of cracking and are cost-effective. As will be seen, some inspection tools are better for picking up certain types of fatigue cracks than are others. The inspection methods or tools that are in common use today include visual inspection (sometimes at low power magnification), ultrasonic inspection, magnetic particle inspection, and use of acoustic emission techniques.

Before cleaning the surfaces to be examined, a visual inspection is essential. Often the most reliable sign of fatigue cracks is the oxide (i.e., rust) stains that develop after the paint film has cracked. Similarly, oxides can be seen on unpainted weathering steel surfaces when cracks develop. They are visually apparent because they differ in appearance from the protective oxide coating that has formed normally on the weathering steel. Magnification (10x) is helpful, as is supplementary lighting. Experience has shown that cracks have generally propagated in depth to between one-quarter to one-half the thickness of the part before the paint film is broken, which permits the oxide to form. Cracks smaller than this are not likely to be detected visually unless the paint, mill scale, and dirt have been removed by blast-cleaning the suspect area. At weld terminations, very small cracks are difficult to detect by visual inspection even on cleaned surfaces unless the crack depth is between 3 and 6 mm. It should also be kept in mind that the inspection usually takes place when the live load stresses are small. This means that an existing crack will not be held open by the stress field.

The following inspection methods are useful:

- Dye penetrant inspection. This is the most common and least expensive inspection method. A low viscosity, high capillary fluid (usually a red dye) is used to penetrate into surface cracks. After cleaning and drying, a second material, called a developer (usually white), is sprayed on in order to draw, by capillary attraction, the penetrant fluid from cracks. When the developer is applied to the opposite face, through-thickness cracks can be detected. When used correctly, this method is reliable for detection of surface cracks emanating from smooth surfaces. However, for cracks growing from weld toes, it is often difficult to distinguish between a crack and the plate/weld toe interface.
- Magnetic particle inspection. When a magnetic field in a steel plate encounters a discontinuity, the field becomes distorted. Fine magnetic particles are sprayed or dusted on the object in order to detect such distortions. Clusters of particles form at crack tip locations. As with dye penetrant inspection, this method works most effectively on smooth surfaces. Accuracy is reduced when used on weld surfaces, but reasonable results can be obtained by an experienced inspector. Even sub-surface cracks can be detected if the depth below the surface is not too great. Equipment is simple and portable.
- Ultrasonic inspection. This method uses high frequency sound waves at a pitch beyond that audible to the human ear. These waves are picked up by a receiver and a crack will cause a distortion in the waves received. This method can be used for any thickness of plate over 3 mm and, once calibrated, it can detect small cracks whether they are embedded or not. Variations in surface roughness affect accuracy. The orientation and size of the crack are not always easy to visualize and, therefore, use of this method requires considerable experience.
- Acoustic emission. This method of assessment uses the high frequency sound wave that is generated by crack extension. Sensitive piezoelectric sensors convert the very high frequency vibrations (several hundred kilohertz) generated by a propagating fatigue cracks into electrical signals that are detected and analyzed. Most available systems are not directly engineered for bridge monitoring, however. In addition, relatively large cracks must be present for the system to be effective.
- X-ray Inspection. Under controlled conditions, radiography can be used to identify the presence of defects and cracks. It is not particularly helpful when the actual sizes

of the crack are desired, however. Its primary use has been to evaluate groove welds where lack-of-fusion may exist.

- Coring. An effective way to establish the type of defect or crack is to core and remove a segment of the crack or discontinuity. This permits a destructive assessment of the section within the cores. In this way, the actual size of the crack can be established and this can often be used to calibrate and interpret ultrasonic and radiographic results. After the core has been removed, the opening should be ground smooth and then inspected with liquid penetrant to ensure that no crack extends beyond the hole. In some cases, a high-strength bolt is inserted into the core opening and preloaded.

7.6 Repair of Fatigue-Cracked Members

Repairing a cracked element is an obvious option, but other possibilities should also be considered. Appropriate measures could also include implementation of damage tolerance strategies and element replacement. When damage tolerance strategies are used, no immediate action is taken to repair the crack or replace the element. (However, often holes are drilled at the crack tip in order to minimize crack extension.) Repair can be delayed, thereby making it possible to avoid repairs at inconvenient times. Furthermore, this strategy often provides the opportunity to determine the causes of cracking more precisely. However, damage tolerance should not be employed when rupture of the element would cause general collapse of the structure; when continued cracking would endanger human life through increased deformations (for example, an increased risk of derailment due to cracking of a railway bridge girder); when monitoring crack growth at regular intervals is not possible; or when further cracking may substantially increase repair costs.

In order to ensure that a damage tolerance strategy is successful, additional measures are recommended. Fracture mechanics analyses should be employed to predict crack growth and to determine critical crack lengths, i.e., crack lengths at which fracture would be expected. Laboratory testing of specimens (Charpy V-notch, CT, etc.) made from steel taken from the structure may be needed. Crack measurement equipment should be calibrated and verified on a regular basis. Also, any modifications to the structure or changes to the applied loading should be assessed in order to verify that the structure can safely tolerate further cracking.

Repair of cracks, when carried out correctly, may result in an adequate solution to fatigue cracking provided that the steel quality is appropriate for both present and future service conditions. However, when repairing fatigue cracks, it is important to keep in mind

that repair welding is rarely successful, and therefore weld repair should be employed as a last resort when no other solution is possible. The following is a list of measures that have been employed successfully for steel structures containing fatigue cracks. These measures are ordered (roughly) from best to worst.

- Place cover plates over the crack in order to provide a load path for forces and to restrict movement of the crack surfaces during fatigue loading. Preferably, these cover plates should be placed on both sides of the cracked plate, and they must be attached with pretensioned high-strength bolts. If this solution is adopted, it is essential to ensure that the fatigue crack growth has stopped. Crack growth may be stopped by changes to the structure itself (reduce the stress range, stop out-of-plane movement, etc.), or in some cases it may be done by drilling a hole at the end of the existing crack. The latter procedure is discussed following.
- Drill a hole at the end of the crack and fill the hole with a pretensioned high-strength bolt. The bolt should be pretensioned according to code provisions for bolted assemblies. See reference [25] for guidance regarding appropriate hole diameters. Care must be taken to ensure that the crack front is intercepted by the hole. (Drilling a hole at the end of an existing crack changes the crack from sharp to blunt, thereby greatly increasing the force required to drive the crack. Use of a pretensioned bolt introduces a local compressive stress, which has the effect of masking the tensile stresses that drive the crack.)
- Cut out and re-fabricate parts of elements in order to reproduce the same conditions that existed at the crack site before cracking occurred. Employ fatigue strength improvement methods to increase fatigue resistance. This measure is most effective for cases in which fatigue cracks have grown from weld toes and when cracking in another, unimproved location is unlikely.
- Air-arc gouge the crack, fill the gouged area with weld metal, grind away weld reinforcement, polish smooth and inspect for weld defects using ultrasonic and X-ray inspection technology. This measure should be accompanied by some modification that reduces the fatigue stress range in the region surrounding the crack.
- Peening the toe of a weld termination that is perpendicular to the stress range is an effective way to prevent small cracks (less than 3 mm deep) from propagating. Peening introduces compressive residual stresses and also changes the size of the weld toe crack. It effectively increases the fatigue resistance by a category.

- Gas tungsten arc remelting has been demonstrated to effectively remove the micro-discontinuities at the weld toe and decrease the stress concentration. It also improves the fatigue resistance by about one category. Experimental field trials demonstrated that it was difficult to execute while the bridge was in service because of vibration. Also, an embedded crack sometimes resulted because the penetration did not follow the crack path. The procedure seems best suited for shop use and new construction.

Finally, any measure that lowers the stress ranges in the area around the crack will contribute to the success of a repair. Care should be taken to ensure that cracking at other locations is not triggered as a result of these measures. Such consequences are most likely when the local stiffness of the structure is modified, thereby altering the sensitivity of the structure to dynamic loading.

When damage tolerance strategies are not appropriate and when no repair option can be implemented, replacement of the cracked element may be warranted in those situations where it is possible to remove and replace the element. In the presence of corrosive environments, and when there is any doubt regarding the grade of steel used in the structure, employ a steel grade that is more suited to the situation.

Replacement using a larger element than that originally present will result in lower stresses at the location where the crack was detected, and, for this reason, use of a larger element is often warranted. However, a larger element alters the stiffness of the structure. Consequently, the effects of this change in stiffness should be studied in order to ensure that problems are not created elsewhere.

After removal of the cracked element, all connections should be inspected for cracking. Reuse old connection material only if it can be demonstrated that it has not been damaged by the incidence of cracking in the element. Although connections may not be cracked, they may be damaged due to excessive movement. Do not reuse bolts that were used in the old element for connecting the new element.

Fabrication work on the new element should be performed where adequate quality of workmanship can be assured. Work on-site should be avoided, especially if such activity does not contribute to reducing built-in-stresses and eccentricities. Therefore, site work should be limited to actions such as drilling under-sized holes to fit and other joining techniques that are intended to ensure good fit and satisfactory alignment.

7.7 Avoiding Future Cracking Problems

If fatigue cracking has been discovered at one location in a structure, it is likely to be present at other similar locations. Consequently, if nothing is done to improve conditions at those places, development of fatigue cracks is probable in the future. Therefore, such locations should be identified and measures for improvement of their fatigue resistance should be considered.

Measures that lower the stress ranges in the structure are the most effective way of preventing further crack growth. Care should be taken to ensure that susceptibility to fatigue cracking is not increased elsewhere as a result of these measures. Such consequences are most probable when the local stiffness of the structure is modified, thereby altering the response of the structure to vibration and other loading.

Effective measures for avoiding future cracking problems usually fall into one of the following categories:

- reduction of applied stress ranges
- reduction of dynamic magnification (impact)
- reduction of number of cycles of damaging stress ranges
- decrease in vibration through damping, addition of mass, or a change in restraint
- use of fatigue-strength improvement methods at critical locations (e.g., gas tungsten arc remelting at weld toes, peening)
- holes drilled in webs will often be effective in prevention of future damage. Holes not only arrest cracks, but they can be used to improve problem details such as flanges that penetrate webs.

Corrosion-induced cracking can be avoided by protecting the structure from the environment, not allowing water and debris to become trapped on the structure, by providing adequate drainage (for example, for de-icing salts) and, finally, through modifying areas sensitive to electrolytic action.

The following general precautions are recommended for the structure as a whole:

- Identify areas in the structure where cracking would create a dangerous condition. Use the same criteria as those used to judge whether further cracking can be tolerated for implementation of a damage tolerance strategy. Mark these areas for modification and inspection.

- If new information is received regarding the structure or if structural modifications are significant, reconsider decisions made regarding the management of the structure.
- Inspect repair locations regularly in order to verify the effectiveness of repair measures.
- Create conditions whereby the structure can be inspected as easily as possible. This involves measures such as keeping the structure clean, providing safe access to critical locations, and designing modifications considering in-service inspection.
- All modifications should be designed with the goal of making the structure as fail-safe as possible. Fail-safe means that the structure can tolerate failure of one or more elements before a catastrophic condition arises. This condition must be preceded by a period that is long enough to identify cracking and to take appropriate action.

Chapter 8 Special Topics

This chapter contains a number of topics that will be of interest in specific cases. The topics include fatigue strength of bolted or riveted members, threaded fasteners, the influence of environmental effects upon fatigue life, the role of residual stresses in fatigue crack growth, fatigue under combined stresses, and comments on the use of fracture mechanics in fatigue strength evaluation.

8.1 Bolted or Riveted Members

Fatigue characteristics of bolted connections, riveted connections, anchor bolts, and threaded rods are discussed in this section. The need for information on all of these topics is self-evident, except perhaps for riveted members. Rivets have not been used in new construction for a considerable period of time, but an understanding of the fatigue life characteristics of riveted connections is needed because of the necessity for evaluating the remaining fatigue life of existing structures. There are tens, perhaps hundreds, of thousands of existing riveted structures still in use in North America. Most of these are bridges, and their remaining fatigue life and safety is a topic of great importance to the owners and to regulatory authorities.

8.1.1 Bolted Members

High-strength bolted joints can be subdivided into two categories; those which are lap or butt splices ("shear splices") and those which are tension-type connections. In the former case, the bolts can be either preloaded or not preloaded, although in new construction most specifications require that the bolts be preloaded if fatigue loading is likely. It has always been common practice in bridge construction to use preloaded bolts.

The fatigue strength of a bolted shear splice is directly influenced by the type of load transfer in the connection. This load transfer can be completely by friction at the interface of the connected parts (preloaded bolts), completely by bearing of the bolts against the connected material (non-preloaded bolts), or by some combination of these two mechanisms. In the case where the load transfer is by friction, fretting of the connected parts occurs, particularly on the faying surfaces near the extremities of the joint. Here, the differential strain between the two components is highest and, consequently, minute slip takes place in this location as load is applied repeatedly. Cracks are initiated and grow in this region, which means that cracking takes place ahead of the first (or last) bolt hole in a line, and the crack

progresses through the gross cross-section of the component. The phenomenon is often referred to as "fretting fatigue."

If the bolts are not preloaded, the load transfer is by shear in the fasteners and an equilibrating bearing force in the connected parts. The local tensile stress in the region of the connected part adjacent to the hole is high, and this is now the location where fatigue cracks can start and grow. Some point at the edge of the hole or within the barrel of the hole is the initiation site for the fatigue crack and growth is through the net cross-section of the connected part.

Both types of fatigue crack behavior have been observed in laboratory tests and, in a few cases, both types have been observed within the same test. If non-preloaded bolts are used, it is highly unlikely that fretting fatigue will occur, however. When preloaded bolts are used, it is prudent that the designer check both possible types of failure.

It is worth noting that there is no history of fatigue failure of high-strength bolts themselves in shear splices. Only the connected material is susceptible to fatigue cracking.

Figure 46 shows the test results that were used to develop the design rule given in the AASHTO Specification. As compared with welded details, it can be observed that there is a great deal of scatter in the results. The data come from a wide variety of sources and test configurations, and this explains some of the dispersion. However, it is likely that most of the scatter is due to two more fundamental reasons. First, the level of residual stress is negligible

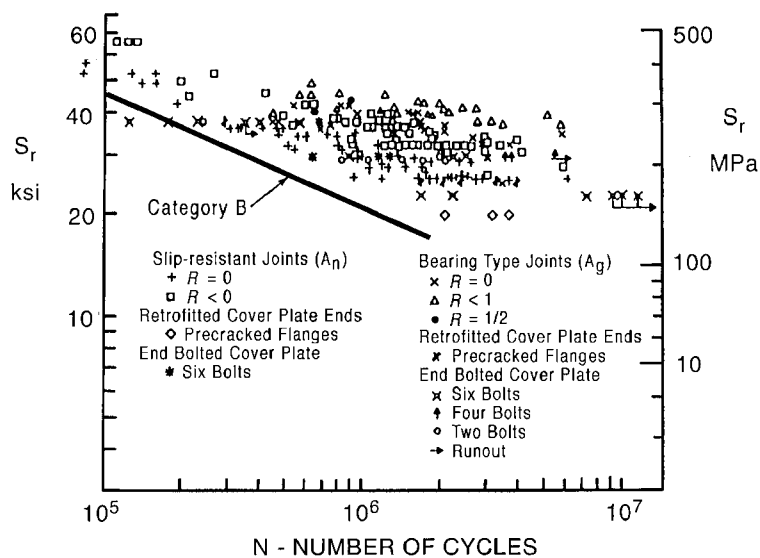


Figure 46 Fatigue Resistance of High Strength Bolted Shear Splices

in mechanically fastened joints, whereas in welded joints it is very high. This means that any portion of a stress range that is compressive will not be as damaging as are the tensile portions. Second, the severity of initial flaws in a mechanically fastened connection is much less than that in a typical welded joint.

In Fig. 46, the data were plotted using the stress range on the net cross-section or the stress range on the gross cross-section, depending upon whether or not the connection had slipped into bearing. This is consistent with the fatigue crack mechanisms discussed above. Also shown in the figure is the AASHTO Detail Category B fatigue life line. It represents a reasonable lower bound, albeit a conservative choice for many of the data. Since Category B is already a superior fatigue life category, the design of bolted shear splices will not be at any significant disadvantage because of this conservatism. A closer evaluation of the data would be warranted only in the case of fatigue life evaluation of an existing structure. It should also be noted that there are very few data in the long-life region.

The AASHTO Specification prescribes Detail Category B for bolted shear splices (AASHTO Table 6.6.1.2.3-1), and requires that stresses be calculated in the gross cross-section of the base metal in slip-critical connections (i.e., preloaded bolts are used) and at the net cross-section when the connections are "high-strength bolted non-slip-critical." Article 6.13.2.1.1 requires that joints subjected to fatigue loading must be designed as slip-critical, i.e., Detail Category B will be used and stresses will be calculated in the gross cross-section. It seems prudent to use slip-critical connections throughout a bridge structure, whether or not a particular joint is subjected to fatigue. Since the structure will be dynamically loaded, preloaded bolts are desirable so that there is no possibility that nuts will vibrate loose. Moreover, since the majority of the joints within the bridge will have to use preloaded bolts in any case, use of preloaded bolts throughout the bridge gives a consistency to the installation process.

Connections that place the bolts in tension are infrequent in bridge construction, but they may occur in bents and frames, for example. Although there are few, if any, reported fatigue failures of high-strength bolted shear splices, fatigue failures of high-strength bolted tension-type connections have occurred from time to time. Some features of the behavior of this type of connection will be reviewed here, but it will not be treated fully. Reference [35] provides a more complete treatment of the subject than can be covered here.

Typical of the configurations that can place bolts into tension is the one illustrated in Fig. 47. This situation arises when a tee is used to connect a tension hanger to a beam lower flange, for example. A significant feature of the connection is that prying forces develop, and this places an additional force in the bolt, thereby increasing the nominal value (total external force divided by the number of bolts). The amount of the prying force is dependent upon the flexibility of the connection, as illustrated in the sketch. The same flexibility introduces bending into the bolt, and this also can have an effect on the fatigue life of the bolt. The threaded portion of the bolt provides the crack initiation location, which as a rule is at the root of a thread.

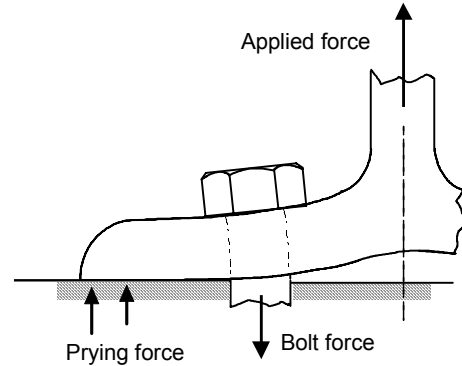


Figure 47 Bolts in Tension

The stress range experienced by the bolt as the assembly undergoes repeated loading is significantly affected by the level of bolt preload [35]. At one extreme, properly preloaded bolts in a very stiff connection will undergo little or no stress range. On the other hand, if the connection is relatively flexible, bolt bending is present, and the bolt preload is low, then the stress range in the bolt threads will be large. An additional complication occurs if the applied load is high enough to produce yielding in the fasteners. In this case, it has been shown that the stress range increases with each cycle [35].

Recommendations for the fatigue design of high-strength bolts in tension-type connections can be found in References 35 and 36. In addition to reflecting the features already mentioned here, the recommendations distinguish between ASTM A325 bolts and ASTM A490 bolts. The latter are somewhat less ductile than the former.

The AASHTO Specification requirements for bolts in tension-type connections follow the same general pattern as that for other details. However, the cases of ASTM A325 and A490 bolts in tension are not set out as separate Detail Categories. Instead, the necessary information for calculating the fatigue life of a high-strength bolt in tension is simply listed in AASHTO Tables 6.6.1.2.5-1 and 6.6.1.2.5-3. These tables provide the constant A and the constant amplitude fatigue stress for use in Eq. 17 and 19 of this document. Other information concerning fatigue of bolts in tension is given in AASHTO Article 6.13.2.10.3, where, among other things, it is noted that the bolt prying force must not exceed 60% of the nominal force in the bolt. It is also pointed out that the stress range is to be calculated using the area of the bolt corresponding to the nominal diameter. This is simply a convenience that can be employed because the ratio between the area through the threads and that

corresponding to the nominal diameter of the bolt is relatively constant for the usual bolt sizes.

The fatigue design of high-strength bolts that are in tension-type connections should reflect the following guidelines:

- Whenever possible, redesign the connection so that the bolts are in shear, not tension.
- Design the connection so that prying forces are minimized. Reference [36] suggests that the prying force should be less than 60% of the externally applied force. Some specifications have even lower limits, although the AASHTO Specification also uses the 60% value.
- Whenever possible, use ASTM A325 bolts rather than A490 bolts.
- Ensure that proper installation procedures are adhered to so that the prescribed bolt preloads will be attained.

8.1.2 Threaded Rods

Threaded rods are used frequently in mast or sign base plates. Under the action of the wind on the mast or sign, fatigue loading will be present, and this can produce a large number of stress cycles, usually at a relatively low stress range. If high-strength bolts that are not preloaded act in direct axial tension, they are equivalent to a threaded rod.

A large number of test results are available [37] and they are shown in Fig. 48. Most of the tests represented in this figure were carried out at constant amplitude loading, but a few tests were done under variable amplitude. (As is customary, the stress range was calculated using the so-called "stress area" of the rod.) Many of the tests were done in a double-nut configuration, that is, a nut was present on each side of a simulated base plate. In this way, a short section of the rod is prestressed, but most of it is not. The effect of a small amount of misalignment was also included in some tests. The results include axially loaded rods (i.e., no preload), rods preloaded to the "snug-tight" level, and rods preloaded by turning the nut on 1/3 turn.

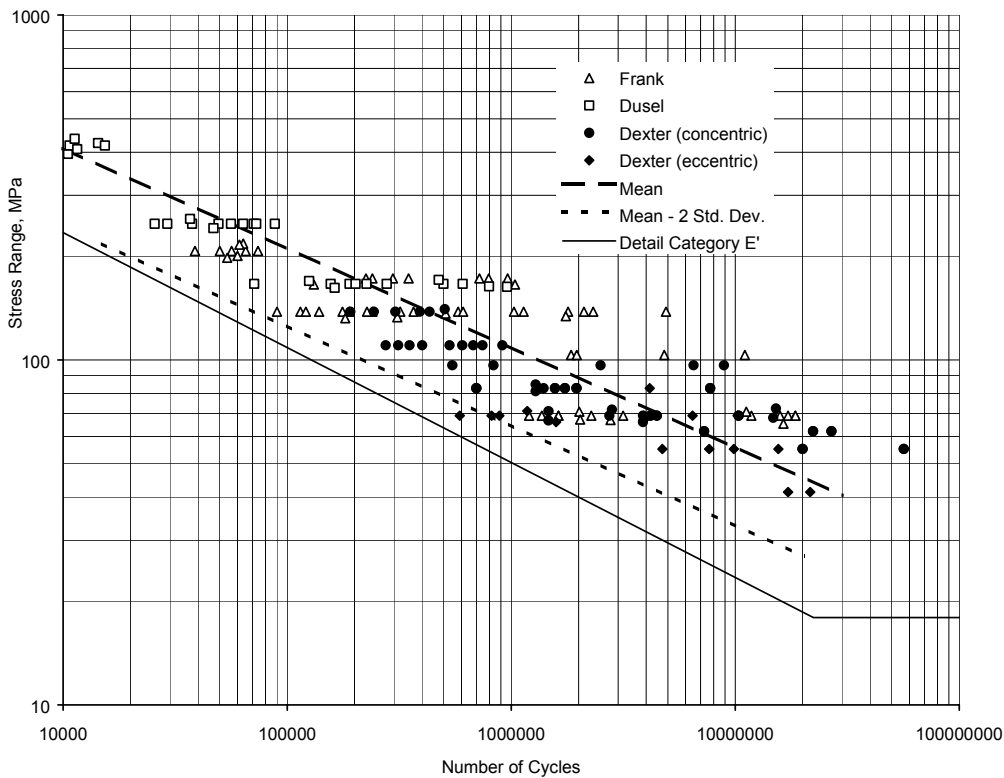


Figure 48 Fatigue Life of Anchor Bolts (Ref. 37)

There is considerable scatter in the results, but it is clear that the threaded rod is an element with poor fatigue resistance. The results do indicate that grade of steel, thread size, method of thread forming, and bolt diameter did not in themselves have a major effect on the fatigue life [37]. The misalignment used in the tests (1:40) likewise did not significantly reduce the fatigue life, assuming that beveled washers are used. The fatigue life of rods tested with no preload and rods tested in the snug-tight condition was similar. A small increase in fatigue life was observed for fully preloaded rods.

Figure 48 also shows AASHTO Detail Category E'. As can be seen, this is a reasonable representation of the data in the region up to about 1 million cycles. The constant amplitude fatigue limit for Category E' (17.9 MPa) clearly is too conservative for these (mostly) constant amplitude tests: a better choice is the Category E constant amplitude fatigue limit (31.0 MPa). Unfortunately, the region of low stress range and a large number of cycles is reflective of where many of the structures that use threaded rods will have to function. A sign baseplate, for example, could have a large number of cycles at low stress range under wind loading. Until more variable stress range data are available, it would be

prudent to use Detail Category E' throughout. The AASHTO Specification does not address the fatigue life of anchor bolts (threaded rods).

8.1.3 Riveted Connections

It has already been explained that the need for fatigue life rules for riveted connections rests in evaluation of existing structures. If a conventional fatigue life examination indicates that a given riveted structure has long remaining fatigue life, then obviously no further effort is necessary. However, when remaining fatigue life is shown to be inadequate, it is necessary that the best possible information be used. The alternative might be replacement of the structure—a costly solution.

As was the case for high-strength bolted shear splices, the experimental evidence is that fatigue cracking in riveted shear splices takes place in the connected material, not in the rivet itself. Thus, the fatigue life can be expected to be a reflection of such features as the size of the hole relative to the part, the method of hole forming (drilled, punched, or sub-punched and reamed), the bearing condition of the rivet with respect to the hole, and the clamping force provided by the rivet.

At the present time, the influences of clamping force, bearing condition, and the method of hole formation have not been examined in any systematic way. The influence of the hole size, *per se*, is not likely to be strong, as long as the hole sizes and plate thicknesses commonly used in structural practice pertain. Thus, the best data available are tests on riveted connections of proportions that are consistent with usual structural practice and are of full size, or at least large size. For the time being, the reflections of clamping force, bearing condition, and hole formation must simply be part of the data pool. For this reason, and because the "defect" presented by a riveted connection is not severe, it is to be expected that the scatter of data will be relatively large.

Figure 49 shows the data: identification of the specific sources from which the test data came can be obtained in Reference [38]. Most of the data come from tests of flexural members, and most of these were members taken from service. For those cases where members taken from service were tested, the previous stress history was examined and deemed to have been non-damaging. A few of the test results are from tension members. In the case of bending members, the moment of inertia of the cross-section included the effect of holes. For the tension members, the stress range was calculated on the net cross-section. (It is not yet clear whether this is justified since the fatigue cracks were observed to grow at right angles to the cross-section.) As was the case with bolted connections, there is a

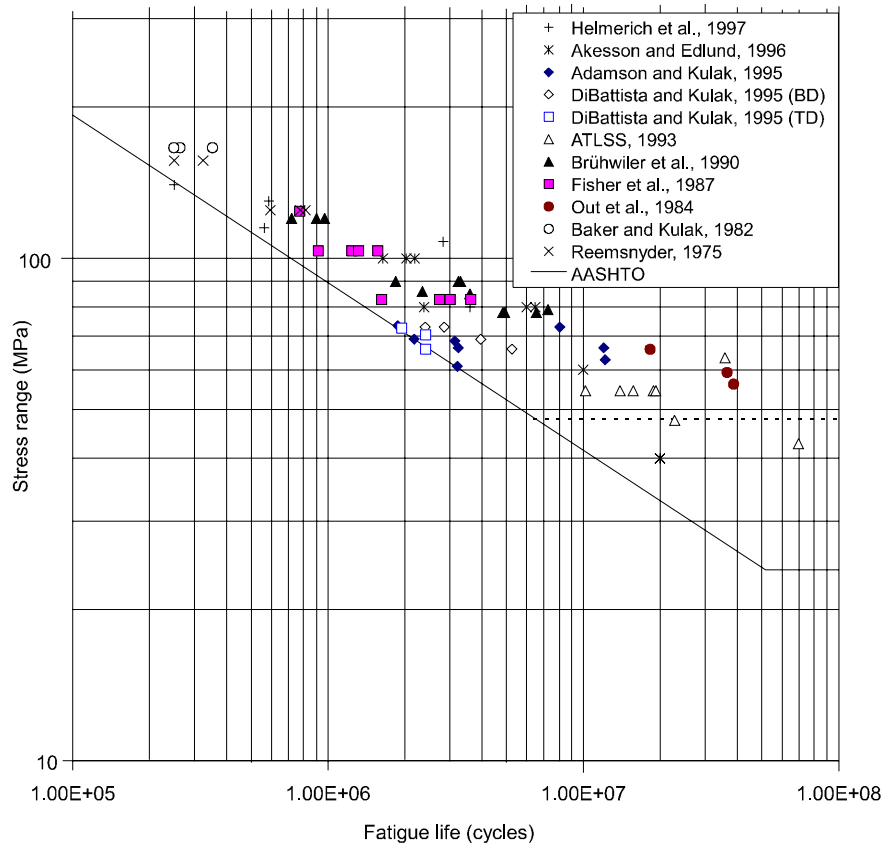


Figure 49 Fatigue of Riveted Connections

considerable amount of scatter in the data, for the reasons described earlier. Almost all the data shown in Fig. 49 come from members made of mild steel, but results from some wrought iron members are also present.

Figure 50 shows a fatigue crack passing through the net section of a riveted member that was tested in tension.

The AASHTO Specification stipulates the use of Detail Category D for riveted connections, and this is shown along with the data in Fig. 49. Category D is a reasonable reflection of the data except for two test results at long fatigue lives. These were variable amplitude tests. It has been suggested that a fatigue limit of 40 MPa should be used, rather than the value of 48.3 MPa that is used for Category D. This change would capture the long life data points better, but it is too conservative in the region of the "knee" of the bilinear fatigue life representation. The issue is discussed further in Reference [38].

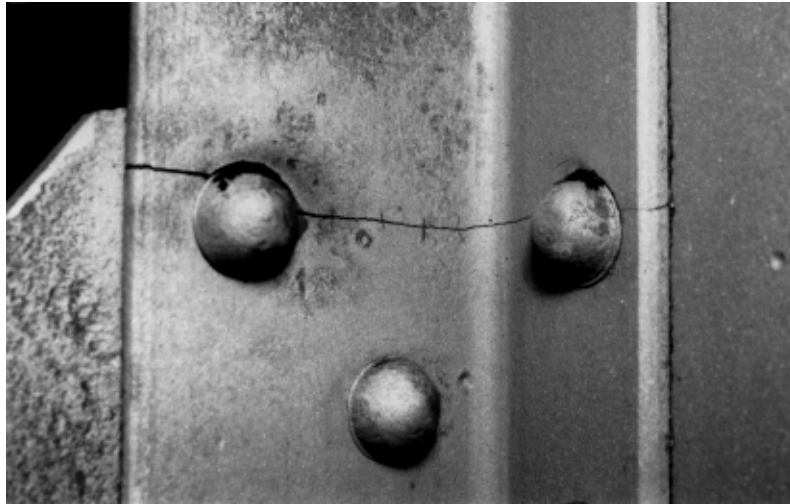


Figure 50 Fatigue Crack Through Net Section of a Tension Member

8.2 Environmental Effects; Use of Weathering Steel

The effects of the environment upon the fatigue life of steel members can show up in one of several ways. Corrosion produces local effects that cause stress concentrations. For instance, corrosive products (e.g., brine) can drip down from an upper level to a lower level and produce both a local reduction in cross-section and a notch effect. Old railway bridge floor system members sometimes show this type of corrosion. For example, the top surface of the lower flange of a girder can often show deterioration of the cross-section as the result of brine that has dripped down from the upper levels. (Ice and salt were formerly used as the refrigerant in railway rolling stock). It is not uncommon to see depressions in the order of 25 to 50 mm diameter, with depths in the order of 3 to 8 mm. In extreme cases, particularly with initially thin members (e.g., bracing members, lacing bars), the local corrosion may completely penetrate the member. Although these are not desirable situations, they are similar to the introduction of a hole: as such, they do not introduce a particularly severe flaw into the member. Since this type of corrosion effect will generally be an issue in the case of evaluation of old bridges, a value judgment can be made as to how much to degrade the fatigue life as compared with a non-corroded member. Fisher et al. have reported on the fatigue life of a number of corrosion-notched beams [39], although the number of test data in which the corrosion effect was specifically examined is quite limited. The ratio of corroded part to original thickness ranged from 0.2 to 0.8. Fisher et al. reported that if the corrosion reduced the thickness by more than one-half, fatigue cracking was likely to start at a notch within the corroded region rather than at the location of a net section (reduced by corrosion) through rivet or bolt holes.

There are also instances in which the entire cross-section has been corroded, more or less in a uniform way. The origin of the corrosion in these cases is a more general source, such as high humidity, usually in a salt-laden atmosphere, or corrosive fumes in proximity to chemical process plants. In the case of a general reduction in cross-section, the fatigue life evaluation can be based on an estimate of the reduced cross-section. In other words, the fatigue strength examination of a corroded member can proceed on the basis of the usual stress range vs. number of cycles relationships, given that the stress range will be calculated using the properties of the reduced section. Of course, the designer should be alert to the presence of notches in this case also.

Figure 51 shows the lower flange of a railroad stringer in which a fatigue crack has occurred at a corrosion notch.

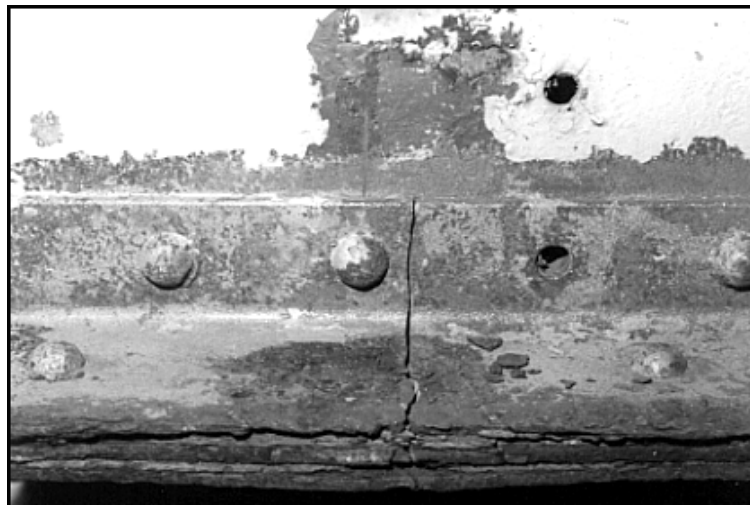


Figure 51 Fatigue Crack at a Corrosion Notch in a Railroad Stringer

In principle, the useful life of a welded bridge structure can be affected by an aggressive environment when it is under sustained load (stress-corrosion cracking), or by the enhancement of an aggressive environment on the effects of cyclic stresses (corrosion fatigue). However, general experience with bridge steels and weldments, including successful use in long-time environmental service applications, have not demonstrated any significant problems with either stress-corrosion cracking or corrosion fatigue.

The effect of a corrosive environment upon crack growth or as it increases stress concentrations has not received much attention, particularly in civil engineering applications. The available laboratory test results, often done at relatively high test rates, do not indicate any significant effect, however [39]. Moreover, experience in the field does not support the

need for inclusion of special rules for bridges or similar structures that are operating in the types of corrosive environments normally associated with that type of structure. In two specific cases, the consequences of operating in a corrosive environment are included explicitly in the design rules. Both of these are clear-cut—offshore structures and the drillpipe used in oil exploration. In both instances, the environment is severe—salt water—and its consequences cannot be avoided. There is not much test data available here either, however, and it must be recognized that corrosion and its effect on fatigue life is time-dependent. Thus, testing in this area takes even longer than it does for the normal situation of testing in air. Designers of civil engineering structures in particularly harsh environments should take special care that detailing of the structure minimizes the possibility of locations for fatigue and that a detailed maintenance strategy is established. In all cases, detailing practice should be to promote drainage of water and to prevent of entrapment of moisture and corrosion products.

Crack growth rate data has been acquired on most commonly used bridge steels under constant amplitude and variable amplitude loading [40, 41]. The scatter bands of the test specimens in air generally bracketed the test data acquired in an aqueous environment. The latter was done with or without a 3 percent solution of sodium chloride. Most of the aqueous data fell between the mean and upper limit of the data acquired in air. However, all of the test data was acquired at relative high levels of ΔK and crack growth rate. Figure 52 shows the

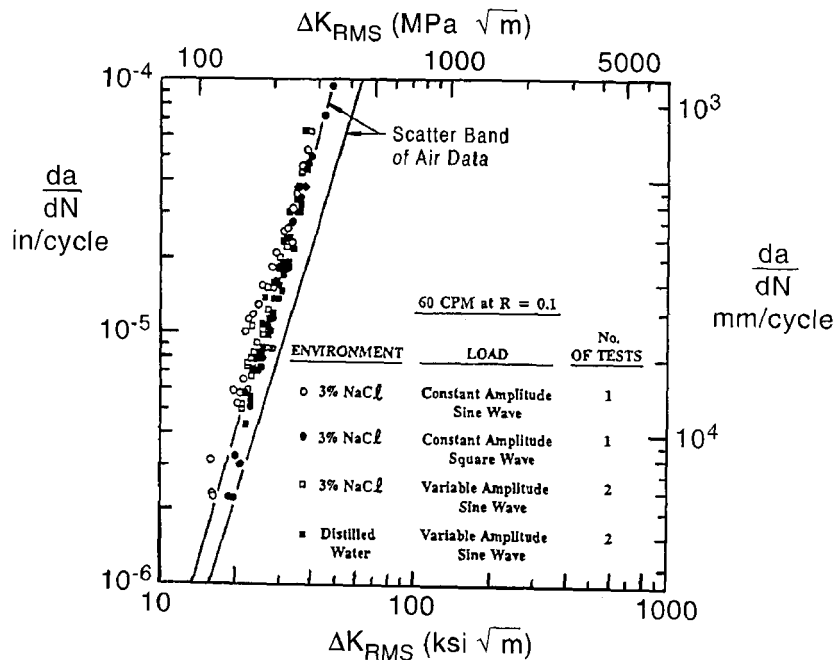


Figure 52 Crack Growth in Aqueous Environment

test data for A588 steel in an aqueous environment with and without the sodium chloride solution. This level of ΔK is only reached after very large cracks have formed. The crack growth threshold appears to increase with decreasing load frequency when subjected to a hostile environment. The general conclusion is that the crack propagation life of bridge steel components under actual operating conditions (wet and dry) in aqueous environments is equal to or greater than that obtained in a room temperature air environment. The laboratory studies which led to the conclusion that environmental conditions have little effect upon the fatigue behavior of bridge components are supported by field experience.

The influence of the environment upon rusting, pitting, and the start of corrosion-fatigue cracking (assuming no prior fatigue crack) may differ from its influence on progressive crack extension when the crack crevice controls the crack tip behavior. As would be expected, rusting and pitting introduces notches and this can affect the crack initiation behavior of the base metal. Studies on weathering steel have demonstrated that only the Detail Category A situation is significantly affected, however. Figure 53 shows the experimental results of cruciform joints, which are a Category C detail, in their as-welded and weathered conditions. It is apparent that the use of weathering steel does not in itself produce a fatigue life that is inferior to that when ordinary grades of steel are used.

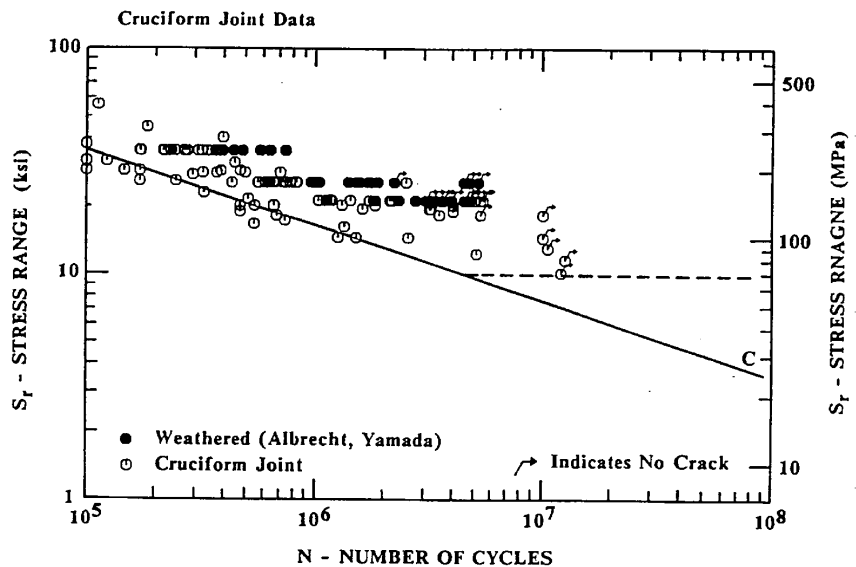


Figure 53 Comparison of Weathered and Unweathered Cruciform Joints

Many civil engineering structures must operate in low temperature environments. Again, there are very few test data in this area. The work of Fisher et al. [39] did include

some tests in which a portion of the fatigue crack growth was done under very low temperatures (-40°C and -73°C). The study showed that the low temperature did not result in sudden fracture until the cracks had become very large.

In summary, it can be concluded that the civil engineering structures most likely to have to endure corrosive environments, especially bridges, can be designed in accordance with the rules that have been developed on the basis of tests in air. Evaluation of existing structures in which corrosion has affected the cross-section can be done by applying judgment and using the results of those tests that are available [39]. In the case of new structures, great care should be taken to ensure that corrosion products from roadway decks are directed away from the members and that road spray from traffic either above or below the bridge is cleaned up periodically. Detailing should be done with a view to minimizing those locations where corrosion products can form and sit, especially in crevices.

8.3 Combined Stresses

Throughout the discussion so far, it has been emphasized that the stresses to be used in the fatigue life evaluation are those corresponding to the nominal stress as obtained from a strength of materials level of analysis. The detail classification stipulated by the governing specification includes the effect of local stress concentrations due to weld shape, discontinuities, triaxial conditions, and so on. Only in exceptional cases, around large openings, for example, will a more sophisticated analysis be required. Occasionally, also, it might be necessary to investigate the combined effect of normal and shear stresses.

When normal and shear stresses are present at the same location but do not occur simultaneously under a given loading event, the individual components of damage can be added according to a Miner's summation, as follows:

$$\left[\frac{\Delta\sigma_e}{\Delta\sigma_r} \right]^3 + \left[\frac{\Delta\tau_e}{\Delta\tau_r} \right]^3 \leq 1 \quad (20)$$

where σ and τ refer to normal stresses and shear stresses, respectively. The subscript e means a calculated equivalent stress range (see Eq. 13, for example) and the subscript r refers to the permissible stress range for the detail.

For a case in which normal and shearing stresses are present in significant quantities at a given location and are concurrently present and in phase at that location during a given loading event, the principal stresses should be calculated. This stress range is then used in the

fatigue life evaluation. (Normal stress is defined as the stress perpendicular to the direction of the potential fatigue crack.) When the principal stress changes direction during the stress cycle, as it does at transverse stiffeners in plate girder webs, for instance, it has been shown that the fatigue resistance need not consider the principal stress [19]. Generally, it should only be necessary to consider the principal stress when its direction does not change during the stress cycle. Hence, use of Eq. 20 should be focused on this case.

In unusual situations, shear stress alone can be significant. There are very few test results, but they show that the general relationship between stress range and number of cycles still exists. The AASHTO Specification recommends that Detail Category E be used for the case of shear stress on a fillet weld throat.

8.4 Effect of Size on Fatigue Life

Most of the test results upon which the fatigue life rules are based were done on specimens where the component parts were in the order of 12 to 25 mm thick. Fabricated steel structures often use plate thickness considerably greater than this, however, particularly in the case of flanges of welded built-up beams. It is generally agreed [42, 43, 44] that the fatigue resistance of thicker elements is less than that of thinner elements. Although a thicker element will have a greater statistical chance of containing flaws, this is not the main reason for the decrease. Rather, it has to do with more severe residual stresses that result when using thicker plates and from the observation that the stress intensity factors at the weld toe increase as plate thickness increases (and the initial flaw size remains constant) [45].

There are several locations within the AASHTO Specification where it is required that fatigue strength be decreased with an increase in plate thickness. For example, the fatigue category for the base metal at the end of partial length cover plates is reduced from Detail Category E to E' (case of plate wider than flange) when the plate thickness exceeds 20 mm. Likewise, the same decrease in fatigue detail category occurs when the plate thickness exceeds 25 mm in a longitudinally loaded groove or fillet welded detail. This would apply to the attachment of flange plates to girder web, for example.

8.5 Role of Residual Stress

Steel structures that are fabricated by welding contain "residual" or "locked-in" stresses that have been introduced as a result of the welding process. These have considerable influence on the propagation of fatigue cracks. The main effect is to significantly reduce the effects of the applied stress levels, *per se*, for standard weldable

structural steels. For modern codes, this has brought about a return to the simple stress range vs. cycle life model for fatigue strength suggested by Wöhler over one hundred years ago. Furthermore, independence of steel grade justifies the use of the relatively large data base of laboratory results taken from tests of different steel grades produced in different countries. During recent modifications to fatigue codes, code developers have taken advantage of such opportunities and, consequently, fatigue design guidelines have been greatly simplified and harmonized internationally.

Consider a weld laid down as shown in Fig. 54. As the weld cools, it tries to contract. However, since the plate and the weld must maintain compatibility of length, the plate restrains the weld during the cooling and contraction process. This puts the weld and a relatively small volume of plate adjacent to the weld into tension. Conversely, the main portion of the plate is being pulled down by the contracting weld, thereby placing it into compression. The stresses set up in the plate and in the weld as a consequence of this process are called *residual* stresses. Since there are

no external forces applied during this process, the equilibrium condition of the cross-section must be reflected in the balance between residual tensile stress and the area over which it acts and the residual compressive stress and its associated area. The actual distribution and magnitude of the residual stress pattern depends upon such factors as the strength of the steel and the weld metal, the geometry of the connected parts, and the size of the weld relative to the connected parts. The important fact, however, is that the magnitude of the tensile residual stress can reach the yield strength of the material.

It follows, of course, that the rolled shapes or built-up members used in structural applications also contain regions of high residual tensile stress. For example, very large residual tensile stresses are present at the junction of the flange and web of a beam that has been built up by welding the component parts together [18]. This junction is also the location of the flaws that are likely to be the source of fatigue crack growth, which means that the flaw is under a condition of initial stress even before load is applied. For the usual condition wherein this initial stress is at or near the yield stress level, this means that stress range, rather than the maximum applied stress, the stress ratio (ratio of maximum stress to minimum

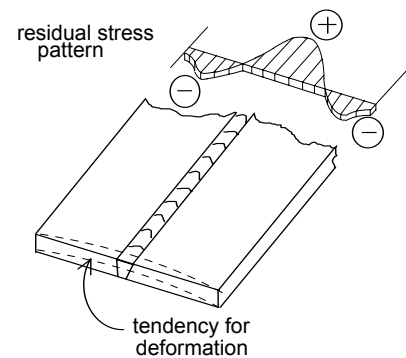


Figure 54 Residual Stresses in a Welded Plate

stress), or some other parameter of applied stress, is the governing condition describing fatigue crack growth. This will be illustrated by the following numerical example.

EXAMPLE 13

Figure 55 shows a rectangular plate and its assumed residual stress pattern. (This could be an idealization of the flange of a welded beam.) According to the designer, the plate will be subjected to a maximum tensile stress of 215 MPa and a minimum compressive stress of 122 MPa. Calculate the actual range of stress that will exist for a flaw at the center of the plate (cf., junction of the web and flange of a welded beam). Compare this range of stress with the stress range that will be computed by the designer, that is, $+215 - (-122) = 337$ MPa. The plate has a yield strength of 300 MPa.

Solution:

1. Initial conditions—The pattern of residual stress is shown in Fig. 55 (a). It shows that the values of the initial stress are as high as the yield stress. Since the yield stress is not exceeded, however, the corresponding strains can be calculated from the elastic relationship, $\sigma = E \epsilon$, and these strains are shown in Fig. 55 (b). There is no force on the member, and we note (by inspection) that the condition $P = \int \sigma dA = 0$ is met. (This can be verified by calculation.)

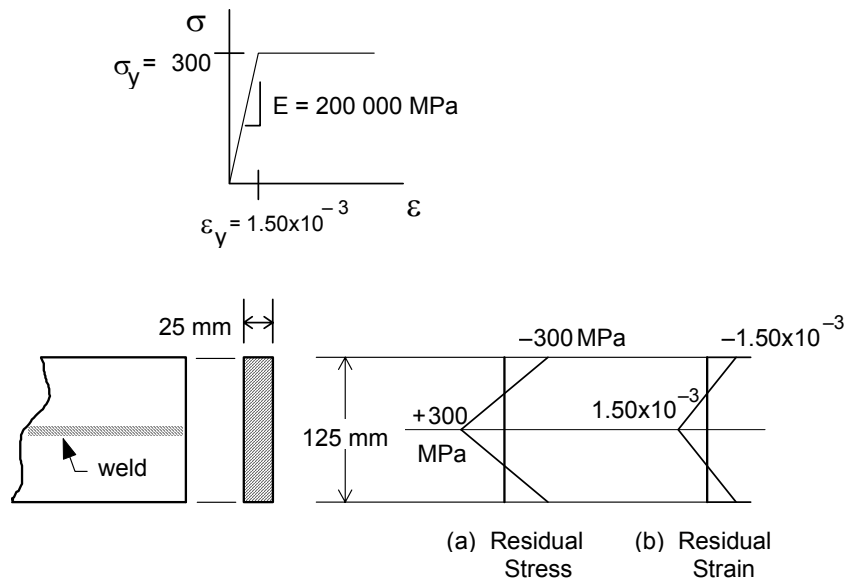


Figure 55 Initial Stress Condition in a Welded Plate

2. Apply tensile force such that the design stress level is +215 MPa, i.e.,

$$P = \sigma A = 215 \text{ N/mm}^2 \times (25 \times 125) \text{ mm}^2 = 672 \times 10^3 \text{ N} = 672 \text{ kN}$$

During application of this force, which is the equivalent of the imposition of a uniform compressive strain over the residual strain of Fig. 55 (b), not all parts of the cross-section respond in the same way. Specifically, the relationship $\varepsilon = \sigma/E$ will not be valid for those regions of the resultant strain diagram where the strain is greater than the yield strain. In Fig. 56, part (a) shows the residual strain (which is simply Fig. 55 (b) repeated), part (b) shows the strain imposed by the tensile force, part (c) is the resultant strain, and the corresponding stress diagram is shown in Fig. 56 (d).

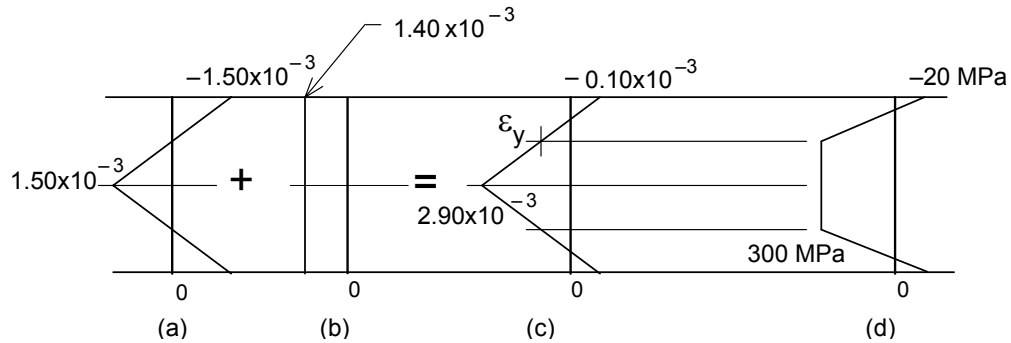


Figure 56 Superimposed Strain (Step 2) and Corresponding Stress

The value of the uniform strain corresponding to imposition of the applied force, 1.4×10^{-3} , was determined by trial so to satisfy the requirement that $\int \sigma dA = 672\,000 \text{ N}$. That the integral is satisfied can be confirmed by first calculating the dimensions of the stress diagram, Fig. 56 (d), and then calculating the force volume obtained when the stress diagram is superimposed on the cross-section.

3. Now, apply a force such that the nominal stress in the cross-section goes to 122 MPa compression. This requires that the 672 kN force be removed and an additional force of $(-122 \text{ N/mm}^2) \times (25 \times 125) \text{ mm}^2 = -381 \times 10^3 \text{ N}$ be applied. Thus, the change in force is $\Delta P = (672 + 381) = 1053 \text{ kN}$. As before, a uniform strain must be applied of sufficient magnitude such that $\int \sigma dA = P = 381 \text{ kN}$. By trial, this has been determined to be a strain of 1.70×10^{-3} .

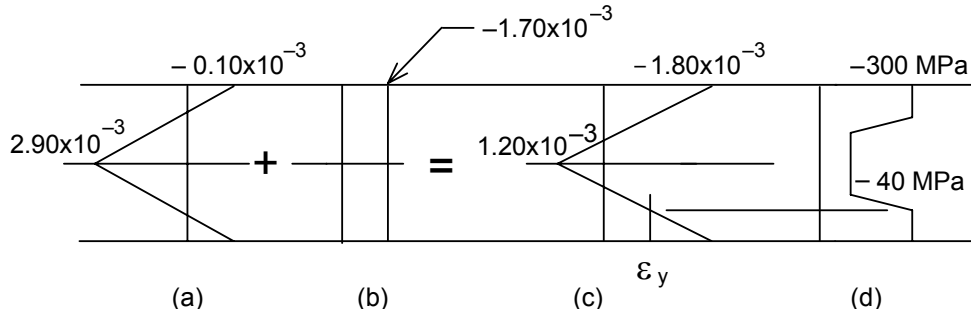


Figure 57 Superimposed Strain (Step 3) and Corresponding Stress

Figure 57 (a) shows the strains that existed at the end of step 2. Figure 57 (b) is the uniform compressive strain that must be applied to satisfy the requirement that a force of 381 kN be imposed. The resultant strains are shown in Fig. 57 (c). The reader can verify the stress values shown in Fig. 57 (d) and that the imposition of these stresses on the cross-section does, in fact, produce the value 381 kN.

4. Finally, examine the stresses in the mid-depth fibre of the cross-section. As shown in Fig. 58, the stress initially was 300 MPa, that is, it was the yield value. Upon initial loading to 672 kN force, the stress remained at this value, even though the strains increased as shown in Fig. 58. The unloading that occurred in Step 3 took the stresses down to 40 MPa compression. Thus, the actual change in stress at the mid-depth fibre was from +300 MPa down to -40 MPa, a total change of

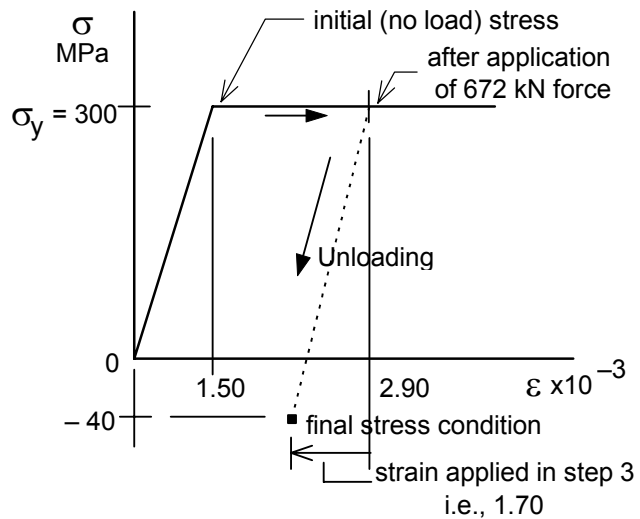


Figure 58 Strains and Stresses at Mid-Depth Fibre

340 MPa. The result is that the actual change of stress, 340 MPa is equal (nearly) to the change of stress calculated by the designer, 337 MPa. The difference between the two values is attributable to round-off errors in the calculations.

(Still with reference to Fig. 58, it should be borne in mind that unrestricted plastic flow of the cross-section cannot occur. The small zone of weld and plate that is at yield is limited

to some finite value of strain because the material adjacent to it remains elastic. Hence, the defect in a high residual tensile stress region is cycled to a limited strain.)

To summarize, in large welded structures there are very high tensile residual stresses near fatigue crack sites and their presence significantly reduces the effects of applied stress levels and steel grade upon crack propagation for standard weldable structural steels. As a result, it is generally agreed that stress range is the only dominant stress parameter. However, there has been a great deal of discussion regarding the best way to treat the following cases:

- the influence of compressive applied stresses
- the fatigue strength of non-welded elements
- the fatigue strength of stress-relieved welded elements
- the difference between results taken from testing small specimens and those taken from testing full-scale elements.

Some of the differences between various codes can be traced to different interpretations of the effect of residual stresses (and other built-in stresses) upon the fatigue strength of structural elements. A selection of approaches to these cases is described next.

Nearly all fatigue guidelines for steel structures recommend that non-welded elements, stress-relieved welded elements, and welded elements be treated in the same manner when the applied stress ranges are tensile. When the applied stress ranges are compressive, or partly compressive, recommendations vary. According to the AASHTO recommendations [2], it is possible to ignore all fully compressive stress ranges. (This was discussed in Section 5.3.2.) However, if a part of the stress range is tensile, then the whole stress range must be considered. European recommendations suggest that the whole stress range should be employed, regardless of whether it is completely or partially compressive, when welded elements are assessed. Eurocode 3 (EC 3) [46] allows a reduction of the compressive stress range to 60% of its magnitude for non-welded and stress relieved elements. The ECCS recommendations [15] are the most conservative; they recommend that 100% of the stress range be used for all elements and all cases. It can be observed that there are no known cases of load-induced fatigue cracking in bridge structures when the cyclic stresses are totally in compression [20].

Authors of the AASHTO provisions argue that, even if fatigue cracks start within tensile residual stress fields, under fully compressive loading cracks will eventually stop when they propagate beyond the influence of these stresses. The developers of the EC 3

document note that a crack growing from an as-welded joint in an element may be dangerous when applied stress ranges are full compressive. Indeed, some test elements have failed due to cracks growing under fully compressive applied loading. Also, the EC 3 provisions reflect an attempt to accommodate those cases where there are no high tensile residual stresses.

For the ECCS document, it was decided to provide conservative recommendations because in most complex structures the magnitudes of built-in stresses are unknown. Built-in stresses do not only originate from welding related residual stresses, but they may also be caused by other effects such as lack of fit, settlement of supports, temperature gradients, and inefficient expansion joints. Therefore, it was decided that no advantage should be given to cases where applied stresses are in compression or where elements contain no tensile residual stresses.

The final point in this section relates to the physical testing of fatigue specimens. Compared with elements that have no tensile residual stresses, the presence of tensile residual stress near potential crack sites in an element reduces its fatigue strength, especially at long lives. Small test specimens may not contain the same high level of tensile residual stress found in full-scale elements. For this reason, most recent research programs have concentrated upon testing of full-scale elements in order to establish code recommendations. Therefore, results taken from tests of small specimens should be employed with caution for design assessments. However, small specimens are useful when exploring variables such as improvement procedures, use of new materials, and so on.

Test programs are sometimes used to obtain a more accurate fatigue strength relationship than is provided in fatigue codes. Whenever possible, in these circumstances it is desirable that the test specimen have the same dimensions as the element under consideration for the real structure.

8.6 Quantitative Design Using Fracture Mechanics

The fatigue strength curves described in Chapter 3 are not capable of providing an engineer with information necessary for several special cases related to fatigue assessments. For example, these curves cannot evaluate the influence of an unusually large defect; they are not able to evaluate the influence of inspection precision upon fatigue reliability; they provide little help in fixing inspection intervals; and, finally, they cannot be used to predict the remaining life of a cracked structure. Fracture mechanics provides the central analytical model employed in fatigue assessments for dealing with these aspects.

Some defects that may be rejected during standard fabrication controls would not, in reality, influence the performance of the structure. The economic consequences of remedial measures are often severe and resulting delays to a project can be long. Quality assurance provisions in many codes are based more upon accepted standard practice, experience, and detection capability than upon scientific accuracy.

Fracture mechanics offers a more rational means of defect assessment. In such analyses, the value for the initial crack length in Eq. 7, Section 2.3 is normally taken to be equivalent to the size of the defect. Equation 7 is then integrated, usually numerically using equal increments of cycles, in order to determine cycle life. If the cycle life is greater than the number of cycles expected over the life of the structure, the defect may be regarded as being acceptable. Reference 47 provides guidelines for appropriate values of W and Y for use in Eq. 3 and for additional criteria, such as those which determine whether two closely spaced defects should be considered to be equivalent to one large initial crack.

A similar approach can be used for the design of structures when fabrication quality cannot be guaranteed and when it is known that inspection technology is unable to detect defects that are more severe than those normally known to occur in steel structures. In these evaluations, it is assumed that defects are present and the minimum detectable defect size becomes the initial crack size for use in Eq. 7. When the cycle life resulting from the integration is less than the number of cycles applied over the life of the structure, either the design is modified or inspection technology that enables greater precision is justified. Such analysis has been used to determine inspection criteria for steel structures in the North Sea, for example. This approach is sometimes called a "fitness for purpose assessment."

Often, determination of intervals between in-service inspections does not account for the behavior of a potentially cracked structure. Crack-growth curves can be predicted for all critical details in a structure, as shown schematically in Fig. 59. Between the crack length when first detection is possible, a_0 , and the critical crack size, a_{cr} , a set number of inspections, n , should be performed. A constant crack-length increment, Δa , should be fixed rather than a constant time interval. The number of inspections should be determined using reliability analyses that take into account crack-detection probabilities and the consequences of failure. More frequent inspections are

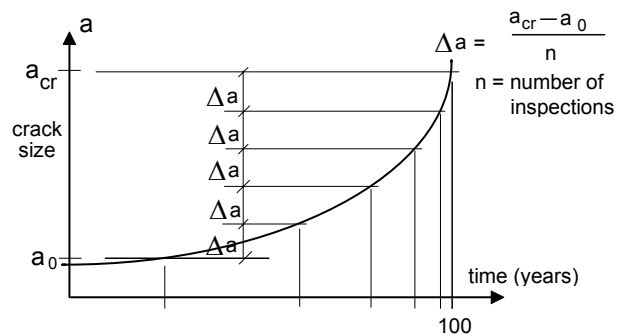


Figure 59 Crack Growth Curve

required as the structure ages. Therefore, fracture mechanic analysis enables a more rational approach for writing those parts of specifications related to inspection.

As the number of structures that approach or exceed their design life grows exponentially each year, so does the number of structures which have a high probability of containing fatigue cracks. Fracture mechanics will become an essential part of the assessment of these structures and, consequently, the decisions concerning their strengthening, repair and replacement. Cracking in several North American steel bridges was reviewed in a collection of case studies [20]. Finally, fracture mechanics analyses may assist in the assessment of complex structures that have connections which are not covered by test results. Test data obtained from simple beams and small specimens may be inapplicable to large structures and to complex loading. This is particularly true for offshore structures, and some of these have been analyzed extensively using fracture mechanics.

REFERENCES

1. Smith, I.F.C. and Hirt, M.A., "Fracture Mechanics in Structural Engineering," *Steel Structures; Recent Research Advances and Their Application to Design*, M.N. Pavolic, Editor, Elsevier, 1986, Chapter VI, 381-402.
2. American Association of State Highway and Transportation Officials, "AASHTO LRFD Bridge Design Specifications," SI Units, First Edition, Washington, D.C., 1994.
3. Griffith, A.A., "The Phenomena of Rupture and Flow in Solids," *Phil. Trans. Royal Soc. London (Series A)*, 221 (1921), 163-198.
4. Irwin, G.R. and de Wit, R., "A Summary of Fracture-Mechanics Concepts," *J. Testing Evaluation*, 11 (1983), 56-65.
5. Rolfe, S.T., "Fracture and Fatigue Control in Steel Structures," *Eng. J. Am. Inst. Steel Constr.*, 14 (1983), 2-15.
6. Smith, R.A., "An Introduction to Fracture Mechanics for Engineers – Parts I, II, and III," *Materials Eng. Applic.*, 1 (1978-79), 121-128, 227-235 and 316-322.
7. Broek, D., *Elementary Engineering Fracture Mechanics*, Martinus Nijhoff, The Hague, Netherlands, 1984.
8. Rolfe, S.T. and Barsom, J.M., *Fracture and Fatigue Control in Structures*, 2nd Ed., Prentice-Hall, Englewood Cliffs, New Jersey, 1987.
9. Pellini, W.S., *Guidelines for Fracture-Safe and Fatigue-Reliable Design of Steel Structures*, Welding Inst., Cambridge, UK, 1983.
10. Tada, H., Paris, P., and Irwin, G., *The Stress Analysis of Cracks Handbook*, Paris Productions, St. Louis, 1985.
11. "J, a Measure of Fracture Toughness," in *ASTM E 813-81 (ASTM Book of Standards 3.01)* (1983), 762-780.
12. Lankford, J., "The Influence of Microstructure on the Growth of Small Fatigue Cracks," *Fatigue Fracture Eng. Materials Struct.*, 8 (1985), 161-175.
13. Paris, P. and Erdogan, F., "A Critical Analysis of Crack Propagation Laws," *Trans. ASME (Series D)*, 85 (1963), 528-534.

14. Suresh, S. and Richie, R.O. , "Propagation of Short Fatigue Cracks," *Int. Metals Rev.*, 29 (1984), 445-476.
15. European Convention for Constructional Steelwork, "Recommendations for the Fatigue Design of Steel Structures," ECCS Technical Committee 6, Rotterdam, 1985.
16. Fisher, J.W. and Viest, I.M., "Fatigue Life of Bridge Beams Subjected to Controlled Truck Traffic," Preliminary Publication, 7th Congress, IABSE, 1964.
17. Gurney, T.R., *Fatigue of Welded Structures*, 2nd Edition, Cambridge University Press, 1979.
18. Fisher, J.W., Frank, K.H., Hirt, M.A., and McNamee, B.M., "Effect of Weldments on the Fatigue Strength of Steel Beams," National Cooperative Highway Research Program *Report 102*, Highway Research Board, Washington, D.C., 1970.
19. Fisher, J.W., Albrecht, P.A., Yen, B.T., Klingerman, D.J., and McNamee, B.M., "Fatigue Strength of Steel Beams With Transverse Stiffeners and Attachments," National Cooperative Highway Research Program, *Report 147*, Highway Research Board, Washington, D.C., 1974.
20. Fisher, J.W., *Fatigue and Fracture in Steel Bridges: Case Studies*, Wiley Interscience, 1984.
21. Broek, D., *The Practical Use of Fracture Mechanics*, Kluwer Academic Publishers, Dordrecht, The Netherlands, 1989.
22. Bardell, G.R., and Kulak, G.L., "Fatigue Strength Behaviour of Steel Beams with Welded Details," *Structural Engineering Report No. 72*, Dept. Civil Engrg., University of Alberta, September, 1978.
23. Bannantine, J.A., Comer, J.J., and Handrock, J.L., *Fundamentals of Metal Fatigue Analysis*, Prentice-Hall, Englewood Cliffs, (New Jersey), 1990.
24. American Railway Engineering Association, "Manual for Railway Engineering," Chapter 15; Steel Structures, AREA, 1994.
25. Fisher, J.W., Yen, B.T. and Wang D., "Fatigue of Bridge Structures – a Commentary and Guide for Design, Evaluation and Investigation Of Cracking," ATLSS Report No 89-02, Lehigh University, Bethlehem, PA, 1989.
26. Matsuishi, M. and Endo, T., "Fatigue of Metals Subject to Varying Stress," Jap. Soc. Mech. Engrg, Fukoda, Japan, March 1968.
27. Downing, S.E., and Socie, D.F., "Simple Rainflow Counting Algorithms," *International Journal of Fatigue*, Vol. 4. No. 1, 1982.

28. Schilling, C.G., Klippstein, Barsom, J.M., and Blake, G.T., "Fatigue of Welded Steel Bridge Steel Members Under Variable Amplitude Loadings," Final Report, NCHRP Project 12-12 Transportation Research Board, Aug. 1975.
29. Smith I.F.C., Castiglioni, C.A., and Keating, P.B. "An Analysis of Fatigue Recommendations Considering New Data," IABSE Periodica, 13, International Association of Bridge and Structural Engineering, Zurich, 1989.
30. Fisher, J.W., Yen, B.T., Wang, D., and Mann, J.E., "Fatigue and Fracture Evaluation for Rating Riveted Bridges," National Cooperative Highway Research Program, NCHRP Report 302, Highway Research Board, Washington, D.C., 1974
31. Fisher, J.W., "Bridge Fatigue Guide: Design and Details," American Institute of Steel Construction, AISC Pub. No. T112-11/77, 1977.
32. Fisher, J.W., "Fatigue Cracking in Bridges from Out-of-Plane Displacements," Canadian Journal of Civil Engineering, Vol. 5, No. 4, December 1978.
33. Fisher, J.W., Jian Jin, Wagner, D.C., and Yen, B.T., "Distortion-Induced Fatigue Cracking in Steel Bridges," National Cooperative Highway Research Program, NCHRP Report 336, Highway Research Board, Washington, D.C., 1990.
34. Cheng, J.J., "Design of Steel Beams with End Copes," Journal of Constructional Steel Research, Vol. 25, 1993.
35. Kulak, G.L., Fisher, J.W., and Struik, J.H.A., *Guide to Design Criteria for Bolted and Riveted Joints*, Second Edition, John Wiley & Sons, Inc., New York, 1987.
36. LRFD Specification for Structural Joints Using ASTM A325 or A490 Bolts. Research Council on Structural Connections, 1988. (Available through the American Institute of Steel Construction, Chicago, IL.)
37. Van Dien, J.P., Kaczinski, M.R., and Dexter, R.J., "Fatigue Testing of Anchor Bolts," Proceedings, Structures Congress XIV, ASCE, Chicago, 1996.
38. Kulak, G.L., "Fatigue Strength of Riveted Connections," IABSE Workshop on Evaluation of Existing Steel and Composite Bridges, IABSE Report No. 76, Lausanne, Switzerland, March 1997.
39. Fisher, J.W., Yen, B.T., and Wang D., "Fatigue Strength of Riveted Bridge Members," Journal of Structural Engineering, ASCE, Vol. 116, No. 11, November, 1990.
40. Carter, C.S., Hyatt, M.V., and Cotton, J.E., "Stress-Corrosion Susceptibility of Highway Bridge Construction Steels, Phase I," Report FHWA-RD-F73-003, FHWA, April 1972.
41. Barsom, J.M. and Novak, S.R., "Subcritical Crack Growth and Fracture of Bridge Steels," NCHRP Report 181, Transportation Research Board, 1977.

42. Gurney, T.R., "Theoretical Analysis of the Influence of Attachment Size on the Fatigue Strength of Transverse Non-Load-Carrying Fillet Welds," *Members Rept.* 91/1979. Welding Inst. Cambridge, 1979.
43. Berge, S., "Effect of Plate Thickness in Fatigue of Cruciform Welded Joints," Rept. MK/R 67, Norwegian Inst. Tech., Trondheim, 1983.
44. Smith, I.F.C. and Gurney, T.R., "Numerical Study of Geometrical Effects in Longitudinal Non-Load-Carrying Fillet-Welded Joints," *Welding Journal*, Vol. 65, American Welding Society, Miami, 1985.
45. Maddox, S.J., "Fatigue Strength of Welded Structures," Second Edition, Abington Publishing, Cambridge, U.K., 1991.
46. European Committee for Standardisation (1992). "Eurocode 3: Design of Steel Structures," ENV 1993-1-1, Brussels.
47. PD 6493 "Guidance on Some Methods for the Derivation of Acceptance Levels for Defects in Fusion Welded Joints," Welding Standards Committee, BSI, UK, 1991.

INDEX

AASHTO:

- average daily truck traffic (ADTT), 55
- basis of design rules, 22, 25
- bolted shear splices, 103
- compressive stresses, 58, 120
- constant amplitude fatigue limit (CAFL), 57
- design example, 59
- design truck, 54
- distortion-induced fatigue, 25, 73, 84
- dynamic load allowance, 55
- effect of component size, 115
- fatigue category, 25
- fatigue design truck, 54, 64
- fatigue resistance, 51, 56
- fracture toughness, 51
- lateral bracing, 69
- load cycles, 64
- redundancy, 51
- riveted connections, 108
- shear studs, 72
- specifications, 2, 25, 54
- stress ranges, 65
- summary of requirements, 58
- tension-type connections, 104
- threaded rods, 107
- webs, 85

Backing bar, 94

Bolted members, 102

- preloaded, 103

- non-preloaded, 104

- tension, 104

Bracing, 77

Bridges

- box girder, 79

- girder, 76

- long-span, 81

- multi-beam, 76

Butt weld (see Groove weld)

Brittle fracture, 1, 17

Charpy V-notch, 6, 11, 54

Combined stresses, 114

Connections:

- bolted, 72, 102

- diaphragm, 76, 80

- groove weld, 93

- fillet weld, 18, 66, 75

- lateral bracing, 69, 83

- lateral connection plate, 69, 83

- riveted, 81, 108

- shear studs, 72

- splice plates, 66

Constant amplitude fatigue limit

- (CAFL), 47, 57

Coped beam, 82

Corrosion, 100, 110

Cover plates, 19, 20, 22, 48, 91

Crack:

- compression zone, 90

- corrosion, 100, 110

- critical length, 7

- discontinuities, 1, 8

- environmental effects, 110

- future cracking, 100

- growth (Paris equation), 9, 10

- growth law, 29

- initiation, 1

- inspection, 7, 88, 95

- length, 4

- location, 4

- low temperature, 113

- mean stress effect, 10

- modes, 3, 13

- pre-existing, 18

- propagation, 10

- repair, 97

- residual stresses, 115

- small, 6

- stress concentration, 4

- stress intensity factors, 5, 9

- sub-critical, 8

Cumulative damage, 34

Cross frames (see Diaphragms)

Cut-off limit, 49

- Diaphragms, 76, 80
- Distortion-induced fatigue cracking, 73
 - summary, 87
 - web gaps, 76, 79
- Environmental effects, 110, 113
- Equivalent stress range, 36
- Eurocode, 120
- European Convention for Constructional Steelwork (ECCS), 49, 120
- Examples, 13, 28, 31, 35, 37, 38, 44, 49, 59, 75, 85, 117
- Fatigue:
 - constant amplitude, 47
 - definition, 1, 8, 16
 - displacement-induced, 25
 - distortion, 2, 73
 - historical background, 16
 - limits, 47
 - limit state, 8
 - load-induced, 25
- Fatigue life (fatigue life assessment):
 - AASHTO, 56, 84
 - anchor bolts, 107
 - basis of design rules, 22
 - bolted, 72, 102
 - combined stresses, 114
 - controlling factors, 24
 - coped beam, 82
 - corrosion fatigue, 111
 - cumulative damage, 34
 - flange splice plates, 66
 - flange-to-web weld, 66
 - fracture mechanics analysis, 29
 - grade of steel, 22
 - lateral bracing attachment, 83
 - minimum stress, 23
 - Palmgren-Miner rule, 34
 - redundancy, 51
 - residual stress, 115
 - riveted, 108
 - shear studs, 72
 - size of component, 115
 - stress corrosion, 111
 - stress cycle counting, 41
 - stress histories, 40
 - stress range, 23
 - threaded rods, 106
 - transverse stiffeners, 67, 73
 - type of detail, 24
 - variable stress ranges, 34
 - web gap, 76
- Fatigue limits, 47
 - constant amplitude, 47
- Fillet welds, 17, 18, 90
- Flaws:
 - in fabricated steel structures, 18, 21
 - mechanical details, 21
 - welded details, 18
- Fracture:
 - toughness, 6, 51, 53
 - surfaces, example, 17, 19, 20,
- Fracture mechanics, 3
 - analysis of fatigue life, 29
 - Charpy test, 6
 - crack-growth model, 17
 - crack-tip opening displacement (CTOD), 5
 - defect assessment, 122
 - inspection interval, 122
 - J*-integral, 5
 - limit state, 6
 - microstructural, 6
 - modes, 3, 13
 - quantitative design, 11, 121
- Groove weld, 93
- Gusset plate, 91, 94
- Inspection, 95
 - acoustic emission, 96
 - coring, 97
 - dye penetrant, 96
 - fracture mechanics, 122
 - magnetic particle, 96
 - methods, 95
 - ultrasonic, 96
 - visual, 95

X-ray, 96

K-factor (see Stress intensity factor)

Long span structures, 81

Longitudinal stiffener, 93

Limit state:

- fracture, 6
- fatigue, 8

National Cooperative Highway Research Program (NCHRP), 16

Palmgren-Miner rule, 34

Rainflow cycle counting, 42

Redundancy, 51

Repair, 97

- Cover plates, 98
- Gas tungsten arc remelting, 99
- Gouge, 98
- Hole drilling, 91, 98
- Methods, 98
- Peening, 98
- Refabricate, 98
- Replacement, 99

Reservoir cycle counting, 42

Residual stresses, 115

- compressive applied stresses, 120
- effect on fatigue life, 24
- stress-relieved elements, 120
- non-welded elements, 120

Riveted connections, 108

Rods (see Threaded rods)

Secondary members, 92

Shear splices, 102

Steel:

- effect of grade upon fatigue life, 22
- toughness, 8

Stiffeners:

- longitudinal, 93
- transverse, 67, 73

Stress:

- combined, 114
- compressive, 58, 120
- constant amplitude, 47, 57, 106
- cycle counting, 41
- dead load, 41
- equivalent, 36
- gross section, 104
- histories, 40
- intensity factor, 5, 9
- live load, 58
- maximum, 23, 116
- mean, 10
- minimum, 23
- net section, 104, 108
- range, 23, 54, 67, 116
- ratio, 24, 116
- residual, 115
- shear, 114
- spectra, 47
- stress-relieved, 120
- tension, 104
- threshold, 50
- variable, 34
- variable amplitude, 47, 57, 106

Stress Corrosion, 111

Temperature, effect of, 113

Threaded rods, 106

Threshold stress, 50

Toughness, 6, 53

Variable amplitude stress ranges, 34

Web gaps, 76, 92

Web stiffener, 67, 73, 93

Weathering steel, 110

Welding:

- defects, 18, 20
- effect on fatigue, 1, 8, 16, 18



**National Steel
Bridge Alliance**



**American Institute
of Steel Construction**